REPUBLIC OF TURKEY

HACETTEPE UNIVERSITY
INSTITUTE OF HEALTH SCIENCES

DETERMINATION OF THE EFFECTS OF ACTINIC KERATOSIS MUTATIONS ON APOPTOSIS

Ayşe ERCAN

Program of Biochemistry
Ph.D. THESIS

ANKARA
2006

REPUBLIC OF TURKEY

HACETTEPE UNIVERSITY
INSTITUTE OF HEALTH SCIENCES

DETERMINATION OF THE EFFECTS OF ACTINIC KERATOSIS MUTATIONS ON APOPTOSIS

Ayşe ERCAN

Program of Biochemistry
Ph.D. THESIS

ADVISOR
Prof. Dr. I. Hamdi ÖĞÜŞ

Co-ADVISOR
Prof. Douglas E. BRASH

ANKARA
2006

To the Director's Office of the Institute of Health Siences of Hacettepe University:

This study has been accepted and approved as a Ph.D. thesis in the program of biochemistry by the examining committee whose members listed below:

Chairperson:	Prof. Dr. İnci ÖZER (Hacettepe University)
Advisor:	Prof. Dr. İ. Hamdi ÖĞÜŞ (Hacettepe University)
Member:	Prof. Dr. Kamer KILINÇ (Hacettepe University)
Member:	Prof. Dr. Orhan ADALI (Middle East Technical University)
Member:	Assoc. Prof. Dr. Yasemin AKSOY (Hacettepe University)

I hereby certify that this thesis has been accepted and approved by the committee above in conformity to the regulations and bylaws of the Hacettepe University Institute of Health Sciences

Prof. Dr. Hakan S. ORER
Director of Institute of Health Sciences

ACKNOWLEDGEMENT

For all the guidance and support he gave me during my Ph.D. education, firstly I would like to thank my advisor Prof. Hamdi ÖĞÜŞ. Being a good mentor to me for nearly 10 years, he lead me in achieveing my goal. I also would like to thank Prof. Nazmi ÖZER for his valuable skills and comments in helping me during my laboratory practices. Both had great contributions on my scientific personality since 1997 as they never forget to teach me the fun side of science.

Special thanks to my co-advisor Prof. Douglas BRASH, who gave me the chance to work in his laboratory at Yale University. Despite being there for a short period of time, I learned too much from him which will always be appreciated. Apart from giving me lectures on how to design and develop a project, how to arrange a functional lab-book and how to discuss my results, he kept on helping me via e-mails even after I got back to Turkey. Needless to say that without his help, I wouldn't have the chance to work on this project.

I would also like to say that I'm really grateful about my lab mates at Brash Lab. Dejan Knezevic, for teaching me the techniques I wasn't familiar with; Wengeng Zhang, for being a kind lab mate and Patrick Rochette, for always being a great company while waiting for my results and discussing for troubleshooting as well as his good conversations everytime I needed.

Meltem MÜFTÜOĞLU is another personality that I specially thank for being a very close friend apart from being a very qualified teacher since she helped me a lot both in Turkey and USA.

Last, but not least, I deeply thank my family for their extreme support, unlimited patience and tolerance. They deserve the best thanks of all. Following every step of this thesis, my father never lost his faith in me and he made me laugh when I was having hard times 9000 km away from home. My mother helped me by coming all the way from home to give me moral support. Whenever I faced problems, my sister never felt any reservations in listening to me patiently. From editing this thesis to catering in the exam, I thank for all of her tremendous efforts.

This research was done at Yale University, New Haven, USA, and was supported by TÜBITAK.

ÖZET

Ercan A., Aktinik Keratozlardaki p53 Mutasyonlarının Apoptoz Üzerindeki Etkisinin İncelenmesi, Hacettepe Üniversitesi Sağlık Bilimleri Enstitüsü Biyokimya Programı Doktora Tezi, Ankara, 2006. Her sene cilt kanseri vakaları artmaktadır ve bu kanserlerin % 95'ni nonmelanoma cilt kanserleri (NMCK) oluşturmaktadır. Güneş yanığı hücreleri olarak da bilinen Aktinik Keratozlar (AK), bir NMCK çeşitidir. Güneş ışığının önemli kısmını oluşturan UV, cilt kanserlerinin etiyolojisine büyük ölçüde katkıda bulunmaktadır. UV, mutasyonlara sebep olan DNA fotoürünlerini oluşturmak suretiyle DNA'da hasarlar yaratmaktadır. UV'nin tanımlayıcı işareti Sitozin'in Timin'e değişimidir ve bu işaret tümör baskılayıcı p53'ün üzerinde de tanımlanmıştır. P53 hücre döngüsünü durdurarak ve apoptozu indükleyerek tümör büyümesini engellemektedir. P53'ün kanserlerin % 50'sinden fazlasında mutasyona uğradığı ve bu mutasyonların büyük kısmının da yanlış kodlanmış nokta mutasyonlar olduğu bilinmektedir. Bu çalışmada amacımız AK'lerde bulunan p53'ün farklı mutant allellerinin UV'ye bağımlı apoptoz üzerine etkilerini tespit etmekti. Bunun için bir dizi biyoinformatik çalışma sonucu 11 nokta mutasyonu tespit edilmiştir. Bu mutasyonlar ekspresyon vektörü üzerinde bölge yönelimli mutagenezle yaratılmıştır. Mutant ve yabanıl tip vektörler primer fare fibroblastlarına transfekte edilmiş ve 1000 J UVB radyasyona maruz bırakılmıştır. Apoptoz yüzdesi flow cytometry'le ölçülmüş, protein ekspresyonunu ölçmek için western blotting uygulanmıştır. Çalışmamızın sonucunda R201C ve L202F mutasyonlarının etkisiz davrandığı bazılarınınsa yüksek endojen apoptoza sahip olmalarına rağmen UV'ye bağımlı apoptoz yüzdesinin düşük olduğu görülmüştür (S241F, G245S, R248W). P128S UV'ye bağımlı apoptoza direnç gösterirken aynı ekzonda yer alan H178Y ve H179Y'de yabanıl tipe göre % 7.2 ve % 5.2 daha fazla apoptoz görülmüştür. A84V ve P92L artmış endojen apoptoza rağmen UV'ye bağımlı apoptoz açısından yabanıl tip gibi davranmışlardır. Mutasyonun kazandığı fiziksel ve kimyasal değişiklik, evrimsel olarak korunmuş bölgede yer alması ve/veya DNA'ya bağlanma bölgesine yakınlığı bu mutasyonların apoptoz açısından davranışını etkilemektedir.

Anahtar Kelimeler: p53, p53 mutasyonu, Apoptoz, AK, UVB

Destekleyen Kurumlar: TÜBİTAK

ABSTRACT

Ercan A., Determination of the Effect of Actinic Keratosis Mutations on Apoptosis, Hacettepe University Institute of Health Sciences, Ph.D. Thesis in Biochemistry, Ankara 2006. Every year the incidence in skin cancers increases where 95% of these are non melanoma skin cancers (NMSC). Actinic Keratosis (AK) is a NMSC characterized by aberrant proliferation and cell differentiation. Ultraviolet (UV) contributes to the etiology of skin cancers. UV damages DNA by creating DNA photoproducts which in turn generates mutations also seen on the p53 tumor suppressor gene. P53 is mutated in more than 50% of cancers, and most of these are missense mutations. In this research our aim was to determine whether different mutant p53 alleles found in AK have different abilities to confer new properties as a response to UVB-induced apoptosis. After a bioinformatic study 11 point mutations were selected and generated by site directed mutagenesis on an expression vector. The mutated and wild type (WT) vectors were transfected into primary mouse fibroblasts and irradiated with 1000 J UVB. The apoptosis percentage was detected with flow cytometry and protein expression levels were determined by western blotting. We found that mutations R201C and L202F behave like null-mutations, while hotspot mutations S241F, G245S, R248W have high endogenous apoptosis but less response to UV-induced apoptosis. P128S was resistant to UV-induced apoptosis but H178Y and H179Y have 7.2% and 5.2% more UV-induced apoptosis compared to WT scores, respectively. Mutations A84V, P92L have increased endogenous apoptosis but behaved like WT p53 to UV-induced damage. The physical and chemical change the mutation acquires, being on an evolutionarily conserved domain and/or close to the DNA binding region effect the behavior of the mutation.

Keywords: p53, p53 mutation, Apoptosis, AK, UVB

Supported by TÜBİTAK.

TABLE OF CONTENTS

ABBREVIATIONS

AD	Activation Domain
AIP1	p53-regulated Apoptosis Inducing Protein-1
AK	Actinic Keratose
Apaf-1	Apoptotic protease–activating factor
ATM	Ataxia Telangectasia Mutated
ATR	Ataxia Telangectasia and Rad3 related
Bax	BCL2-associated X protein
BCC	Basal Cell Carcinoma
Bcl-2	B-cell leukemia/lymphoma 2
BSA	Bovine Serum Albumine
CPD	Cyclobutane Pyrimidine Dimer
CDK	Cyclin Dependent Kinase
CS	Cockayne Syndrome
Cyt c	Cytochrome c
DBD	DNA Binding Domain
DMEM	Dulbecco's Modified Eagle Medium
EGFP	Enhanced Green Fluorescence Protein
FADD	Fas-associated death domain
FBS	Fetal Bovine Serum
GADD45	Growth Arrest and DNA Damage-inducible protein 45
HPV E6	Human Papilloma Virus E6
HRP	Horse Radish Peroxidase
IPTG	Isopropyl-β-D-thiogalactopyranoside
KO	Knockout mouse
MDM-2	Minute Double Murine 2
mt	Mutant
NER	Nucleotide Excision Repair
NLS	Nuclear Localization Signal
P53R2	P53 Inducible Ribonucleotide Reductase
PBS	Phosphate Buffer Saline

PI	Propidium Iodide
PRD	Proline Rich Domain
SCC	Squamous Cell Carcinoma
Smac/Diablo	Second mitochondria-derived activator of caspase/direct IAP-binding protein with low pI
SV 40	Simian Virus 40
TFIIH	Transcription Factor II-H
TNF-α	Tumor necrosis factor alpha
UV	Ultraviolet
WT	Wild Type
X-Gal	5-bromo-4-chloro-3-indolyl β-D-galactopyranoside
XP	Xeroderma Pigmentosum

LIST OF FIGURES

LIST OF TABLES

1. PREFACE

Apoptosis, a form of programmed cell death characterized by cell shrinkage, membrane blebbing, nuclear breakdown and DNA fragmentation is essential for the development, maintenance of tissue homeostasis, and elimination of harmful cells (31). The presence of toxic agents, DNA damage, induced death receptor signal, the ectopic expression of nuclear oncogenes and the withdrawal of survival signals such as growth factors, cytokines, hormones are factors that initiate apoptosis (6). The tumor suppressor P53 is the key regulator that mediates apoptosis.

P53 is a sequence specific transcription factor responsible for maintaining the integrity of the genome (66). It's a tetrameric protein that has a very short half-life. Therefore in undamaged cells the levels of p53 remains very low (17). Mdm-2, which is one of the downstream target elements of p53, is responsible for keeping P53 at low levels by ubiquitinating and mediating the degradation of the protein (24). Depending on the stimuli, P53 contributes to the activation of two major pathways that control the tumor growth; the arrest of the cell cycle and the regulation of apoptosis (68). After cellular exposure to various DNA-damaging agents (such as ionizing radiation, UV radiation, chemoterapeutic agents, hypoxia, virus infection) P53 accumulates and activates the transcription of several downstream target element (66, 17).

P53 is known to be mutated in more than 50 % of human cancers (67). In the latest version of International Agency for Research on Cancer TP53 Mutation Database (released in October 2006), 23.544 somatic mutations and 376 germline mutations have been reported where 73.7 % of these are missense mutations. Most of these mutations take place on the DNA binding domain of the protein, especially on the evolutionarily conserved regions (59). P53 is inactivated by allelic loss, small deletions and point mutations (48). Some point mutation may confer new characteristic to the gene such as gain of function, loss of function or dominant-negative properties (26).

Ultraviolet (UV) is the major component of sunlight in which everybody is exposed. In the light spectrum it takes place between X-ray and visible light and is divided in three subtypes; UVA, UVB and UVC. Though UVC has the lowest wavelength, thus the highest energy, in reality it's greatly absorbed by the ozone

layer and doesn't affect organisms directly. UVB is the UV type that cause the biggest damage. It induces the production of thymine dimers between two adjacent pyrimidine bases on the same DNA strand (51). These reactions occur very frequently and they are very common. Fortunately, most of these genetic lesions are corrected very shortly after they are created, before they can leave a permanent damage. Nucleotide Excision Repair system is one of the mechanisms in which the organism use to repair the damaged portion of the DNA (53). The damage caused on the DNA by UV light is very distinctive; the mutation signature caused by UV is C to T transitions at dipyrimidine sites, and CC to TT substitution in 10 % of the cases (54).

The skin, the largest organ of the body, protects, absorbs, excretes, communicates, synthesizes, controls evaporation, and regulates the body temperature. This multifunctional shield is exposed to sunlight and is target to developing cancers as a result of accumulating UV-induced mutations. Skin cancers are classified as melanoma and nonmelanoma. Every year the frequency of the incidence in skin cancer is increasing and 95 % of these are non melanoma skin cancers (NMSC) (brash 91). Unlike the melanomas that originate from melanocytes, the NMSCs, namely Basal Cell Carcinoma (BCC), Squamous Cell Carcinoma (SCC) and Actinic Keratosis (AK), originate from the basal layer of the epidermis and develop on sun-exposed areas of the body, like the face, ear, neck, lips, and the backs of the hands (45). BCCs are common, they spread by local invasion and they tend to remain diploid. SCCs are less frequent but are more aggressive; they have a greater tendency to metastasize and they become aneuploid. AKs, also known as sunburn cells, are characterized by aberrant proliferation and cell differentiation. If left untreated in most of the cases AKs will regress but there's also a chance that they can turn into carcinoma or SCC (54). Therefore AKs are thought to be the first step in the development of skin cancer. It is thus a precursor of cancer or a precancer.

The aim of this work was to determine whether different mutant p53 alleles found in human precancers have different abilities to confer new properties as a response to UVB-induced apoptosis. For this purpose 11 mutations found in AK lesions were generated by site directed mutagenesis on an expression vector. To determine the mutations to generate, a bioinformatic study was performed (as

described in detail in section 3.1). The wild type and mutated vectors were transiently transfected into the mouse primary fibroblast cells. The primary mouse fibroblasts were preferred over cell lines (such as HeLA, HACaT, Saos2) as these cell lines are already defected in apoptosis and independent inactivation of cell cycle arrest. Another reason for working with the primary mouse cells is that the transient transfection into these cells allows wild-type and mutant p53 alleles to be co-transfected to check for dominant negative phenotypes. The cells were radiated with UVB 72 hours post transfection in order to allow the mutated protein to be expressed and the DNA synthesis to be resumed. 19 hours post UVB readiation the cells were harvested and subjected to Annexin Assay to determine the percentage of apoptosis. Similarly, the protein expression levels were determined for p53 and Mdm-2 by western blotting.

2. INTRODUCTION

2.1 History of P53

Antibodies against SV40 large T antigen from tumours produced by SV40-transformed cells coimmunoprecipitated a cellular protein called p53, named after having a molecular mass of 53 kDa (1). From this observation it was concluded that p53 interacted with SV40 large T antigen (2). Later it was discovered that viral oncoproteins and DNA tumor viruses like the adenovirus E1B, human papillomavirus HPV E6 protein (3), Epstein ± Barr virus nuclear antigen (4), Hepatitis B virus X protein (5) and human cytomegalovirus IE84 protein have the ability to bind p53. Moreover it was found that many transformed cell lines, as well as primary human cells from patients with various types of tumours, contained an elevated level of p53, whereas non transformed cells contained only minute amounts of p53 (6). This difference was attributed to stabilization in transformed cells of the normally short-lived protein (7). p53 was also identified by its ability to be immunoprecipitated from a variety of transformed cell lines with antibodies produced by certain tumour-bearing animals (8, 9). Similarly, anti-p53 antibodies were also identified in sera from cancer patients (10, 11).

In later works on p53, Reich and Levine arrested the cell growth rate with serum deprivation in mouse 3T3 cells and showed that the cells exhibited very low levels of p53 mRNA and p53 protein. The mRNA and protein levels of p53 increased remarkably and reached a peak near the G1/S phase when the cells were induced to grow by serum stimulation. The results reported in that work demonstrate an increase in the synthesis and steady-state levels of p53 protein and mRNA prior to DNA synthesis in late G1, and suggest a role for p53 in the progression of cells from a growth-arrested state to an actively dividing state (12). Similarly Milner and McCormick treated normal resting T lymphocytes with Concanavalin A and stimulated the DNA synthesis and mitotic division (13). These experiments show that the increased expression of p53 is accompanied by a nearly proportional increase in the growth fraction of a given population. Thus the increased expression of p53 observed in the large majority of tumors simply reflects the increased number of cycling cells frequently found in a neoplastic tissue (14).

2.2 Structure of P53

The Human tumour suppressor gene p53 is localized on the short arm of the chromosome 17 (17p13). The human p53gene encompasses approximately 20 kb of genomic DNA and consists of 11 exons and shows a high level of conservation through species of vertebrates (15). The product of the gene is a 393 amino acid nuclear phospho-protein found in very low levels in normal, undamaged cells (Figure2.1). The low level of p53 protein in normal cells is due mainly to the short half-life of the protein (6–20 min) (16, 17). P53 has been divided into a number of discreet motifs.

The acidic N-terminal region (amino acids 1-39) encodes the transactivation domain. This region has been shown to interact with components of the transcriptional machinery such as TATA-Binding Protein (TBP) and the Mdm2 protein which negatively regulates p53's transactivation function. The region between amino acids 40-100 contains series of repeated proline residues that are conserved in the majority of p53. This proline-rich region has been shown to be important for p53's tumor suppressor function (19, 20).

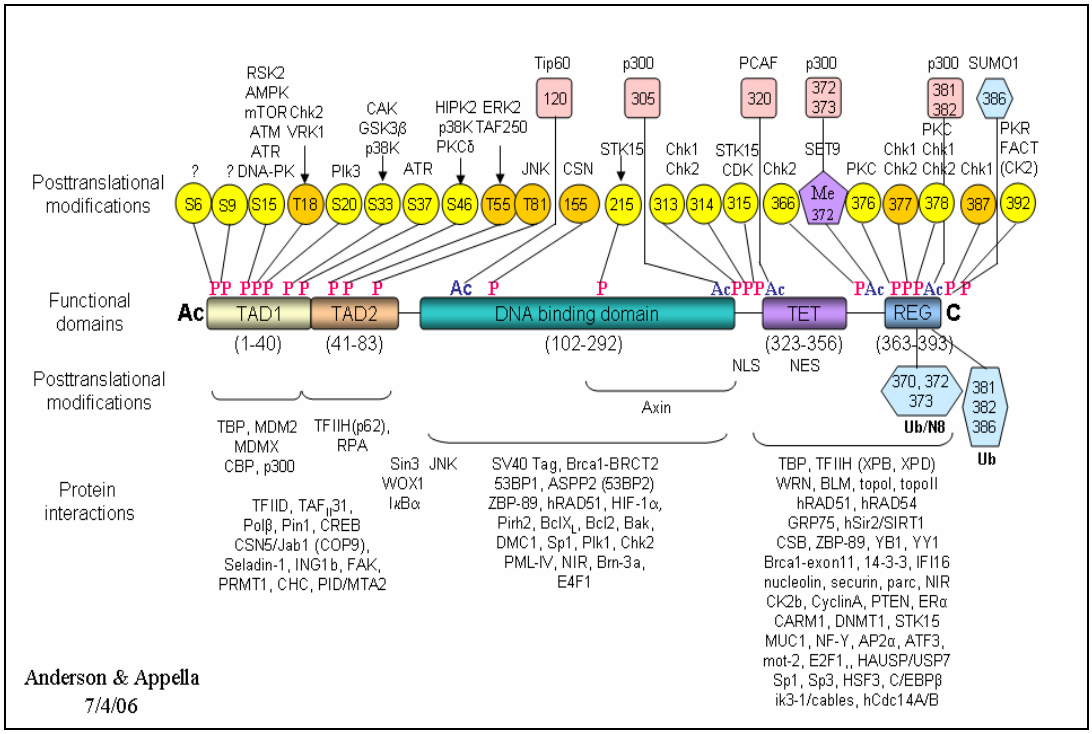

Figure 2.1. Structure of the p53 gene (18).

The large central region (codons 101-306) on the protein confers sequence specific DNA binding activity to the polypeptide (17). It is the target of 90% of p53 mutations found in human cancers and mutations on this region disrupt DNA binding by p53. The oligomerization domain (codons 307-355) consists of a beta-strand, followed by an alpha-helix necessary for dimerization, as p53 is composed of a dimer of two dimers. Many mutant alleles of p53 are a result of this oligomerization and they confer a dominant negative property to the tetramer. A nuclear export signal is also localized in this oligomerization domain (15).

The carboxy-terminus of p53 (codons 356-393) contains 3 nuclear localization signals and a non-specific DNA binding domain that binds to damaged DNA. This region is also involved in downregulation of DNA binding of the central domain. p53 is substantially modified posttranslationally via serine targeted phosphorylations at both the N-terminus and the C-terminus, as well as acetylation at lysine residues in the C-terminus (17). For an efficient binding of p53 to recognition sites of targets or for transcriptional activation the integrity of these domains is strictly required (21).

P53 is active as a tetramer (22). Most of the p53 mutations in human cancers are found outside the oligomerization domain, hence sparing tetramerization. Experimental evidence showed that wild-type p53 tetramerizes with mutant proteins to form a heterotetramer (23).

2.3. The Function of P53

The basal level of p53 remains very low unless there's damage in the DNA. The cell maintains the level of p53 through the binding of the E3-ubiquitin ligase protein Mouse Double Minute 2 (MDM2). It was demonstrated that the E3 activity of MDM2 is dependent on its RING finger domain and that MDM2 ubiquitinates both p53 and itself (24). MDM2 is also responsible for the negative regulation of p53 by binding to its N-terminal domain and repressing its transcriptional activation. This binding blocks p53 mediated gene expression. P53 can in turn bind to MDM2 and trigger its expression. There's a regulatory loop between p53 and MDM2; where p53 induces MDM2's expression which turns off p53's activity (25).

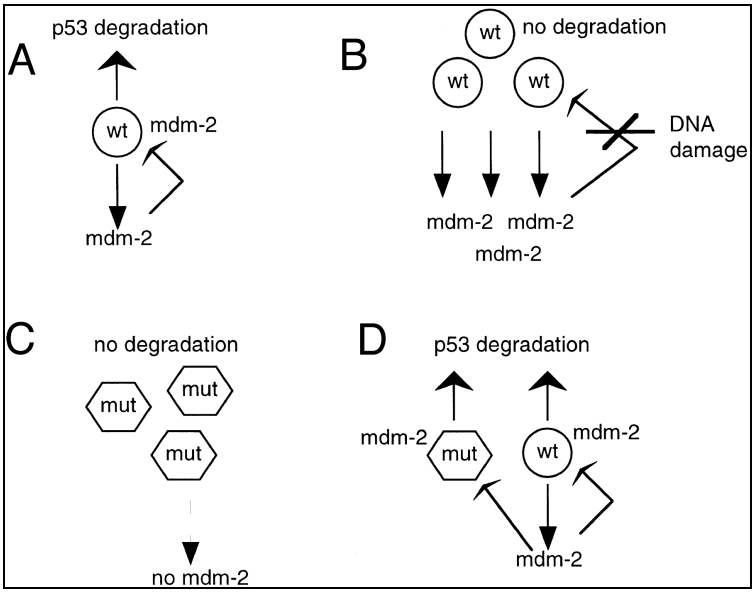

Figure 2.2. The regulation of the p53 stability by Mdm2 (26).

As it can be seen from Figure 2.2, depending on the wild type (wt) or mutated (mt) state of P53 there are different regulations for P53's stability. In figure 2.2.A, mdm-2 is transcriptionally induced by wt p53 which in turn degrades it. In the presence of a DNA damage, figure 2.2.B, the degradation of wt p53 by mdm2 is prevented. In that case p53 accumulates and depending on the stimuli transactivates it's downstream genes. When P53 is mutated it cannot transactivate mdm2, thus P53 accumulates (Figure 2.2.C). If there's a wt p53 allele, mdm-2 is transactivated by wt p53 and both mt p53 and wt p53 are subject to degradation by mdm-2 (F'gure 2.2.D) (26).

Following the DNA damage, p53 can play role in three major mechanisms; p53 can activate the transactivation of target genes which in turn will play a role in cell cycle arrest, apoptosis or regulate p53 negatively. It can repress the downstream target genes such as antiapoptotic proteins, viral and cellular oncogenes and cyclins. Or it can activate the genes that are involved in DNA repair mechanisms (Figure 2.3) and the damage can be removed by nucleotide excision repair, base excision repair, mismatch repair, homologous recombination or non-homologous end joining.

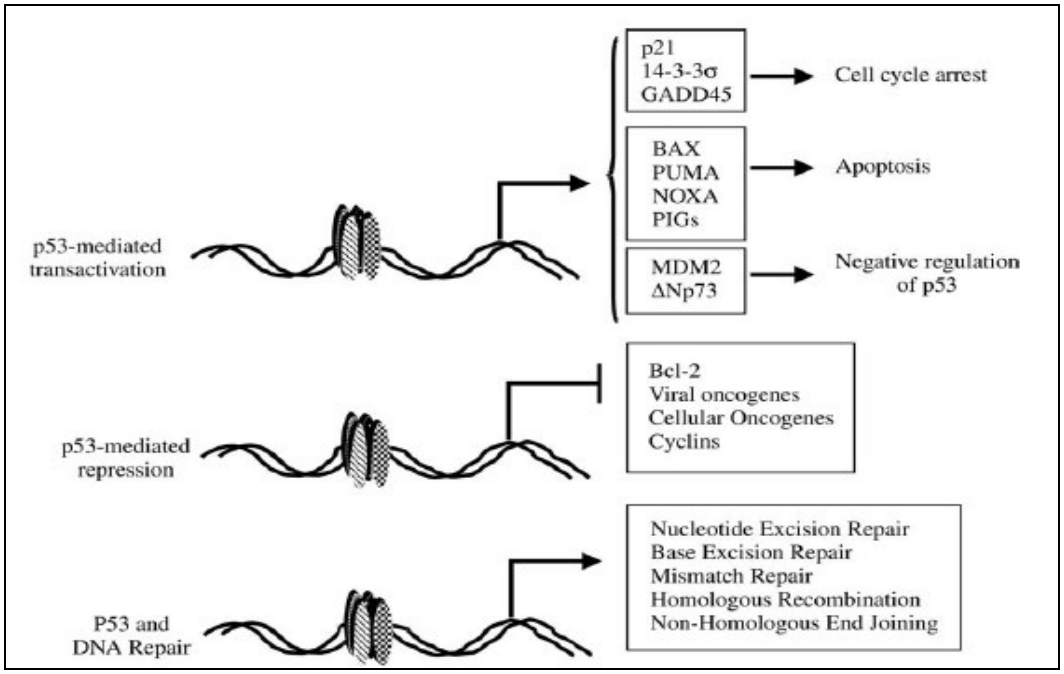

Figure 2.3.The three main role of the p53 gene (69).

In response to some forms of DNA damage P53 can inhibit the cellular growth by two mecahnisms; First, it can induce apoptosis, as it will be explained in the next session. Second, it can inhibit the progress of the cell cycle until the damage is repaired (27). The cell cycle progression into the S phase requires the enzyme Cyclin Dependent Kinase 2 (Cdk2), which can be inhibited by p21 (also termed WAF1 or CIP1). p53 turns on the transcription of p21, which in turn binds to a number of cyclin and cdk complexes such as cyclin D1–Cdk4, cyclin E–Cdk2, cyclin A–Cdk2, and cyclin A–Cdc2 (28). Mice deficient in the p21 gene develop normally, and but fibroblasts derived from these mice are partially deficient in their ability to arrest cells in G1-to-S phase in response to DNA damage (29). The progression into the M phase requires Cdc2 which can be inhibited by p21, GADD45 or 14-3-3-σ. p53 regulates the expression of these inhibitory proteins to induce growth arrest at the M phase (17). The DNA damage due to UV activates the Ataxia Telangectasia Mutated (ATM) kinase which phosphorylates and activates CHK2 checkpoint homolog (Chk2). Activated Chk2 phosphorylates Cdc25 and targets it for degradation. A second pathway from activated ATM/ATR (Ataxia Telangectasia and Rad3 related) kinase stabilizes p53, by phosphorylating the protein at a site that binds with Mdm-2, thus inhibiting its rapid degradation (30).

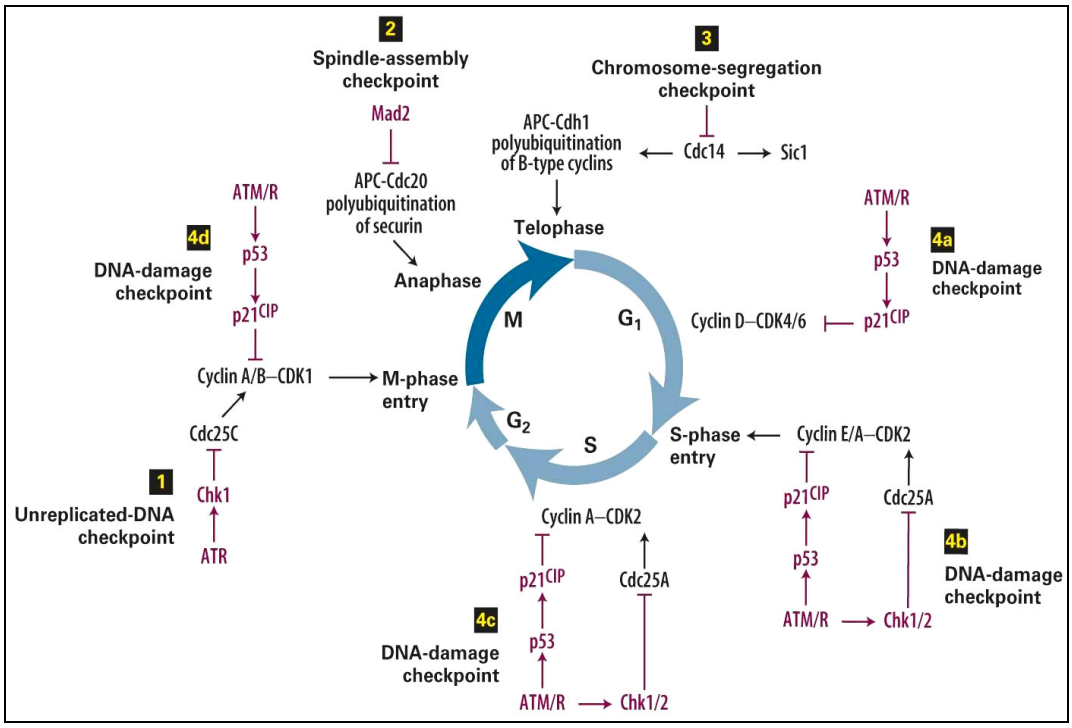

Figure 2.4. The role of p53 in the cell cycle regulation (30).

2.4. Apoptosis

Apoptosis is defined as the programmed cell death that occurs in response to multiple physiological factors. Naturally occuring apoptosis is essential for the proper embryonic development of the organism, as well as the maintenance of the immune response (31). The presence of toxic agents, DNA damage, induced death receptor signal, the ectopic expression of nuclear oncogenes and the withdrawal of survival signals such as growth factors, cytokines, hormones are other factors that initiate apoptosis (6). Different cells exhibit different thresholds to various apoptotic stimuli. For example splenic lymphocytes readily undergo apoptosis when exposed to ionising radiation whereas myocytes are resistant to apoptosis on similar exposure (32). The apoptotic process is characterized by morphological and biochemical changes, including the blebbing of the plasma membrane, condensation of the chromatin, exposure of phosphatidyl serine on the outer plasma mebrane and DNA fragmentation. Cells undergoing apoptosis are rapidly phagocytosed by surrounding cells. Therefore in a light microspcope, apoptosis can be justified by the presence of “apoptotic bodies” inside neighboring cells. Another characteristic feature of

apoptosis, DNA fragmentation, can be seen in agarose gel electrophoresis as a laddering formation of 80-120 base pair fragments of DNA. The DNA ladder is an early morphological sign of apoptosis and is widely used for the its detection (33).

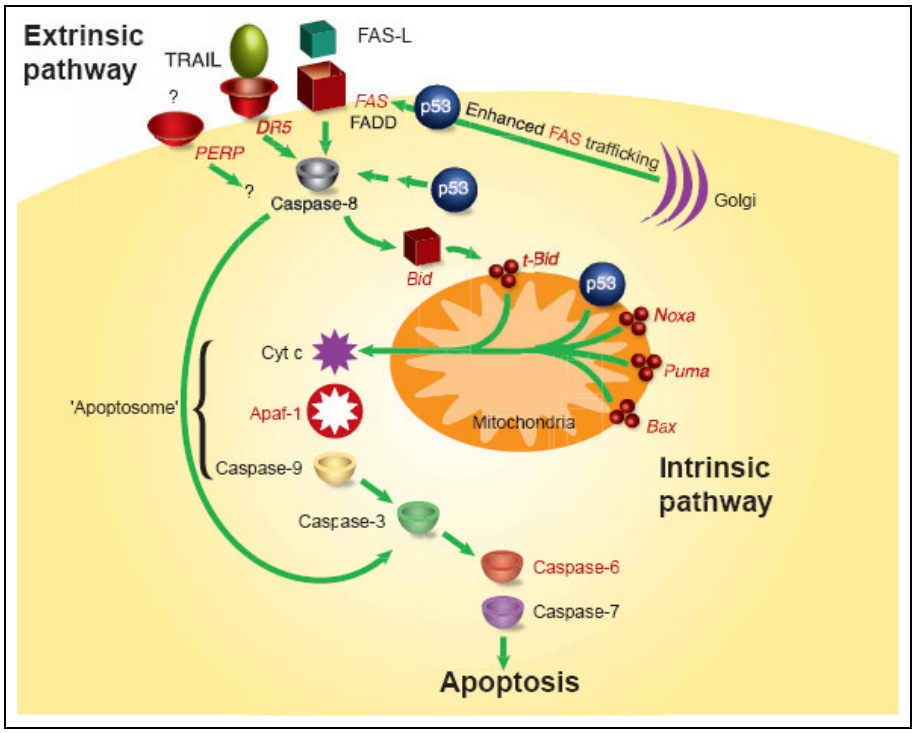

Figure 2.5. The Extrinsic and Intrinsic Apoptotic Pathways (36)

There are two pathways that trigger apoptosis; the "extrinsic" and the "intrinsic" pathways (Figure 2.5). The intrinsic apoptosis pathway is triggered by cellular stress, caused by factors such as DNA damage and heat shock (34). Following the stress signal Bax dimerizes and translocates to mitrochondria. Bad is phosphorylated and activated by 14-3-3 sequestration. Bid is activated and together with Bax and Bad they bind to the outer membrane of the mitochondria. This complex activate the pro-apoptotic protein Bak and initiate the release of Cytochrome c from mitochondria. Cytochrome c forms a complex called apoptosome with Adenosine Triphosphate and Apaf1, which in turn activates the initiator caspase 9. This complex then activates the effector caspase, caspase 3. Other than these proteins released from mitochondria, Smac/DIABLO and Omi/HtrA2, inhibit IAPs (inhibitor of apoptosis proteins) which prevent the activation of caspase 3, thus prevent apoptosis (34, 35).

The extrinsic pathway begins outside the cell with the binding of the Fas ligand (FasL or CD95L) to the transmembrane Fas receptor (CD95) which is a member of death receptor family. This binding results in the clustering of receptors on the target cell and initiates the extrinsic pathway. Fas clustering recruits an adaptor protein known as Fas-associated death domain (FADD). FADD and the initiator pro-caspase 8 forms a complex, also known as death-inducing signal complex (DISC). Pro-caspase 8 is activated by autocatalysis. The activated caspase 8 cleaves in turn pro-caspase 3, which then undergoes autocatalysis to form active caspase 3, the initiator caspase (37).

Active caspase-8 can also cleave BID protein to tBID, which acts as a signal on the membrane of mitochondria to facilitate the release of cytochrome c in the intrinsic pathway (38). The extrinsic and intrinsic pathways merge at caspase 3 level. The apoptotic activity of p53 is essential for the elimination of defective and potentially carcinogenic cells. p53 induces apoptosis by multiple mechanisms involving both transcription-dependent and -independent pathways. These include the generation of reactive oxygen species, depolarization of the mitochondrial membrane, and the activation of caspase cascades. Disruption of an appropriate apoptotic response is implicated in the development of many disease states, including cancer, atherosclerosis and several degenerative diseases. (25)

2.5. Apoptosis and Necrosis

The cell deaths defined by apoptosis and necrosis are morphologically and biochemically different from each other (39). The stimuli that trigger apoptosis can be pathological or physiological whereas for necrosis it's always pathological. Apoptosis is energy dependent, necrosis is not. Necrosis is not dependent to mitochondria, and there are no role for the cytochrome c release. In necrosis, contrary to apoptosis there are no caspase activation but instead there's pro-inflammatory signalling and cytokine production. Thus the necrotic response generates an inflammatory response where there's leakage of the lysosomal enzymes and the dead cells are ingested by macrophages and neutrophils. Morphologically in necrosis, the cell and the organelles swell, the chromatin condenses and the membrane assimetry is lost and the cell membrane explodes (40).

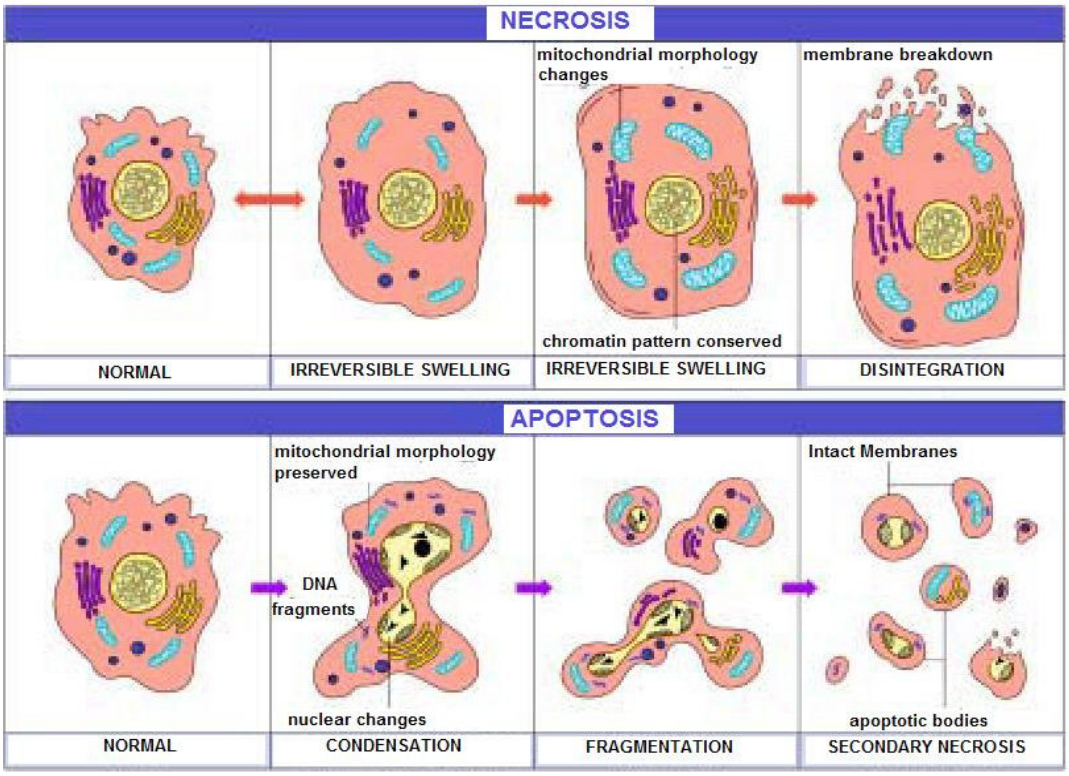

Figure 2.6 The morphological changes occuring during apoptosis and necrosis

2.6. The P53 Family

p63 and p73 are member of the p53-family and they display a high homology to p53. The most prominent homology is found in the DNA Binding domain with 63%. The critical residues for proper folding and for binding to the target DNA sequences are also strictly conserved. At the sequence level, p63 and p73 are more similar to each other than each is to p53, suggesting the possibility that the ancestral gene is a gene resembling p63/p73, while p53 is phylogenetically younger (41). These proteins have striking similarities but also surprising diversities, possibly because both genes give rise to proteins that have p53-agonistic functions, p53-antagonistic functions, and entirely novel functions (42). p63 and p73 are able to bind to p53 DNA binding sites, transactivate p53-responsive genes and induce apoptosis when exogenously expressed in the cells. These different p53-family members seem to cross-talk and cross-regulate between each other (43). P63 and p73 genes are approximately 65 kb and contain 14 and 15 exons respectively. In p53, as well as in p73, exon 1 is non-coding and the mRNA from this exon might influence the translation process. Unlike p53, p63 and p73 encode several polypeptides (41).

2.7. The Organization of the Skin and Skin Cancers

The skin, which is the largest organ of the body, covers the internal organs and protects them from injury, serves as a barrier between microbes and internal organs, and prevents the loss of too much water and other fluids. The skin regulates body temperature and helps rid the body of excess water and salts. Certain cells in the skin communicate with the brain and allow for temperature, touch, and pain sensations. Most skin cancers are classified as nonmelanoma, usually occurring in either basal cells or squamous cells. These cells are located at the base of the outer layer of the skin or cover the internal and external surfaces of the body. The top layer of the skin is the epidermis. The epidermis is thin, averaging only 0.2 mm (about 1/100 of an inch). It protects the deeper layers of skin and the organs of the body from the environment. The outermost part of the epidermis is called the stratum corneum, or horny layer. It is composed of dead keratinocytes (the main type of cell of the epidermis) that are continually shed. Below the stratum corneum are layers of living keratinocytes, also called squamous cells. These cells form an important protein called keratin. Keratin contributes to the skin's ability to protect the rest of the body. The lowest part of the epidermis, the basal layer, is formed by basal cells. These cells continually divide to form new keratinocytes, which replace older keratinocytes that wear off of the skin surface. The basement membrane separates the epidermis from the deeper layers of skin. Cells called melanocytes are also present in the epidermis. These skin cells produce the protective brown pigment called melanin. Melanin is what makes the skin tan or brown. It is formed to protect the deeper layers of the skin from the harmful effects of the sun. The middle layer of the skin is called the dermis. The dermis is much thicker than the epidermis. It contains hair follicles, sweat glands, blood vessels, and nerves that are held in place by a protein called collagen. Collagen, which is made by skin cells called fibroblasts, gives the skin its resilience and strength. The last and deepest layer of the skin is called the subcutis. The subcutis and the lowest part of the dermis form a network of collagen and fat cells. The subcutis conserves heat and has a shock-absorbing effect that helps protect the body's organs from injury (44).

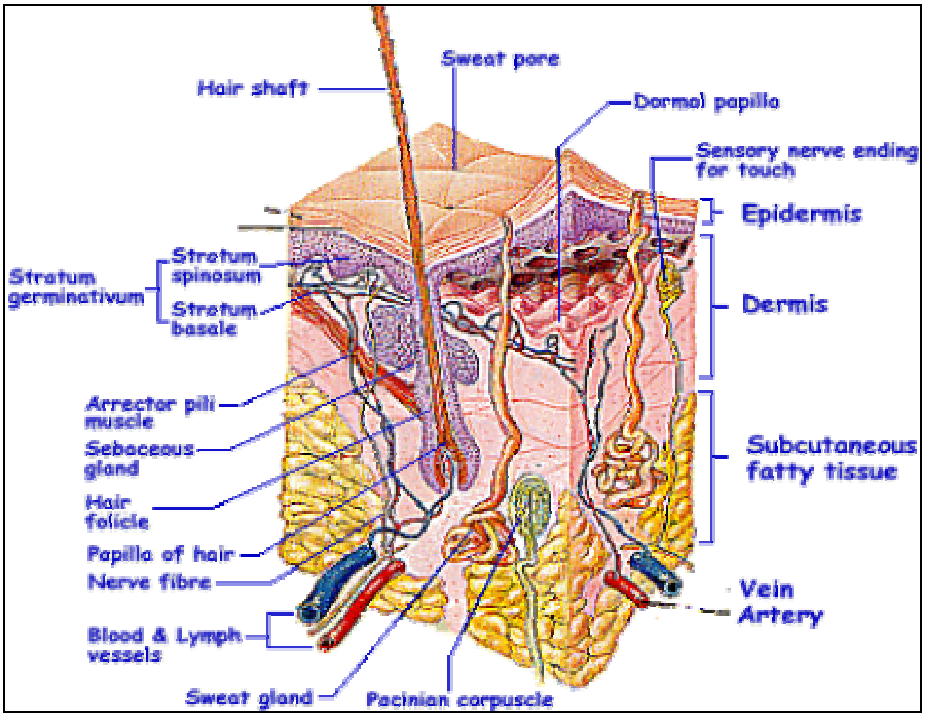

Figure 2.7. The organization of the skin

Some skin conditions are more likely to develop as we get older. These can include the followings: Seborrhoeic keratosis which is a type of benign skin tumour that looks like a brown wart. Solar keratoses are spots of skin that are inflamed, scaly and dry. Common sites include the bridge of the nose, cheeks, upper lip and backs of the hands. Skin cancer (squamous cell) can develop in them, so examination by a doctor is advised.

Bowen's disease is a type of slow-growing and scaly skin patch. It may be a pre-cancerous change. Sun exposure is thought to be a cause.

According to the National Cancer Institute, skin cancer develops in 1 million people every year in US. The disease develops in nearly 50% of all people older than 65. But the risk is highest for adults of any age with excessive sun exposure, especially those with light skin and light-colored eyes (45).

According to the cells type they originate and their ability to metastasize we can classify the skin cancers in 2 general classes as melanoma and non-melanoma.

Melanoma: Melanoma is a malignant tumor that originates in melanocytes, the cells which produce the pigment melanin that colors our skin, hair, and eyes and is heavily concentrated in most moles. Although melanoma accounts for only about 4% of all

skin cancer cases, it causes most skin cancer-related deaths. When melanoma metastases, cancer cells can also be found in the lymph nodes and possibly also in other parts of the body, such as the liver, lungs, or brain. In these cases, the cancer cells are still melanoma cells, and the disease is called metastatic melanoma. The majority of melanomas are black or brown. However, melanomas occasionally stop producing pigment. When that happens, the melanomas may no longer be dark, but are skin-colored, pink, red, or purple.

Most skin cancers are classified as nonmelanoma, usually occurring in either basal cells or squamous cells. These cells are located at the base of the outer layer of the skin or cover the internal and external surfaces of the body. Chronic exposure to sunlight is the cause of almost all skin cancers. Most nonmelanoma skin cancers develop on sun-exposed areas of the body, like the face, ear, neck, lips, and the backs of the hands. Rarely, however, tumors develop on non-exposed areas. Depending on the type, they can be fast or slow growing, but they rarely spread to other parts of the body (45).

Basal cell carcinoma: these cancers arise in the basal cells, which are at the bottom of the epidermis. They spread by local invasion and they have a tendency to remain diploid (46). BCCs usually occur on areas of the skin that have been exposed to the sun. It is most common on the face. They are characterized by an open sore that bleeds, oozes, or crusts and remains open for three or more weeks; a reddish patch; a shiny bump**,** or nodule, that is pearly or translucent and is often pink, red, or white; a scar-like area which is white, yellow or waxy, and often has poorly defined borders (47).

Squamous cell carcinoma: It is less frequent, SCCs may occur on all areas of the body including the mucous membranes, but are most common in areas exposed to the sun. They show a greater cornification, have a greater tendency to metastasize and they become aneuploid (48). An open sore that bleeds and crusts and persists for weeks; an elevated growth with a central depression that occasionally bleeds; a wart like growth that crusts and occasionally bleeds is the characterization for a SCC (47).

Actinic keratosis is also known as solar keratosis. Actinic keratosis is a type of flat, scaly growth on the skin. The growths may appear as rough red or brown patches on the skin. They may also appear as cracking or peeling of the lower lip that does not

heal. Without treatment, a small number of these scaly growths may turn into squamous cell cancer (47). If treated early, almost all AKs can be eliminated without becoming skin cancers. But untreated, about two to five percent may progress to squamous cell carcinoma (SCC). AK can be the first step in the development of skin cancer. It is thus a *precursor* of cancer or a *precancer* (45).

Figure 2.8. The non-melanoma skin cancers.

For basal cell or squamous cell cancers, a cure is highly likely if detected and treated early. Melanoma, even though it can spread to other body parts quickly, is also highly curable if detected early and treated properly. The 5-year relative survival rate for patients with melanoma is 92%. For localized melanoma, the 5-year survival rate is 98%; survival rates for regional and distant stage diseases are 64% and 16% respectively. About 83% of melanomas are diagnosed at a localized stage. The American Cancer Society estimates there will be about 10,710 deaths from skin cancer in 2006 – 7,910 from melanoma and 2,800 from other skin cancers (47).

2.8. The UV Spectrum

The sun emits radiation that ranges from X-ray to infrared (49). UV radiation is defined as the portion of electromagnetic spectrum which takes place between the visible light and X-Ray. There are three kind of Ultraviolet light (UV) that reaches the earth; UVA (315-400 nm), UVB (280-315 nm) and UVC (100-280 nm). As a result of resonance, in the cells, all nucleotide bases absorb UV light, and nucleic acids are characterized by a strong absorption at wavelengths near 260 nm (50).

Taking place in the lowest wavelength portion, UVC has the highest energy. It's directly absorbed by the DNA and is the most potent mutagen. But since UVC radiation is almost completely absorbed by the ozone layer, it does not affect the skin directly, thus it doesn't contribute to the formation of skin cancers *in vivo*. Because

of its ability to kill bacteria germicidal lamps are designed to emit UVC radiation. Among the three subtypes of UV light, UVA has the lowest energy. It's the most commonly encountered type of UV light. It's absorbed by cellular chromophores and also needed for the formation of vitamine D. Its excitation generates reactive oxygen species, which cause DNA strand breaks and chromosome translocations (49). UVB is the most destructive one because most of the UVB isn't absorbed by the ozone layer and it has enough energy to cause photochemical damage. It's in large part responsible for the formation of skin cancers.

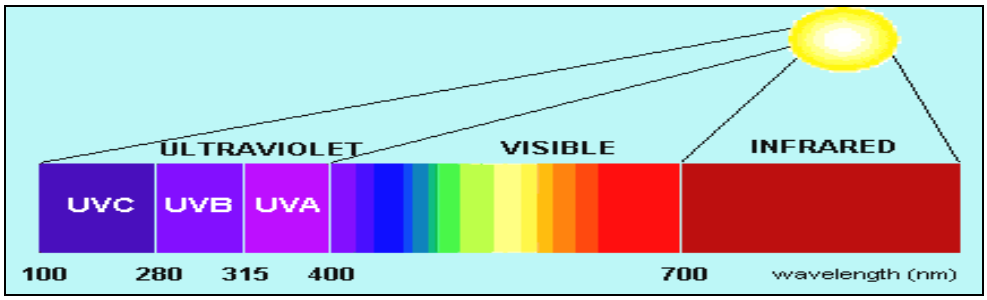

Figure 2.9. The light spectrum

2.9. UV Radiation and DNA Damage

The double bond in a pyrimidine base absorbs the ultraviolet light; it opens and becomes available to react with neighboring molecules. If this occurs between the two adjacent pyrimidine bases on the same DNA strand, the UV-modified base forms covalent bonds (Figure 2.10).

Two new structures, called pyrimidine dimers are formed between the neighboring bases: between the Carbon 5 and Carbon 6 of adjacent pyrimidine residues a cyclobutyl ring is formed and this new structure is named the "cyclobutane pyrimidine dimer (CPD)". When there's a formation of a CPD a bend or a kink is introduced into the DNA. The other reaction takes place between the Carbon 6 of one pyrimidine and the Carbon 4 of its neighbor. This structure is called "pyrimidine pyrimidone (6-4) photoproduct". (51). These reactions occur very frequently and they are very common; for every second that the cells are exposed to sun, 50 to 100 reactions occur continuously. Fortunately, most of these genetic lesions are corrected seconds after they are created, before they can do permanent damage.

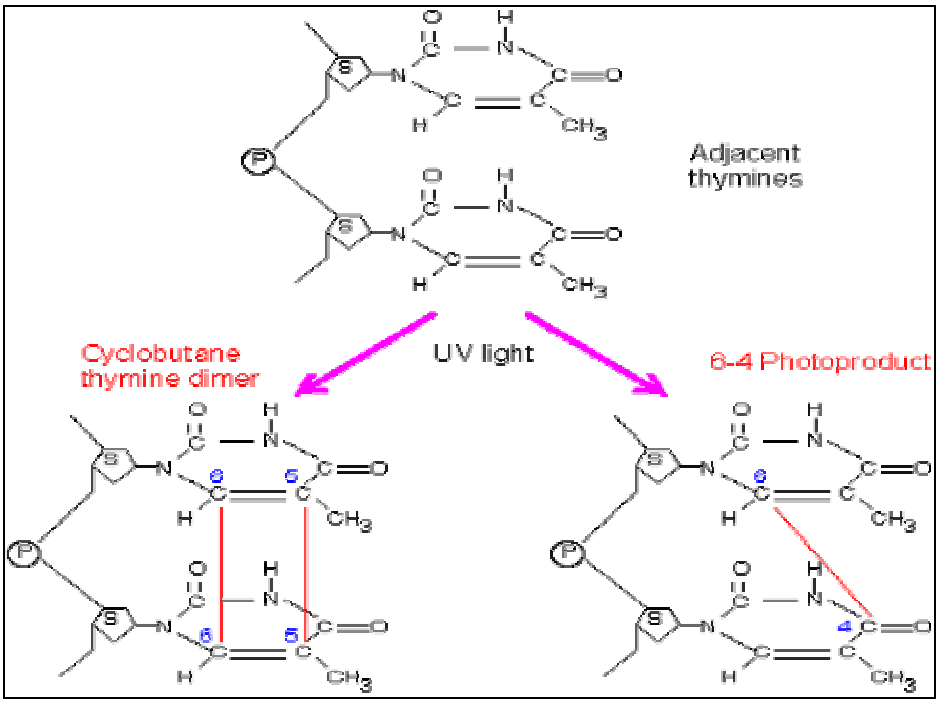

Figure 2.10. The Formation of thymine dimer residues.

To identify and remove the damage caused by UV from the DNA, cells use the nucleotide excision repair (NER). The following figure illustrates how the NER system repairs damaged DNA. Approximately thirty proteins are involved in this repair process. The enzymes of this mechanism were identified from patients with xeroderma pigmentosum (XP), a disease where patients develop skin cancers due to lack of NER-system enzymes. There are two different ways to detect and repair the damage; in transcription-coupled repair the proteins CSA, ERCC8, CSB and ERCC6 recognize the DNA lesion where transcription may be stalled. In global genomic repair, the XPC and hHR23 proteins recognize the lesions with a possible role for XPE. A complex including TFIIH is formed at the lesion and the two helicases XPB and XPD unwind the DNA in the neighborhood of the lesion. XPA may be required for recruitment of additional components to the repair complex. The endonucleases XPF/ERCC1 and XPG then cleave the damaged region. The gap is subsequently filled by DNA polymerases δ and ε nick is sealed by DNA ligase. Lastly, defects in bypass repair synthesis of UV damage are caused by DNA polymerase η and lead to the variant form of XP (50, 52). If the damage goes uncorrected, the genetic information may be permanently mutated (53).

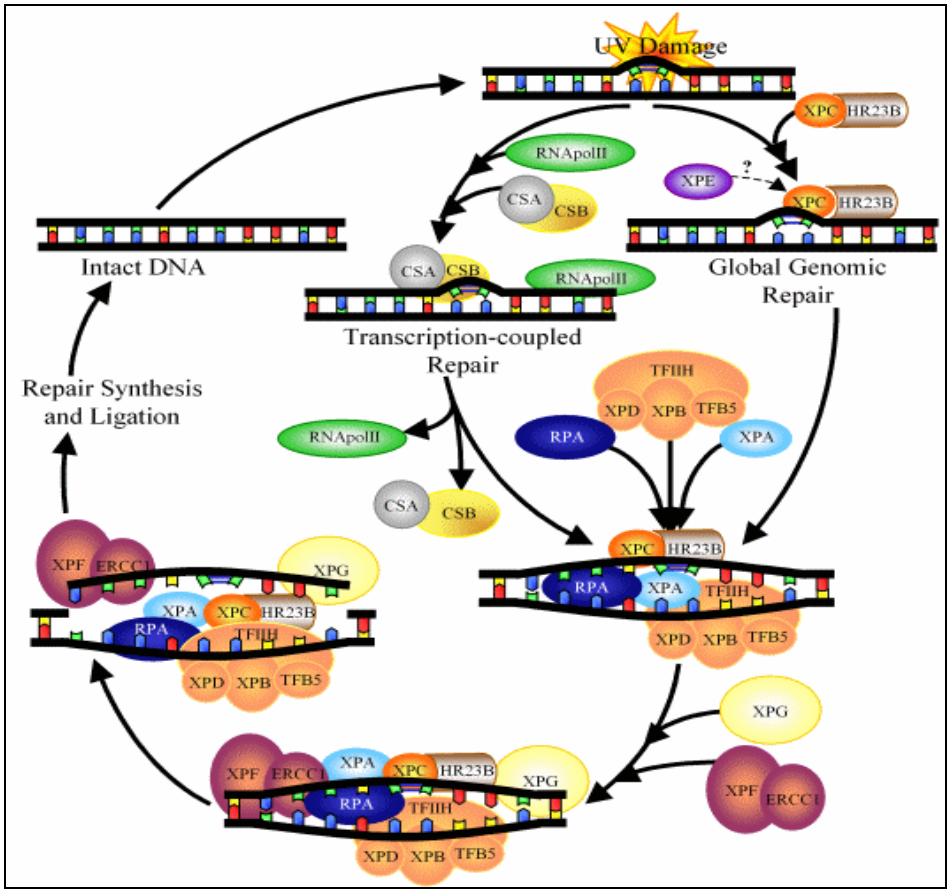

Figure 2.11.The Nucleotide Excision Repair System (55)

Many times, these dimers cause no problems because they are still read correctly. There are three mechanism that can explain why the signature mutation of UV damage is C to T transition; first of these explanation is based on the function of the polymerase which inserts an adenine opposite the abasic sites. Therefore on the opposite of a noncoding photoproduct the polymerase will place an adenine, which on the next replication will become a Thymine. Another explanation is that in fact the presence of the cyclobutane dimer leads to the insertion of an Adenine on the opposite strand. The third mechanism suggests that in the presence of a cyclobutane dimer the amino group of the Cytosine deaminates and becomes an Uracil. If this base change is not repaired by one of the DNA repair mechanisms the Uracil will code as a Thymine and result as a transition (54).

Because of these mutations, the connection between ultraviolet damage to DNA and cancer is quite clear. These CC to TT mutations often show up in the p53 tumor suppressor gene in skin cancers, compromising its watchdog function.

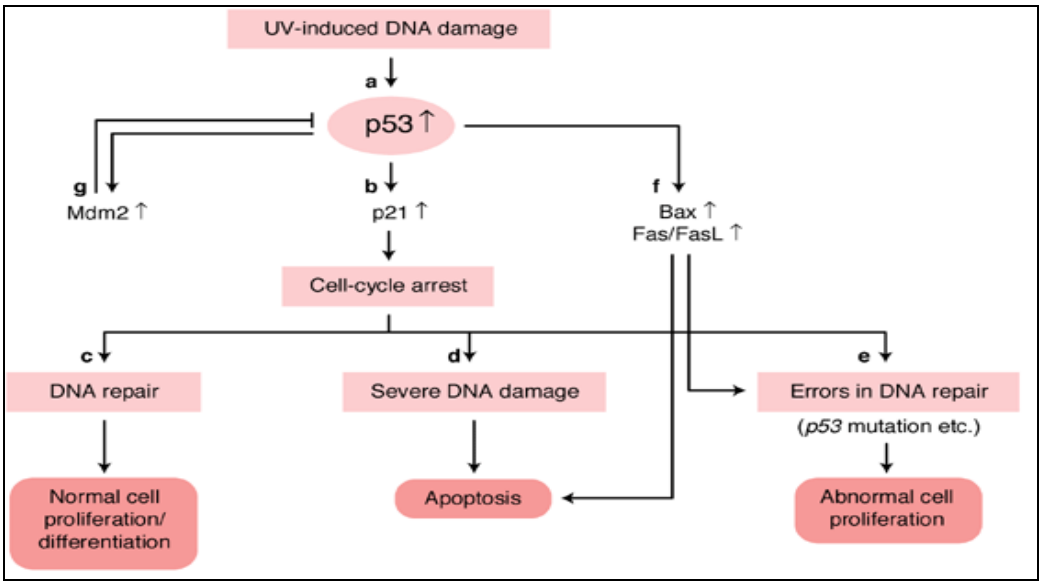

Figure 2.12.The role of p53 in cell-cycle arrest, DNA repair and apoptosis following UV irradiation (56)

Despite the ability of mammalian cells to repair UV-induced DNA damage, some damage will remain. Skin cells contain mechanisms to prevent such DNA damage from leading to skin carcinogenesis. (a) The accumulation of p53 protein after exposure to UV irradiation plays a central role in these mechanisms. (b) p53 induces p21, which inhibits formation of complexes required for the cell cycle and thereby leads to cell-cycle arrest. (c) Cell-cycle arrest can provide the cell with time to achieve successful DNA repair and the cell proliferates as normal. (d) If the DNA damage caused by UV irradiation is too severe and cannot be repaired, apoptotic pathways are activated to eliminate damaged cells. (e) If normal DNA repair is not achieved, for instance because of mutations in *p53*, the cell proliferates abnormally, which can lead to carcinogenesis. (f) As a transactivator of transcription, p53 can induce apoptosis by upregulating the expression of apoptosis-promoting (pro-apoptotic) genes such as *Bax, Fas/Apo-1,* death receptor 5 (*DR5*) or insulin-like growth factor-binding protein 3 (*IGF-BP3*), or by downregulating the expression of apoptosis-suppressing (anti-apoptotic) genes such as *Bcl-2,* cellular inhibitor of apoptosis protein 2 (*c-IAP2*) and neuronal apoptosis inhibitory protein 1 (*NAIP1*) (56). If apoptosis is not achieved, for instance because of mutations in *p53* or dysregulation of the *Fas–FasL* interactions, then this might also result in the

development of skin cancer. (g) The tumour suppressor activity of p53 is in turn inhibited by the Mdm2 protein, which targets p53 for rapid degradation. The gene encoding Mdm2 is itself activated by p53, thereby providing a negative autoregulatory loop (24).

2.10. MUTATIONS and P53

Mutation defines a permanent change that occurs in the nucleotide sequence of the DNA. The change may involve a few base pairs or a large scale chromosome abnormality. The small scale mutations may be the result of a base substitution, an insertion of a base or a deletion of the base. In the substitution mutations one or more nucleotide base is replaced by the same number of base. Based on the change of the nucleotide the mutation may be referred as transition or transversion. If as a result of the mutation a purine (Adenine and Guanine) is substituted by a purine, or a pyrimidine (Cytosine and Thymine) by a pyrimidine, the mutation is called a transition. If a purine becomes a pyrimidine (or a pyrimidine becomes a purine) then the substitution mutation is called a transversion. Based on the consequence of the nucleotide the mutations can be classified as silent, missense or nonsense mutation. A silent mutation occur when the base replaced codes for the same amino acid. For example the nucleotides TGT and TGC code for the the same amino acid, Cysteine. The transition from Thymine to Cysteine of the third nucleotide will reveal the same amino acid thus will be classified as a silent mutation. In missense mutations the resulting replacement of the nucleotide will code for a different codon. For example the replacement of the second Thymine in TGT (which codes for Cysteine) with a Guanine will result in Tryptophane. The nonsense mutations occur when the nucleotide substitution codes for a stop codon and truncates the protein. If the second Thymine in TGT becomes Adenine it reveals TGA which is a stop codon.

In deletion mutations one or more nucleotides are removed from the DNA. The deletions may alter the reading frame of the gene and cause frameshifts. The result is a non-functional protein and the mutation is irreversible. The well known example to this type of mutation is the deletion of the “ATAG” sequence from the APC gene.

In insertion mutations one or more nucleotides are added to the DNA. Like deletions, insertions cause frameshifts too. Huntington's Disease and Myotonic Distrophy are diseases caused by the insertion mutations. Insertion and deletion mutations are usually seen in the repetitive sequence of the gene (50).

When a gene that regulate the cell cycle is altered or fail to work, usually human cancers develop. These key genes in this process are tumor suppressors, oncogenes and DNA repair genes. The alteration on the DNA structure of these genes are the result of a spontaneous mutation or the invasion of a tumor virus.

The tumor suppressor genes's products proteins inhibit mitosis. When mutated, the mutant allele behaves as a recessive; that is, as long as the cell contains one normal allele, the tumor suppression continues. Oncogenes, by contrast, behave as dominants; one mutant, or overly-active, allele can predispose the cell to tumor formation (52).

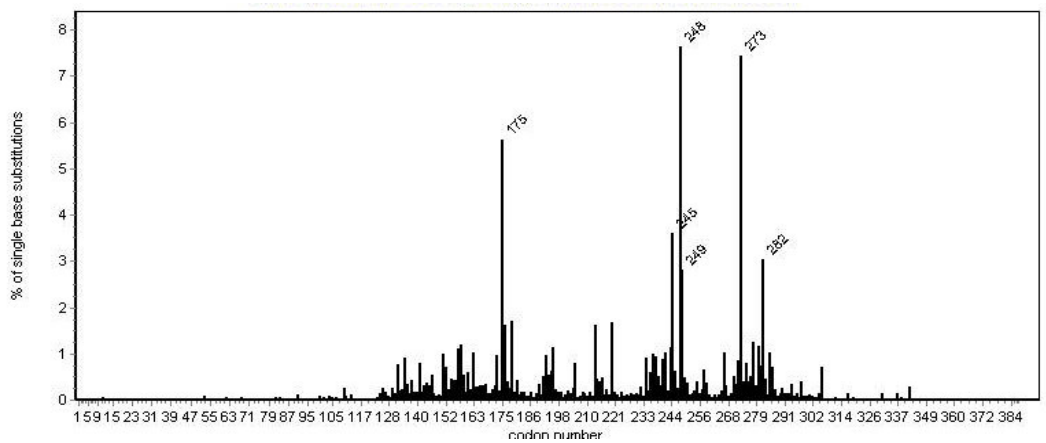

Figure 2.13 Codon distribution of the somatic mutations at single base substitution sites (59)

TP53 is the most frequently mutated gene in human cancer, with a predominance of missense mutations scattered over 200 codons (57). Up to now 23,544 somatic mutations and 376 germline mutations have been reported. From these somatic mutations 73.7 % are missense mutations, whereas 7.5 % are nonsense mutations. According to the mutation pattern 24.7 % of all these mutations are

transitions at CpG sites, 8.6 % are deletions and 2.9 % are insertion mutations (59). (Figure 2.13)

The P53 protein is inactivated as a result of the mutations which can lead to the absence of a protein (in 10 % of the cases) or usually in the expression of a mutant protein. The missense mutations may confer new properties to the mutated P53. The mutant p53 can inactivate wild type p53 and drive it to a mutant conformation. In that case the mutant p53 is considered to have a dominant negative (DN) effect. The same mechanism is also seen in prions and infectious proteins (26). In the case of the Gain-of-function the mutant p53 acquires new functions. This occurs in the presence of a second wt allele (59). Another property the mutant p53 can obtain is the Loss-of-function, where wt p53 loses its activity to transactivate its downstream genes (26).

Table 2.1 Table showing the p53 mutations and the cancer types (59)

CANCER TYPE	P53 MUTATIONS (%)
LUNG	70
STOMACH	45
BREAST	20
COLON	60
LİVER	20
PROSTATE	10-30
HEAD/NECK	60
EOSOPHAGUS	40
LEUKEMIA	10
LYMPHOMIA	30
OVARY	60
BLADDER	60
NON-MELANOMA SKIN	80

3. MATERIALS AND METHODS

3.1. Materials

pRcCMV-p53WT vectors, the transfection agent Lipofectamine 2000 were purchased from Invitrogen (San Diego, CA, USA). pEGFP-f was purchased from Clontech (USA). All the antibodies (Pab240 for p53, MDM2 D-12 for Mdm2, β-actin,) used in western blotting were ordered from SantaCruz Biotech (USA). Nucleotides were ordered from Yale W.M Keck Foundation Biotechnology Resource Laboratory (New Haven, CT, USA). QuickChange Site Directed Mutagenesis Kit, the restriction enzyme DpnI, *pfu* Turbo Polymerase, 5-bromo-4-chloro-3-indolyl β-D-galactopyranoside (X-Gal), Isopropyl-β-D-thiogalactopyranoside (IPTG), XL1-Blue Supercompetent Cells were purchased from Stratagene (LaJolla, CA, USA). Dimethylformamide (DMF), Betaine, Sodium Chloride (NaCl), Sodium Hydroxide (NaOH), Caseine hydrolysate (NZAmine), Collagenase type I, Bovine Serum Albumine (BSA), Trizma Base, Glycine, β-mercaptoethanol, Sodium Dodecyl Sulfate (SDS) were ordered from Sigma (St Louis, MO USA). The antibiotics Kanamycin and ampicilin were purchased from American Bioanalytics (USA). Tryptone, yeast extract, agar were ordered from DIFCO (USA). The restriction enzyme XbaI was ordered from New England Biolabs (Beverly, USA). The Qiaprep Spin Miniprep Kit, Endofree Plasmid Maxi Kit, QiaQuick Gel Extraction Kit were purchased from QIAGEN (Valenci, CA, USA). Betadine was ordered from Frederick Purdue Company (USA). Phosphate Buffer Saline (PBS), Dulbecco's Modified Eagle Medium (DMEM), Fetal Bovine Serum H.I. (FBS), OptiMEM 1X Medium, Trypsin-EDTA %25, the antibiotic Penicilamine/Streptomycin (Pen/Strep), the DNA 1 kb Ladder marker were ordered from GIBCO-BRL (CA, USA). Vybrant 6 Apoptosis Kit was ordered from Molecular Probes (Eugene, OR, USA). The Pierce NE-PER Nuclear&Cytoplasmic Extraction Reagent, BCA Protein Assay Kit, Supersignal Substrate were purchased from Pierce Biotechnology (Rockford, IL, USA).

Centrifuges Sorvall GLC-2B and Eppendorf 515D, the flow cytometer LSR-II from BD Biosciences, the Maxirotator from Labline, the western blotting transfer aparatus and the spectrophotometer Smartspec Plus from BioRad, the thermocycler from PerkinElmer were used.

3.2. Bioinformatics

15,000 tumors with TP53 mutations have been published leading to the description of more than 1,500 different TP53 mutants. The frequency of these mutants is highly heterogeneous with 11 hot spot mutants found more than 100 times, whereas 306 mutants have been reported only once (61). In order to decide which mutation will be used, a serie of bioinformatic software and processable p53 mutation data were analyzed. The p53 mutation data were provided from different groups; Ishioka's group (62) have created 2314 missense mutations by using site-directed mutagenesis and used a yeast-based functional assay to express and evaluate these p53 mutations. Therefore, by using this mutation analysis they were able to detect the transactivation activity of different p53 mutations on 8 downstream genes. Another data source was the TP53 mutation Database, published in International Agency for Research on Cancer (IARC)'s web site (59, 63) The Database is a Microsoft Access Application and provides information on p53 mutations effect, codon distribution, function pattern and analysis, tumor spectrum. Information on 21,587 somatic mutations reported in 1,876 original publications, 283 germline mutations reported in 129 publications (published between 1989 and December 2004) and functional information on more than 425 mutant proteins can be accessed using this database. The Database contains different types of datasets like Somatic dataset, Prevalence dataset, Prognosis dataset, Germline dataset, Mutation dataset, P53MUTfunction dataset and the Cell-lines dataset.

Cluster and TreeView are programs that provide a computational and graphical environment for analyzing data from DNA microarray experiments, or other genomic datasets. The program Cluster organizes and analyzes the data in a number of different ways. TreeView allows the organized data to be visualized and browsed.

All the linearized data concerning the SCC, BCC and AK mutations provided from Ishioka was uploaded in the Cluster and Treeview programs and the dendrogram was obtained.

3.3. Generation of the pEGFP-f-p53 Vector

In order to generate the pEGFP-f-p53 Vector, 2 other vectors were used. pRcCMVp53WT vector has a p53 cDNA insert of 1.8 kb. The insert was excised with the *Xba*I digestion enzyme and the p53 cDNA was obtained. The digestion product was loaded on a 2 % agarose gel and the p53 cDNA fragment was extracted from the gel using the QiaQuick Gel Extraction Kit. Similarly the pEGFP-f vector was digested with the same enzyme, and the p53 cDNA insert was ligated upstream of the EGFP promoter. The ligation was done with the T4 DNA ligase. The newly synthesized EGFP-p53 vector was cloned into the XL1-Blue Supercompetent cells and the blue clones were selected against Kanamycin resistance. The plasmid DNA was isolated and sequenced in order to see whether the p53 cDNA is placed in the right direction.

3.3.1. pRcCMVp53WT

The pRcCMVp53WT plasmid is 7344 bp kb long and has a fragment containing human wild-type p53 cDNA cloned into the polylinker of the eukaryotic expression vector pRcCMV. The dianostic digest of the plasmid with XbaI leads to the generation of 2 fragments of 1.85 kb and 5.5 kb long. (64). The plasmid has a neomycin resistance gene.

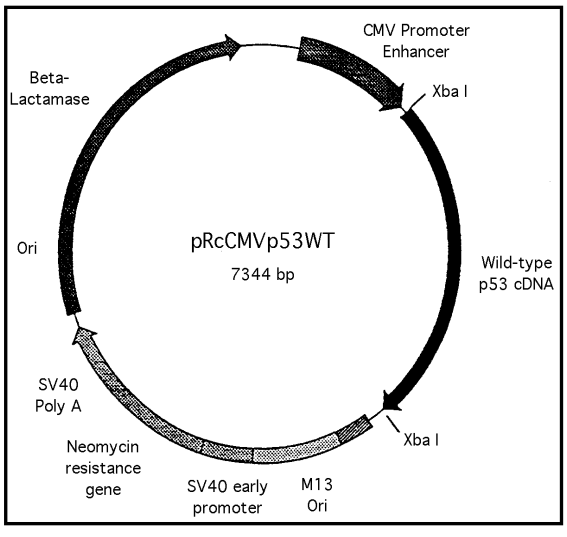

Figure 3.1. The PRcCMVp53WT vector.

3.3.2. pEGFP-f

EGFP-F encodes the farnesylated enhanced green fluorescence protein, a modified form of EGFP that remains bound to the plasma membrane in both living and fixed cells. The vector contains the 20-amino-acid farnesylation signal from c-Ha-Ras fused to the terminus of EGFP. This farnesylation signal directs EGFP to the inner face of the plasma membrane. This vector was designed for use as a cotransfection marker and because it remains attached to the plasma membrane it cen be detected by fluorescence microscopy in permeabilized cells after ethanol fixation. Suitable host strains for propagation in *E.coli* are DH5α, HB101, JM109 or XL-1 Blue. The plasmid confers resistance to Kanamycin (30 μg/ml) to *E.coli* hosts.

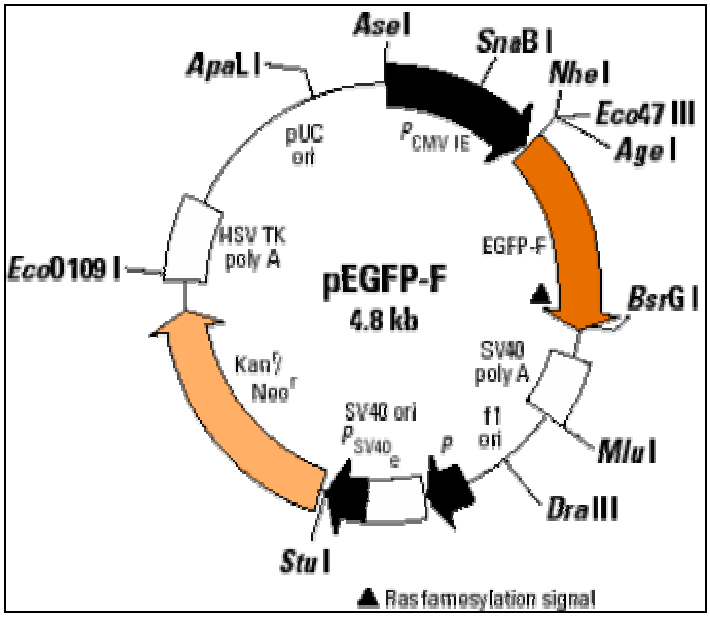

Figure 3.2. The EGFP expression vector.

(1401).CTCCTGAGGATCCAGATCTCGAGCTCAAGCTTCGAATTCTGCAGTCGACG

SauI HindIII

GTACCGCGGGCCCGGGATCCACCGGATCTAGATAACTGATCATAATCA…(1500)

XmaI XbaI

3.3.3. Human p53 cDNA Sequence

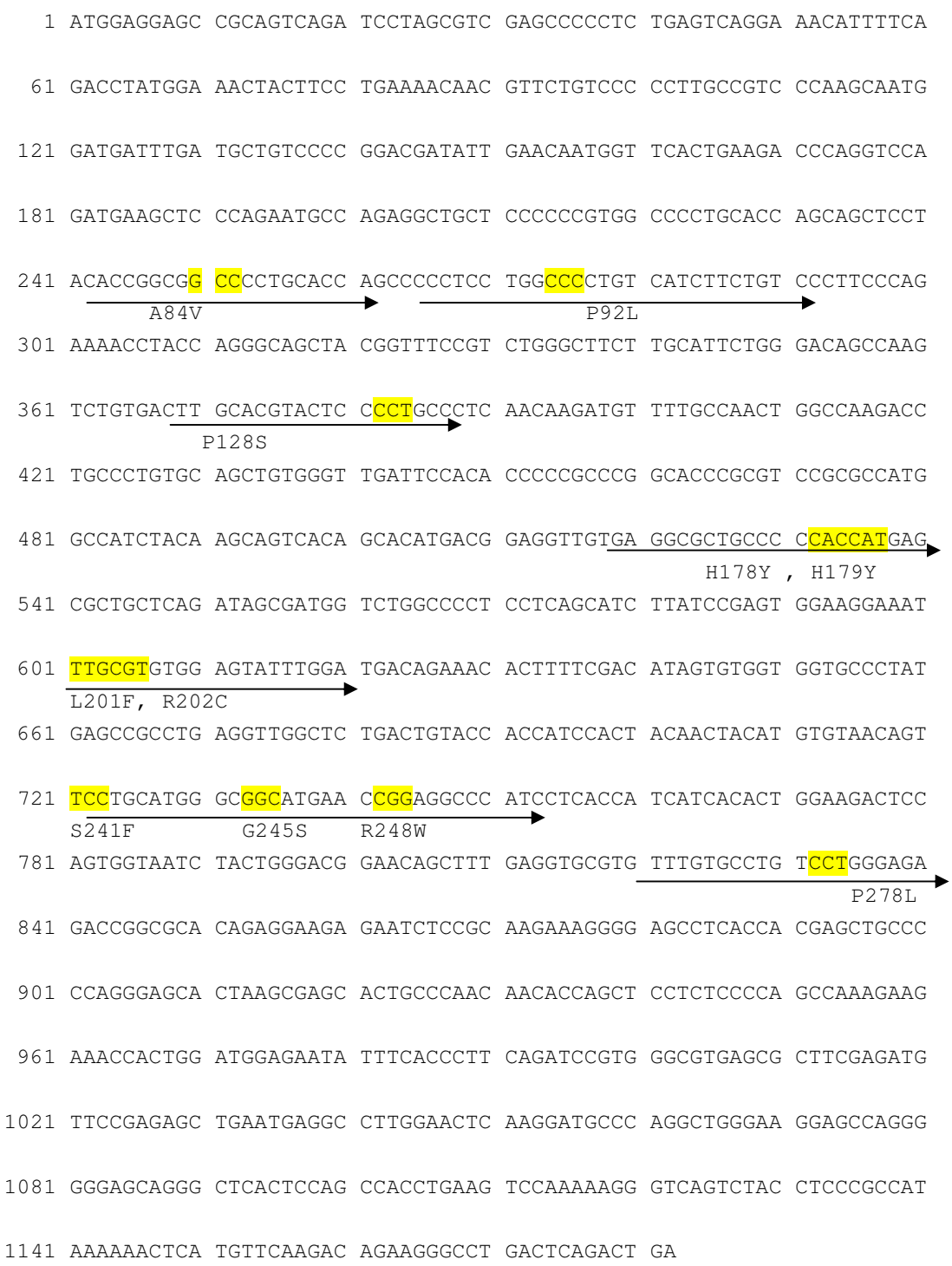

3.3.4. Digestion With The Restriction Enzyme

The Recognition site for the *Xba*I restriction enzyme is as follows:

A 50 µl reaction containing 1 µg of DNA and 20 units of *Xba*I and 47 µl NEB Buffer (10 mM Tris-HCl, 50 mM NaCl, 10 mM $MgCl_2$, 1 mM Dithiothreitol, pH 7.9) was incubated for 16 hours at 37ºC.

3.3.5. DNA Isolation From Gel

(QiaQuick Gel Extraction Kit, Cat.No 27804)

This protocol is designed to extract and purify DNA of 70 bp to 10 kb from standard or low-melt agarose gels in TAE or TBE buffer. Up to 400 mg agarose can be processed per spin column.

1. The DNA fragment was excised from the agarose gel by the help of a scapel. By removing the extra agarose, the size of the gel was minimized as much as possible.
2. The gel slice was weighed in a colorless tube, and 3 volumes of Buffer QG was added to 1 volume of gel (100 mg ~ 100 µl).
3. The mixture was incubated until the gel slice has completely dissolved, at 50°C for 10 minutes. During the incubation to help dissolve gel the mixture was vortexed every 2–3 minutes.
4. After the gel slice has dissolved completely, the color of the mixture was checked if it was yellow. is yellow. Buffer QG contains a pH indicator which is yellow at pH ≤7.5 and orange or violet at higher pH, allowing easy determination of the optimal pH for DNA binding. The adsorption of DNA to the QIAquick membrane is efficient only at pH ≤7.5.
5. 1 gel volume of isopropanol was added to the sample and mixed.
6. A QIAquick spin column was placed in a clean 2 ml collection tube
7. To bind DNA, the sample was applied to the QIAquick column.
8. The flow-through was discarded and placed in the QIAquick column back, in the same collection tube.

9. 0.5 ml of Buffer QG was added to QIAquick column and centrifuged for 1 minute at 13,000 rpm (~17,900 x *g*). This optional step will remove all traces of agarose and is only required when the DNA will subsequently be used for direct sequencing, in vitro transcription or microinjection.
10. To wash, 0.75 ml of Buffer PE was added to the QIAquick column and centrifuged for 1 minute at 13,000 rpm (~17,900 x *g*).
11. The flow-through was discarded and the QIAquick column was centrifuged for an additional 1 minute at 13,000 rpm (~17,900 x *g*).
12. The QIAquick column was placed into a clean 1.5 ml microcentrifuge tube.
13. To elute DNA, 50 µl of Buffer EB (10 mM Tris·Cl, pH 8.5) or H2O was added on the center of the column and the clooumn was let to stand for 1 minute, and then centrifuged for 1 min at 13,000 rpm (~17,900 x *g*).

3.3.6. Ligation Reaction

The 1.8 kb DNA fragment excised from the agarose gel containing the p53 cDNA was ligated into the 4.8 kb fusion vector pEGFP-f using T4 DNA Ligase. The T4 DNA ligase catalyzes the formation of phosphodiester bonds between adjacent 5'-phosphate of DNA fragment containing the p53 cDNA and 3'-hydroxyl residue of pEGFP-f.

A ligation mixture containing 5 µl p53 cDNA, 5 µl pEGFP-f, 10 µl distilled water was added to a tube of Ready-To-Go-T4 DNA Ligase (1.2 U bacteriophage T4 DNA ligase) incubated for 2 hours at 16 °C. 1 µl of the resulting plasmids was transformed into XL1 Blue Supercompetent cells to repair single-strand nicks.

3.4. Bacterial Transformation

Bacterial transformation is the process by which bacterial cells take up naked DNA or plasmids. Bacteria which are able to uptake DNA are called "competent" and are made so by treatment with calcium chloride in the early log phase of growth. The competent bacteria will take up DNA following a heat shock step. DNA molecules, plasmids, which are introduced by this method, will then be replicated in the bacterial host cells. To aid the bacterial cells' recovery, the cells are incubated briefly with non-selective growth medium following the heat shock treatment. When the transformation is coupled with antibiotic selection techniques, bacteria can be induced to uptake certain DNA molecules, and those bacteria can be selected for that incorporation.

3.5. Site-Directed Mutagenesis

11 Mutations were created using Stratagene's QuikChange Site Directed Mutagenesis Kit. The primers were designed according to the following properties; both of the mutagenic primers contained the desired mutation and they anneal to the same sequence on opposite strands of the plasmid. The primers were between 25 and 45 bases in length, with a melting temperature (*T*m) of =78°C (± 5° C). The desired mutation takes place in the middle of the primer with approximately 10–15 bases of correct sequence on both sides. The primers optimally should have a minimum GC content of 40% and should terminate in one or more C or G bases. The primers need not be 5´phosphorylated but must be purified either by fast polynucleotide liquid chromatography (FPLC) or by polyacrylamide gel electrophoresis (PAGE). Otherwise, failure to purify the primers results in a significant decrease in mutation efficiency.

The mutations A84V, P92L, P128S, R201C, R202C, H178Y, H179Y, S241F, G245S, R248W, and P278L were created using the template pEGFP-WTp53. The sequence of the designed forward and reverse primers is shown below; (The underline highlights the codon subject to mutation. The lowercase letter shows the base to be mutated. The percent of the GC base content, the base number and the Tm temperature were also indicated)

A84V FORWARD

5’-CTACACCGGCGGtCCCTGCACCAGC-3’

A84V REVERSE

5’-GCTGGTGCAGGGaCCGCCGGTGTAG-3’

GC = 69 %, Tm = 80, 25 base pairs

P92L FORWARD

5’-CCCCCTCCTGGCtCCTGTCATCTTCTG-3’

P92L REVERSE

5’-CAGAAGATGACAGGaGCCAGGAGGGGG-3’

GC = 63 %, Tm = 78.6, 27 base pairs

P128S FORWARD

5’-CTTGCACGTACTCCtCTGCCCTCAAC-3’

P128S REVERSE

5’ –GTTGAGGGCAGaGGAGTACGTGCAAG-3’

GC = 57.7 %, Tm = 75.3, 26 base pairs

H178Y FORWARD

5’ –GAGGCGCTGCCCCtACCATGAGCGCTG-3’

H178Y REVERSE

5’ –CAGCGCTCATGGTaGGGGCAGCGCGAG-3’

GC = 70.3 %, Tm = 81.6, 27 base pairs

H179Y FORWARD

5’ –CGCTGCCCCCACtATGAGCGCTGCTC-3’

H179Y REVERSE

5’ –GAGCAGCGCTCATaGTGGGGGCAGCG-3’

GC = 69.2 %, Tm = 80.1, 26 base pairs

L201F FORWARD

5’ –GAGTGGAAGGAAATTTtCGTGTGGAGTATTTGG-3’

L201F REVERSE

5’ –CCAAATACTCCACACGaAAATTTCCTTCCACTC-3’

GC = 42.4 %, Tm = 75.4, 33 base pairs

R202C FORWARD

5’ –GTGGAAGGAAATTTGtGTGTGGAGTATTTG-3’

R202C REVERSE

5’ –CAAATACTCCACACaCAAATTTCCTTCCAC-3’

GC = 40 %, Tm = 75, 30 base pairs

S241F FORWARD

5’ –CTACATGTGTAACAGTTtCTGCATGGGCGGCATG-3’

S241F REVERSE

5’ –CATGCCGCCCATGCAGaAACTGTTACACATGTAG-3’

GC = 50 %, Tm = 77, 34 base pairs

G245S FORWARD

5’ –CCTGCATGGGCaGCATGAACCGGAG-3’

G245S REVERSE

5’ –CTCCGGTTCATGCtGCCCATGCAGG-3’

GC = 65.3 %, Tm = 80, 25 base pairs

R248W FORWARD

5’ –GCGGCATGAACtGGAGGCCCATCCTC-3’

R248W REVERSE

5’ –GAGGATGGGCCTCCaGTTCATGCCGC-3’

GC = 65.3 %, Tm = 80, 26 base pairs

P278L FORWARD

5’ –GTTTGTGCCTGTCtTGGGAGAGACCGGCG-3’

P278L REVERSE

5’ –CGCCGGTCTCTCCCAaGACAGGCACAAAC-3’

GC = 62 %, Tm = 77, 29 base pairs

3.5.1. Mutant Strand Synthesis Reaction

In order to create the mutant strand, the following reaction mixture was prepared in a final volume of 50 µl and then subjected to PCR:

Table 3.1 The PCR reaction for site directed mutagenesis

Reagent	Volume(µl)	Concentration	Final Concentration
PCR reaction buffer	5	10 X	1 X
pEGFP-WTp53 template plasmid	2	5 ng/µl	10 ng
forward primer	1.25	100 ng/µl	125 ng
reverse primer	1.25	100 ng/µl	125 ng
dNTP mix	1	10 mM/each	200 uM
PfuTurbo DNA polymerase	1	2.5 U/µl	2.5 U
double-distilled water	39.5	-	-

The 10 X PCR Reaction Buffer contains: 100 mM KCl, 100 mM(NH4)2SO4, 200 mM Tris-HCl (pH 8.8), 20 mM MgSO4, 1% Triton X-100, 1 mg/ml nuclease-free BSA.

The cycling parameters for the QuikChange Site-Directed Mutagenesis method is as followed;

Cycle 1 ……..95°C 3 minutes……1 times

Cycle 2 ……..95°C 30 seconds

55°C 1 minute

68°C 1 minute/kb of plasmid length (8 minutes)

Cycle 2 was repeated 16 times and the reactions were placed on ice for 2 minutes.

3.5.2. *Dpn*I digestion of the products

1 µl of the *Dpn* I restriction enzyme (10 U/µl) is added directly to each amplification reaction. Each reaction is mixed gently and thoroughly by pipetting the solution up and down several times. the reaction mixtures were spun down in a microcentrifuge for 1 minute and immediately each reaction were incubated at 37°C for 1 hour to digest the parental (the nonmutated) supercoiled dsDNA.

3.5.3. Transformation of XL1-Blue Supercompetent Cells

1. The XL1-Blue supercompetent cells were gently thawed on ice. For each control and sample reaction to be transformed, 50 µl of the supercompetent cells was aliquoted to a *prechilled* 14 ml BD Falcon polypropylene round-bottom tube.
2. 1 µl of the *Dpn* I-treated DNA from each control and sample reaction was transferred to separate aliquots of the supercompetent cells.
3. The transformation reactions were swirled gently to mix and the reactions were incubated on ice for 30 minutes.
4. The transformation reactions were heated for 45 seconds at 42°C and then placed on ice for 2 minutes.
5. 0.5 ml of NZY+ broth (10 g NZ amine, 5 g of yeast extract, 5 g of NaCl were added to deionized H_2O to a final volume of 1 liter. The pH was adjusted to 7.4 using NaOH. The mixture was autoclaved and prior to use 12.5 ml of 1 M $MgCl_2$, 12.5 ml 1 M $MgSO_4$ and 20 ml of 20% (w/v) glucose were filtered added to the mixture) preheated to 42°C was added to the transformation reactions and the mixture was incubated at 37°C for 1 hour with shaking at 225–250 rpm.
6. 10 µl of each transformation reaction is plated on agar plates containing 80 µg/ml X-gal, 20 mM IPTG and 30 µg/ml kanamycin.
7. The transformation plates were incubated at 37°C for >16 hours. The expected colony number is between 10 and 1000 colonies, depending upon the base composition and length of the DNA template employed. The insert of interest is sequenced to verify that selected clones contain the desired mutation.

To prepare the LB agar plates 10 g of NaCl, 10 g of tryptone, 5 g of yeast extract, 20 g of agar were added to deionized H_2O to a final volume of 1 liter. The pH was adjusted to 7.0 with 5 N NaOH. The mixture was autoclaved and poured into petri dishes (~25 ml/100-mm plate). To obtain the LB–Kanamycin Agar after cooling the 1 liter mixture to 55°C, 10 ml of 30 mg/ml filter-sterilized Kanamycin was poured into petri dishes (~25 ml/100-mm plate)

For blue–white color screening, 2% of X-gal 5-bromo-4-chloro-3-inodyl-α-D-galactopyranoside (X-gal) in dimethylformamide (DMF), 100 µl of 10 mM isopropyl-1-thio-α-D-galactopyranoside (IPTG) were added on agar plates 30 minutes prior to plating the transformations.

3.6. DNA Isolation From Plasmid

For the isolation of plasmid DNA, and the confirmation of the mutagenesis by sequencing, a number of independently transformed bacterial colonies were picked randomly and their plasmid DNA were purified using QIAPREP Spin MiniPrep and Endofree Pasmid Maxi Kits, according to the manufacturer's manual (QIAGEN, Valencia CA). QIAGEN plasmid purification systems uses an unique anionexchange resin developed exclusively for the purification of nucleic acids. Plasmid purification on QIAGEN resin is based on the interaction between negatively charged phosphates of the DNA backbone and the positively charged DEAE groups on the surface of the resin. The salt concentration and pH conditions of the buffers used determine whether DNA is bound or eluted from the column. QIAGEN plasmid purification protocols are based on the alkaline lysis procedure, followed by the binding of plasmid DNA to Anion-exchange resin under appropriate low salt and pH conditions.

3.6.1. DNA Isolation Using Qiagen Miniprep

(QIAprep Spin Miniprep Kit, Cat.No 27104)

1. A single bacterial blue colony from LB-agar plate was picked and transferred into 5 ml LB medium containing ampicilin (0.1 mg/ml) and the culture was incubated overnight at 37 C in a shaking incubator at 250 rpm.

2. The saturated overnight culture was centrifuged at 10,000 x g for 5 minutes. The supernatant was discarded.
3. The cell pellet was resuspended in 250 ul of Cell Resuspension Solution (50 mM Tris-HCl (pH 7.5), 10 mM EDTA, 100 ug/ml RNAse A) by pipetting up and down.
4. From the Cell Lysis Solution (0.2 M NaOH, 1% SDS) 250 ul was added and incubated at room temperature for 5 minutes.
5. After the incubation 350 ul of the Neutralization Solution (1.32 M potassium acetate, pH 4.8) was added, mixed immediately, inverted vigorously 4-6 times and centrifuged at 10,000 x g for 15 minutes.
6. Tthe supernatant was applied to a QIAPrep column by pipetting and centrifuged for 1 minute at 10,000 x g. the flow-through was discarded.
7. The QIAPrep column was washed with 750 ul of Column Wash Solution (80 mM potassium acetate, 8.3 mM Tris-HCl (pH 7.5), 40 uM EDTA and 55 % ethanol) and centrifuged for 1 minute at 10,000 x g.
8. The flow-through was discarded and the column was recentrifuged at 10,000 x g for 2 minutes to get rid of the residual column wash.
9. The QIAPrep column was placed in a clean 1.5 ml eppendorf, 50 ul of TE Buffer (10 mM Tris-HCl pH 8.0, 1 mM EDTA) was applied to the column and waited for 1 minute. The tube was the centrifuged for 1 minute at 10,000 x g and the column was discarded.

The colonies containing the mutated plasmid were identified by sequencing.

3.6.2. DNA Isolation Using Qiagen Maxiprep

(EndoFree Plasmid Maxi Kit, Cat. No. 12362)

Plasmids and cosmids up to 50 kb in size can be purified using EndoFree Plasmid Kits. This protocol is designed for purification of up to 500 µg endotoxin-free plasmid DNA using the EndoFree Plasmid Maxi Kit. Endotoxin-free DNA improves transfection into sensitive eukaryotic cells and is essential for gene therapy research.

1. A single colony from the selective plate was picked and inoculated in 4 ml LB medium containing ampicilin (0.1 mg/ml) and incubated at 37 C for 8 hours in a shaking incubator. After 8 hours 3 ml saturated bacterial culture

was added into 1 liter LB/ampicilin culture and the cells were grown overnight at 37 C in a shaking incubator at 250 rpm.

2. The bacterial cells were harvested by centrigation at 6000 x g for 20 minutes at 4 C.
3. The bacterial pellet was resuspended in 10 ml of Cell Resuspension Solution (50 mM Tris-HCl (pH 7.5), 10 mM EDTA, 100 ug/ml RNAse A) by pipetting up and down.
4. 12.5 ml of Cell Lysis Solution (0.2 M NaOH, 1% SDS) was added and incubated at room temperature for 5 minutes.
5. After the incubation 10 ml of the chilled Neutralization Solution (1.32 M potassium acetate, pH 4.8) was added, mixed immediately, inverted vigorously 4-6 times and centrifuged at 10,000 x g for 15 minutes.
6. The lysate was poured into the barrel of a QIAFilter cartridge and incubated at room temperature for 10 minutes.
7. The cap from the QIAFilter Cartridge outlet nozzle was removed. The plunger was inserted gently QIAFilter Maxi Cartridge and the cell lysate was filtered to a 50 ml tube.
8. 2.5 ml Buffer ER was added to the filtered lysate. The tube was mixed by inverting 10 times and incubated for 30 minutes on ice.
9. A QIAGEN-tip 500 was equilibrated by applying 10 ml Equilibration Buffer (750 mM NaCl, 50 mM MOPS pH 7.0, 15 % isopropanol, 0.15 % Triton X-100) and the column was allowed to empty with gravity flow.
10. The filtered lysate was applied to the equilibrated QIAGEN-tip
11. The QIAGEN-tip was washed 2 times with Wash buffer (1.0 M NaCl, 50 mM MOPS, pH 7.0, 15 % isopropanol)
12. The DNA was eluted with 15 ml of Elution Buffer (1.25 M NaCl, 50 mM Tris-HCl pH 8.5, 15 % isopropanol).
13. 0.7 volumes (10.5 ml) of room temperature isopropanol was added to the eluted DNA and mixed by inversion. The samples were centrifuged immediately at 16,000 x g at 4 C for 30 minutes. The supernatant was discarded.

14. The DNA pelet was washed with 5 ml 70 % ethanol and centrifuged at 16,000 x g at 4 C for 15 minutes. The supernatant was discarded and the pellet was allowed to air dry.
15. The DNA was resuspended in 1.5 ml TE Buffer (10 mM Tris-HCl pH 8.0, 1 mM EDTA).

3.7. Sequencing the Mutated Plasmid

One Blue colonie was selected and the DNA was isolated using QIAPREP Spin MiniPrep according to the manufacturer's manual. A reaction of 500 ng Plasmid DNA, 2µl of 4 mM sequencing primers (forward and reverse separately) were mixed and the final volume was completed to 18 µl with ddH_2O, then sent to W.M. Keck Foundation Biotechnology Research Laboratory at Yale University. The results were read using the sequencing program Chromas.

The primers used to amplify the p53 gene for sequencing were designed as below. Sequencing primer-1 amplifies a region of 460 bp long (between 51-510) and Sequencing primer-2 amplifies a region of 600 bp long (between 301-900).

SEQUENCING PRIMER -1 FORWARD

5' –TGAGTCAGGAAACATTTTCA -3'

35 % GC, Tm = 48°C

SEQUENCING PRIMER – 1 REVERSE

5' –CGTCATGTGCTGTGACTGCT -3'

55 % GC, Tm = 58.7°C

SEQUENCING PRIMER – 2 FORWARD

5' –TCTGTGACTTGCACGTACTC -3'

50% GC, Tm = 54 °C

SEQUENCING PRIMER – 2 REVERSE

5' –GGGCAGCTCGTGGTGAGGCT-3'

55% GC, Tm = 58.7°C

3.8. Cell Culture

Holes were poked in a bed of crushed ice as to be one newborn mouse per hole. The newborns were put on the fingers of a latex glove, one newborn per fingertip. The enclosed newborns were put on ice holes. Newborn mice are anesthetized in ice (more than 30 minutes). Subsequently, they were rinsed in Betadine, 3 times in 70% ethanol and then the skin was removed. Skins were rinsed in PBS without calcium or magnesium, with 1% antibiotic/antimycotic. Flattened skins with dermal side down were placed in Petri dishes with 10ml of 0.25% Trypsin-EDTA and incubated at 4ºC over night.

Primary Murine Fibroblasts dermis were separated from epidermis by forceps pulling the layers apart, and placed in a Petri dish containing 5ml collagenase type I (0.35% wt/vol) and thereafter minced by scissors into small pieces. The solution was transferred to 20 ml collagenase and stirred at 37ºC for 45 minutes. The solution was filtered through a cell strainer and centrifuged at 500g for 5 minutes in a Sorvall GLC-2B centrifuge. The cells were resuspended in DMEM high glucose with 10% fetal bovine serum and 1% penicillin/streptomycin. The suspension wais then placed in a large flask (1 mouse per 150 cm^2 flask) and grown at 37ºC, 5% CO_2 until it reached 60-80% confluency.

3.9. Counting the Cells

A device used for determining the number of cells per unit volume of a suspension is called a counting chamber. The most widely used type of chamber is called a hemocytometer, since it was originally designed for performing blood cell counts.

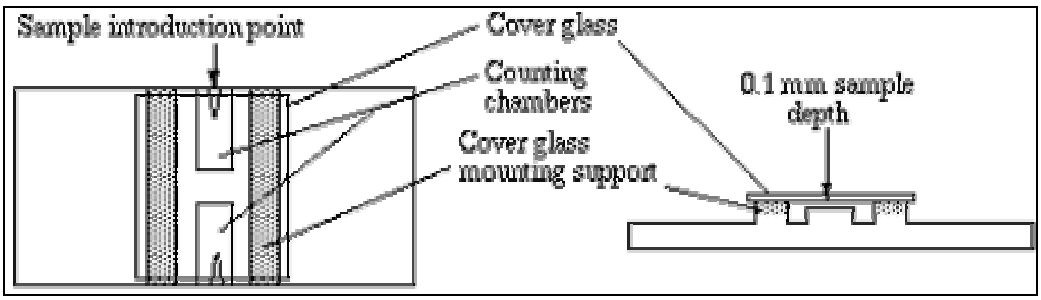

Figure 3.3. The picture of a hemocytometer

To prepare the counting chamber the mirror-like polished surface is carefully cleaned with lens paper. The coverslip is also cleaned. Coverslips for counting chambers are specially made and are thicker than those for conventional microscopy, since they must be heavy enough to overcome the surface tension of a drop of liquid. The coverslip is placed over the counting surface prior to putting on the cell suspension. The suspension is introduced into one of the V-shaped wells with a pasteur or other type of pipet. The area under the coverslip fills by capillary action. Enough liquid should be introduced so that the mirrored surface is just covered. The charged counting chamber is then placed on the microscope stage and the counting grid is brought into focus at low power. One entire grid on standard hemacytometers with Neubauer rulings can be seen at 40x (4x objective). The main divisions separate the grid into 9 large squares (like a tic-tac-toe grid). Each square has a surface area of one square mm, and the depth of the chamber is 0.1 mm. Thus the entire counting grid lies under a volume of 0.9 mm-cubed.Cell suspensions should be dilute enough so that the cells do not overlap each other on the grid, and should be uniformly distributed. To perform the count, determine the magnification needed to recognize the desired cell type. Systematically the cells are counted in selected squares so that the total count is 100 cells.

To determine a cell count using a standard hemocytometer; To get the final count in cells/ml, first divide the total count by 0.1 (chamber depth) then divide the result by the total surface area counted. For example suppose you counted 125 cells (total) in the four large corner squares plus the middle combined. Divide 125 by 0.1, then divide the result by 5 mm-squared, which is the total area counted (each large square is 1 mm-squared). You shoud get 125/ 0.1 = 1250. 1250/5 = 250 cells/mm-cubed. There are 1000 mm-cubed per ml, so you calculate 250,000 cells/ml. Sometimes you will need to dilute a cell suspension to get the cell density low enough for counting. In that case you will need to multiply your final count by the dilution factor. For example, suppose that for counting we had to dilute a suspension of Chlamydomonas 10 fold. Suppose we obtained a final count of 250,000 cells/ml as above. Then the count in the original (undiluted) suspension is 10 x 250,000 which is 2,500,000 cells/ml.

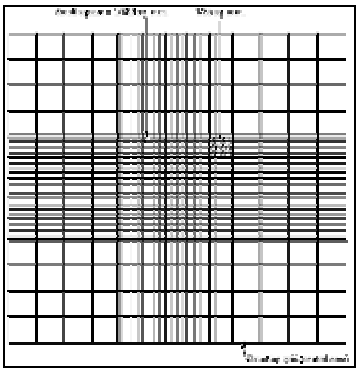

Figure 3.4. The detailed schematic representation of a hemocytometer grid

3.10. Vector Transfection

16 hours before the transfection, the cells were plated in antibiotic-free DMEM media at 60% confluency (350000 cells per 60 mm plate). The cells used in transfection experiments were no older than 5th passage. On the day of transfection, the cells were washed three times with 1X PBS and the media of the cells was replaced with DMEM high glucose at room temperature. 3 μg of DNA and Lipofectamine 2000 at a ratio of 1:3 (vol:vol) were diluted separately in 500 ul OptiMEM. After 10 minute of incubation, the DNA-OptiMEM mixture was added dropwise to the Lipofectamine-OptiMEM mixture. The samples were incubated at 37°C for 20 minutes. At the end of the incubation the DNA/Lipofectamine mixture was added to the cells, and then gently swirled around to distribute the solution thoroughly. The plates were placed in the incubator at 37°C for 4 hours. Following the incubation, the cells were washed one time with 1X PBS and the media was replaced with DMEM high glucose containing 1% Pen/Strep and 10% FBS H.I. The next day the media was replaced with fresh regular media with antibiotics. The vector is expressed 48 hours post-transfection.

3.11. UV Radiation

20 hours before collecting the samples for the annexin assay the cells were washed twice with 1X PBS and 2 ml of 1X PBS (enough to cover the cells) was added before radiation. The cells were exposed to UVB from 3 broadband FS20T12-UVB lamps filtered through a Kodacel filter (Eastman Kodak, Rochester, NY) to remove wavelengths below 290 nm. The lamp output was 250-420 nm with peak

emission at 313 nm, and after filtering contained 72.6% UVB, 27.4% UVA, and 0.01% UVC as measured by an IL1700/790 spectroradiometer with double monochromator (International Light, Inc., Newburyport, MA). The dose rate was 2.2 J/m2/sec.The cells were covered by an UVB filter so that the final lamp output was >99% UVB. After the radiation, 1X PBS was replaced with regular DMEM containing FBS and Pen/Strep antibiotic. The UVB output of the lamp was measured prior to each session by a UVX meter (UV Products, Upland, CA).

3.12. Annexin Assay

In normal viable cells, phosphatidylserine (PS) is located on the cytoplasmic surface of the cell membrane. However, in apoptotic cells, PS is translocated from the inner to the outer leaflet of the plasma membrane, thus exposing PS to the external cellular environment. The human vascular anticoagulant, annexin V, is a 35–36 kD Ca2+-dependent phospholipidbinding protein that has a high affinity for PS. Annexin V labeled with a fluorophore or biotin can identify apoptotic cells by binding to PS exposed on the outer leaflet. Vybrant 6 apoptosis kit was used to perform the Annexin Assay. Apoptosis was induced in the cells by irradiating them with UVB 20 hours prior the experiment. The positive and negative control samples were included for each set of experiment. The media containing floating cells was also collected. The cells were washed with 1X PBS and trypsinized. The cells were collected in a 15 ml polypropylene Falcon tube and centrifuged at 900 x g using a Sorvall GLC-2B centrifuge. The pellet was washed with ice cold 1X PBS and centrifuged again. The supernatant was discarded and the pellet was resuspended in 100 ul of 1X Annexin-Binding Buffer buffer and transferred to a 1.5 ml Eppendorf tube. 5ul of Biotin-Annexin V complex was added, and incubated at room temperature for 15 minutes. The cells were centrifuged at 900 x g using an Eppendorf microfuge. The pellet was resuspended in 100 µl of 1X Annexin Binding Buffer, and 1µg of 1mg/ml Alexa Fluor 350 Streptavidin solution was added. The mixture was incubated on ice for 30 minutes. At the end of the incubation period, the cells were centrifuged and the pellet was resuspended in 500 µl of 1X Annexin Buffer. 1 µl of 1mg/ml PI stock solution was added to the cells while they are still on ice (70). The cells were analyzed using LSR-II flow cytometry.

3.13. Principle of Flow Cytometry

Flow cytometry uses the principles of light scattering, light excitation, and emission of fluorochrome molecules to generate specific multi-parameter data from particles and cells in the size range of 0.5um to 40um diameter. Cells are hydro-dynamically focused in a sheath of PBS before intercepting an optimally focused light source (See Figure 3.5). Lasers are most often used as a light source in flow cytometry.

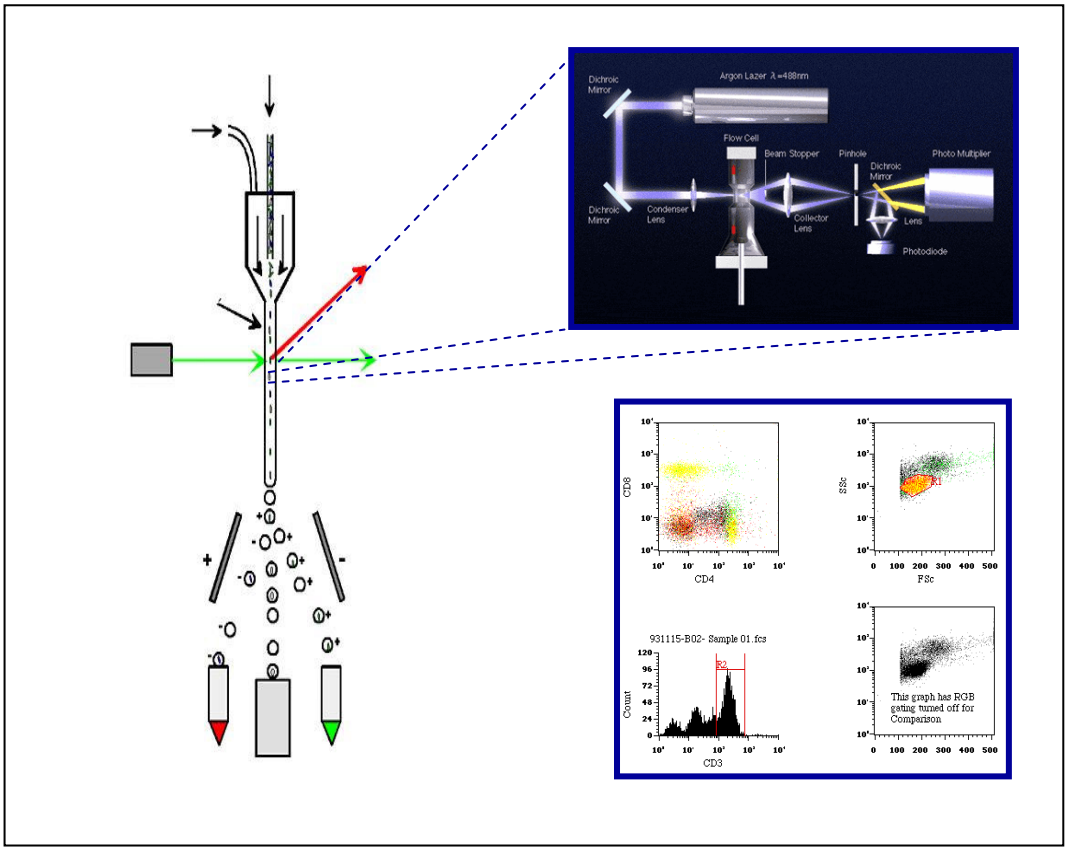

Figure 3.5. the schematic representation of the flow cytometry.

One unique feature of flow cytometry is that it measures fluorescence per cell or particle. This contrasts with spectrophotometry in which the percent absorption and transmission of specific wavelenths of light is measured for a bulk volume of sample. Scattered and emitted light from cells and particles are converted to electrical pulses by optical detectors. Collimated (parallel light waveforms) light is picked up by confocal lenses focused at the intersection point of cells and the light source. Light is send to different detectors by using optical filters.

The most common type of detector used in flow cytometry is the photomultiplier tube (PMT). The electrical pulses originating from light detected by the PMTs are then processed by a series of linear and log amplifiers. Logarithmic amplification is most often used to measure fluorescence in cells. This type of amplification expands the scale for weak signals and compresses the scale for "strong" or specific fluorescence signals. After the different signals or pulses are amplified they are processed by an Analog to Digital Converter (ADC) which in turn allows for events to be plotted on a graphical scale(One Parameter, Two parameter Histograms). Flow cytometry data outputs are stored in the form of computer files using the FCS 2.0 or 3.0 standard. Data corresponding to one sample can be stored as a listmode file and/or histogram file.

When making a reading in the flow cytometry machine there are 4 types of control. In every experiment these controls were used to qualibrate the machine:

Control No 1: This tube consist of WT p53 mouse fibroblast cell which have NO transfection and NO UVB radiation. The biggest difference of this tube from the "-Tfx –UV" sample is that, this control has NO Alexa Fluor 350 and NO PI treatment. The cells in this plate are used to determine the FSC (Forward Scatter Signal) and SSC (Side Scatter Signal) parameters in the data acquisition window of the machine. The FSC and SSC parameters give an idea about the shape, the complexity, and the granulosity of the cells.

The following controls are used to determine the fluorochromes. GFP, Alexa Fluor 350 and PI (Propidium Iodide) have their own excitation and emmission values. For a correct reading these excitation and emmission peaks should be well separated from each other otherwise they will overlap.

The excitation and emmission values for the most common fluorochromes are indicated in Appendix 2.

Contol No 2: This tube consist of WT p53 mouse fibroblasts cells transfected with EGFP vector only (not EGFP-WTp53 vector). They are NOT radiated with UVB, and NOT treated with Alexa Fluor 350 and PI. This tube is used to set up the FL1 parameter. The excitation and emmission values for EGFP are 489 nm and 508 nm respectively.

Contol No 3: This tube consist of WT p53 mouse fibroblasts cells which have NO transfection. They are radiated with 1000 J/m^2 UVB, and treated with Alexa Fluor 350 only. This tube is used to set up the FL2 parameter. The excitation and emmission values for Alexa Fluor 350 are 346 nm and 445 nm respectively.

Contol No 4: This tube consist of WT p53 mouse fibroblasts cells which have NO transfection. They are radiated with 1000 J/m^2 UVB, and treated with PI only. This tube is used to set up the FL3 parameter. The excitation and emmission values for PI are 536 nm and 617 nm respectively.

3.14. Nuclear and Cytoplasmic Protein Extraction

(NE-PER® Nuclear and Cytoplasmic Extraction Reagents (CER), Cat.No 78833)

The nuclear and the cytosolic protein fractions were obtained using Pierce NE-PER Nuclear and Cytoplasmic extraction kit.This kit enables stepwise separation and preparation of cytoplasmic and nuclear extracts from mammalian cultured cells or tissue. Non-denatured, active proteins are purified in less than two hours. Addition of the first two reagents to a cell pellet causes disruption of cell membranes and release of cytoplasmic contents. After recovering the intact nuclei from the cytoplasmic extract by centrifugation, the nuclei are lysed with a third reagent to yield the nuclear extract. Extracts obtained with this product generally have less than 10% contamination between nuclear and cytoplasmic fractions—sufficient purity for most experiments involving nuclear extracts.

This procedure reflects reagent volumes based on samples with a packed cell volume of 20 ml (~40 mg of cell paste approximately equivalent to 2 x 106 HeLa cells).

1. Isolate 20 ml packed cell volume (~40 mg) of cells in a 1.5 ml microcentrifuge tube by centrifugation at 500 x *g* for 2-3 minutes.
2. Using a pipet, carefully remove and discard the supernatant, leaving cell pellet as dry as possible.
3. Add 200 µl of ice-cold CER I to the cell pellet.
4. Vortex the tube vigorously on the highest setting for 15 seconds to fully resuspend the cell pellet. Incubate the tube on ice for 10 minutes.

5. Add 11 µl of ice-cold CER II to the tube.
6. Vortex the tube for 5 seconds on the highest setting. Incubate tube on ice for 1 minute.
7. Vortex the tube for 5 seconds on the highest setting. Centrifuge the tube for 5 minutes at maximum speed in a microcentrifuge (~16,000 x *g*).
8. Immediately transfer the supernatant (cytoplasmic extract) fraction to a clean pre-chilled tube. Place this tube on ice until use or storage (see Step 13).
9. Resuspend the insoluble (pellet) fraction produced in Step 7, which contains nuclei, in 100 µl of ice-cold NER.
10. Vortex on the highest setting for 15 seconds. Return the sample to ice and continue vortexing for 15 seconds every 10 minutes, for a total of 40 minutes.
11. Centrifuge the tube at maximum speed (~16,000 x *g*) in a microcentrifuge for 10 minutes.
12. Immediately transfer the supernatant (nuclear extract) fraction to a clean pre-chilled tube. Place on ice.
13. Store all extracts at -80°C until use.

3.15. BCA Protein Assay

In order to determine the protein amount in the cytoplasmic and nuclear fractions the BCA Protein Assay was done. This colorimetric assay detects a protein concentration varying from 125-2000 µg/ml, and the color intensity is proportional to the concentration of protein in the samples.

Bovine Serum Albumin (BSA) at 2mg/ml concentration was diluted serially to generate the standard curve. The blank contains the Pierce CER-1 or CER-2 buffers used in preparing the cytosolic and nuclear protein fractions.The standards and the samples were prepared according the following table:

BCA working solution was prepared mixing 1 part mixture A and 50 parts mixture B. 95 ul of this working solution was added to 5 ul of total volume of blanks, standards and samples. The mixture was immediately vortexed and incubated at 37°C for 30 minutes. The absorbance was read using Biorad Spectrophotometer at 562 nm.

Table 3.2 The reagent volumes for preparing the BSA standard

BSA concentration (µg/ml)	**0**	**0.4**	**0.6**	**0.8**	**1**	**1.2**	**1.6**	**2**	**blank**	**sample**
Volume BSA (µl)/sample	0	1	1.5	2	2.5	3	4	5	2	2
Volume dH_2O (µl)	5	4	3.5	3	2.5	2	1	0	3	3

3.16. Western Blotting

The samples are mixed with the appropriate volume of 5X sample buffer (0.063M TRIS, 10% glycine, 5% β-mercaptoethanol, 3% SDS, 0.02% bromophenol dye in water) and boiled at 95ºC for 5 minutes. The acrylamide gels (Bio-Labs) are assembled and immersed in running buffer (3g TRIS base, 14.4g Glycine, 10ml 10% SDS in 1L of water). The samples are loaded and run at 200V until the dye reaches the bottom of the gel. After the proteins have separated, they are transferred to nitrocellulose paper overnight in transfer buffer (3g TRIS, 14.4 Glycine, 150mL Methanol, water to 1 liter) at 4ºC. Transfer apparatus is assembled by making a "gel sandwich" composed of 2 sponges, 4 filter papers, a nitrocellulose paper and the gel in a way that the nitrocellulose paper and the gel are adjacent. The samples were immersed in a transfer apparatus (Bio-Rad) and transferred at 30V overnight. Following the transfer, the nitrocellulose paper was immersed in a dish containing 50ml of 5% non-fat dry milk for 1 hour. The antibodies were diluted in 3ml of 1% milk (or in 5% BSA if the antibody is phospho-specific) according to manufacturer's recommendations (all antibodies were purchased from Santa Cruz Biotech), placed in a plastic bag and sealed together with the nitrocellulose paper for 1-2 hours shaking on a Lab Line shaker 4631. The primary antibody was removed by washing 4 times for 10 minutes in 50ml BB buffer (50ml 1M Tris-Cl, pH 7.4, 30ml 5M NaCl, 5ml 10% Tween-20, water to 1L). The nitrocellulose blot was then incubated in 40ml of the appropriate secondary antibody (diluted 1:10,000 in 1% milk) for 1 hour with shaking. The secondary antibody was removed by washing in 50ml BB buffer 4 times for 10 minutes.The Super-signal substrate was prepared by mixing 2ml of reagent A with 2 ml of reagent B and applied on top of the nitrocellulose paper for 6

minutes. The paper was briefly dried and placed between sheet protectors in a developing cassette. It is exposed for 1 minute (or until the desired signal strength is obtained) using ECL film (Amersham) that produce linear signals proportional to the antibody binding.

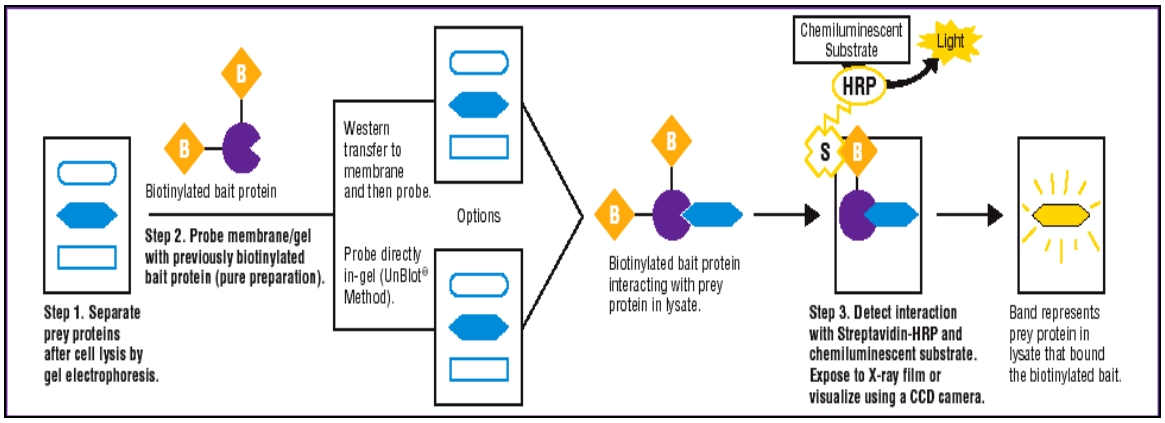

Figure 3.6. The mechanism of the supersignal substrate to detect HRP.

The Supersignal Substrate from Pierce is a highly sensitive enhanced chemiluminescent substrate for detecting horseradish peroxidase (HRP) on immunoblots. The substrate's intense signal output enables detection of picogram amounts of antigen. The sensitivity, intensity and duration of the signal allow for easy detection of HRP using photographic or other imaging methods. Blots can be repeatedly exposed to film to obtain optimal results or stripped of the immunodetection reagents and reprobed.

4. RESULTS

4.1. The Result of Bioinformatic Analysis

The relationship between apoptosis and the p53 mutations is obvious. What we don't know exactly is which mutations confer which property to the protein and what changes in functions we can see as a result. In previous researches Dr Brash's laboratory published the p53 mutations found in AK's, BCC's and SCC's. In order to decide which mutations to work with, the linearized data (sent from Dr Ishioka) was uploaded to a clustering software and a dendrogram was obtained (Figure 4.1.). The data uploaded in the software consists of the missense mutations found in non-melanoma skin cancers. The nonsense mutations and frameshift mutations were not included thus they don't appear in the dendrogram.

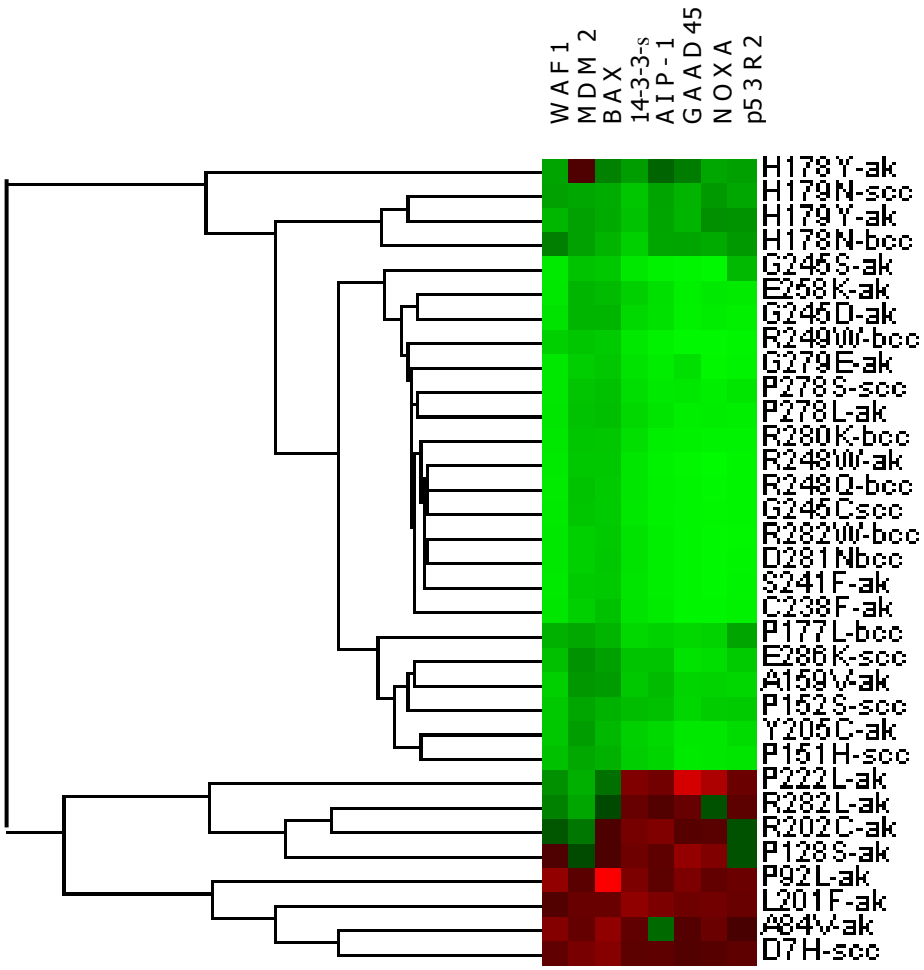

Figure 4.1. The dendrogram of the non-melanoma skin cancer missense p53s mutations created by Treeview Clustering Software.

The letter-number tags on the right of the dendrogram represent the missense mutations in non-melanoma skin cancers and each of the rows cover the original codon, the codon number, the mutated codon and the type of skin cancer. For instance, the second row from the bottom, namely A84V-ak, outlines that the original codon is Alanine (A), that the codon where the mutation takes place is 84, the mutated codon is Valine (V), and that this is a mutation found in AK's (-ak).

There are 19 AK's, 7 BCC's and 7 SCC's missense mutations. For this research 11 of these 19 AK's missense mutations were chosen. The mutations were chosen from different regions of the dendrogram, so at the end of all the experiments comparing the "expected" and the "obtained" behavior would be much more reflecting. It can be seen from the dendrogram that according to the clustering software the mutations found in codons 84, 92, 201, 202 and 128 fall in the same group. That's why it can be expected that they have similar behaviours in apoptosis. The other six mutations are clustered in different groups and thus they should have an apparently different pattern on apoptosis. These 11 mutations are distributed between the exons 4 and 8. The codons 84 and 92 take place in the proline-rich domain, all the others are in the DNA-binding domain. Only 4 of these mutations are hot-spot mutations (mutations on codons 241, 245, 248 and 278) and of all these 11 mutations 6 were not investigated previously.

The dendrogram represented here gives us only a rough idea about the behavior of these mutations on apoptosis. The linearized data collected to obtain the dendrogram is the result of a yeast-based *in vitro* assay. In order to see the real effects of these mutations on apoptosis, transient transfection of the EGFP-p53-expressing vector is done.

In this research 11 point mutations were created on the p53 cDNA by site-directed mutagenesis, to better understand the molecular functions and the effects of the protein on apoptosis. The p53 cDNA was cloned below the strong CMV promoter in the mammalian expression vector pEGFP-f. The point mutations were created one by one on this new vector. The Widt type (WT) and mutated pEGFP-p53 expression plasmids were transiently transfected into the mouse primary fibroblast cells. The percentage of apoptosis after UVB treatment were analyzed using flow cytometry. The protein expression levels after UVB treatment were also analyzed.

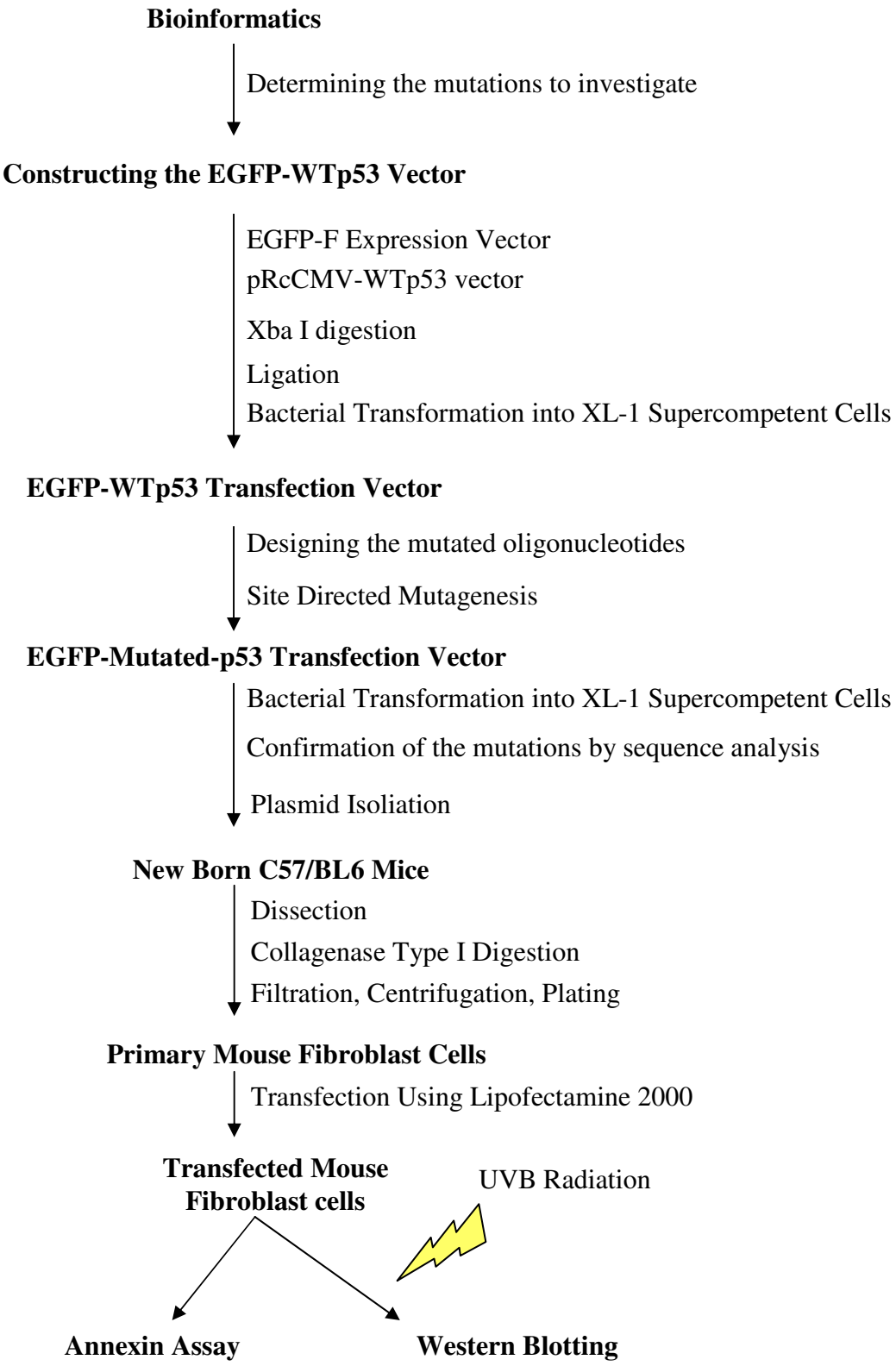

Figure 4.2. Flow chart of the experiments done in this research.

4.2. The Preparation of the pEGFP-p53 Expresion Vector with Restriction Enzyme Digestion

The mammalian expression vector pRcCMV-p53WT has a molecular weight of 7344 bp. As shown in the previous section in Figure 3.1 the pRcCMV vector has a p53 cDNA insert of 1.8 kb. Digesting the vector with the endonuclease XbaI will generate two fragments; the 1.8 kb p53 cDNA and the 5.5 kb empty pRcCMV vector. In figure 4.14 the original and the digested vectors are shown. The plasmids were run in 0.7 % agarose gel. In Figure 4.15 a total of 3 μg XbaI digested pRcCMVp53WT vector was run on agarose gel. The 1.8 kb p53 cDNA inserts were excised from the gel and purified.

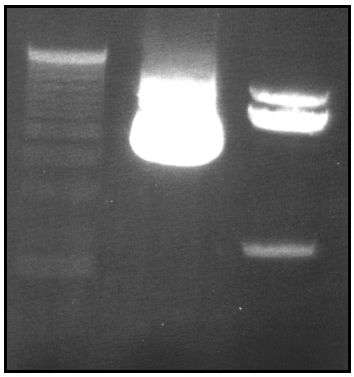

Figure 4.3. Agarose gel electrophoretic representation of the pRcCMV-p53WT vector and the digested product. Lane 1 Marker (GIBCO-BRL), Lane 2 pRcCMVp53WT vector, Lane 3 digested vector.

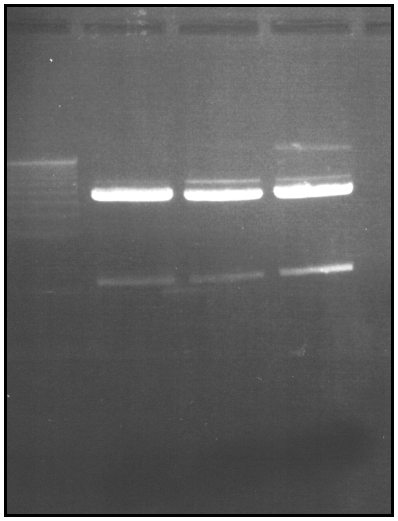

Figure 4.4 Agarose gel electrophoretic representation of the digested vector on low melting gel agarose.

4.3. The cloning of the p53 cDNA insert in pEGFP-f vector

The expression vector pEGFP-f, as shown in the previous section in Figure 3.2 has a size of 4.8 kb. The digestion of the vector with XbaI will generate a cut downstream of the strong mammalian CMV promoter and upstream of the EGFP protein. Thus inserting the p53 cDNA in that region will guarantee that every time there's a GFP signal, the p53 cDNA is also expressed. The vector was digested with XbaI and the p53 cDNA insert was ligated with T4 DNA ligase. In order to confirm that the p53 cDNA insert was ligated on the correct direction, the product was sequenced with an automated sequence analyzer.

Figure 4.4 shows the agarose gel electrophoresis of the expression vector EGFP-f and the EGFP-p53 with mutations created on.

Figure 4.5 shows the sequencing analysis of the EGFP-p53WT ligated correctly. The sequenced and confirmed expression vector was used in the following experiments of the research. 11 point mutations were created one by one, the sequences of these mutated vectors also were analyzed and confirmed.

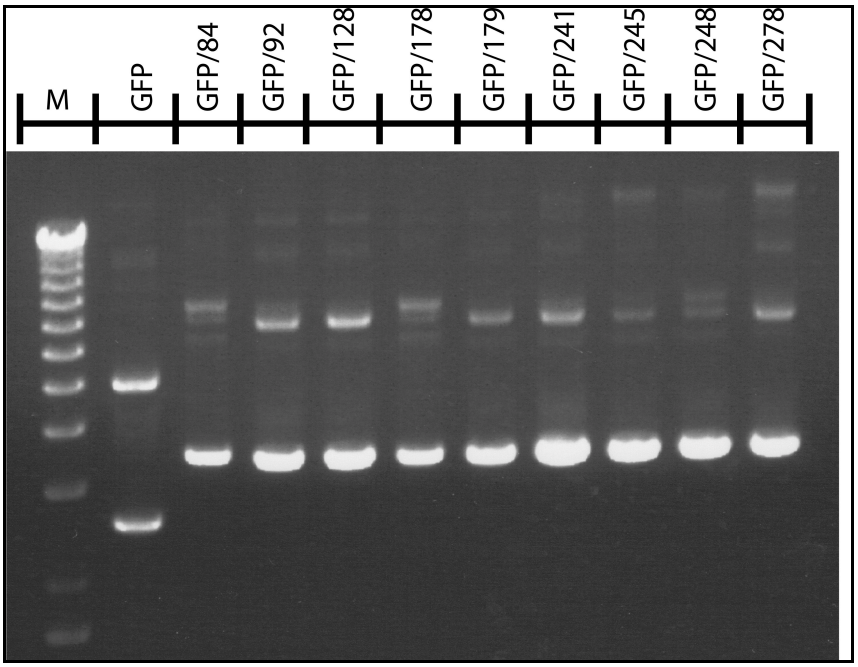

Figure 4.5 Agarose gel electrophoresis of EGFP-f and EGFP-f-p53 with mutations created on. The plasmids were run on a 0.7 % agarose gel.

4.4. The Confirmation of the EGFP-p53 Ligation

The ligation of the EGFP-p53 expression vector was verified and confirmed by using an automated sequence analyzer.

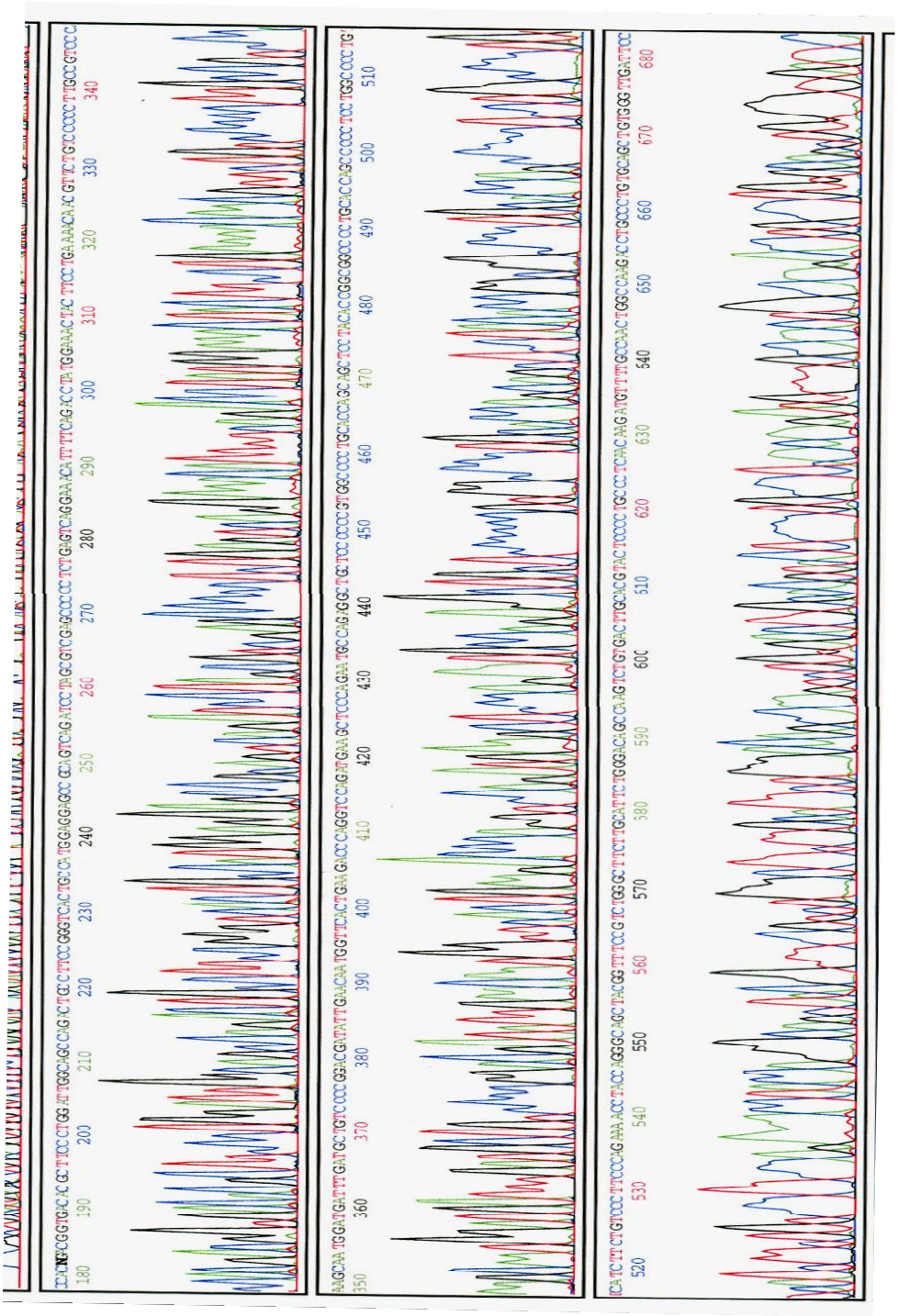

Figure 4.6. Sequence analysis of the EGFP-WTp53 vector

4.5. Confirmation of the Point Mutation Generation Using Sequencing

After generating the 11 point mutations by site directed mutagenesis in the p53 gene cloned to the expression plasmid (pEGFP-p53), the results were verified by using an automated sequence analyzer. Sequencing Primer-1 and Sequencing Primer-2 (explained in the previous section 3.8) were used in order to sequence the p53 gene. The sequence analysis confirmed that all the mutations shown in the previous section were successfully created. The complete coding sequence of the human p53 cDNA was shown in the previous section (Section 3.6). The standard genetic code is shown in the Appendices as Figure 1. The mutated codons were indicated with the red arrows. The forward and revese sequences of the point mutations generated were shown below. (From **Figure 4.7** to **Figure 4.17**).

A84V FORWARD SEQUENCE

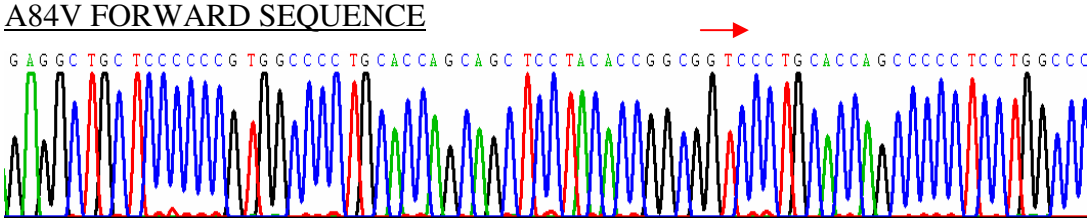

A84V REVERSE SEQUENCE

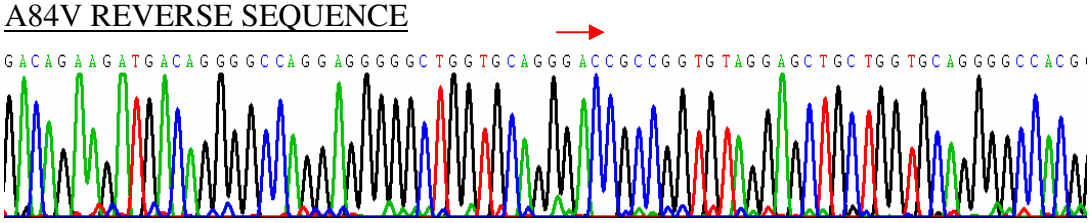

Figure 4.7. The sequence analysis of A84V mutation in the p53 cDNA.

P92L FORWARD SEQUENCE

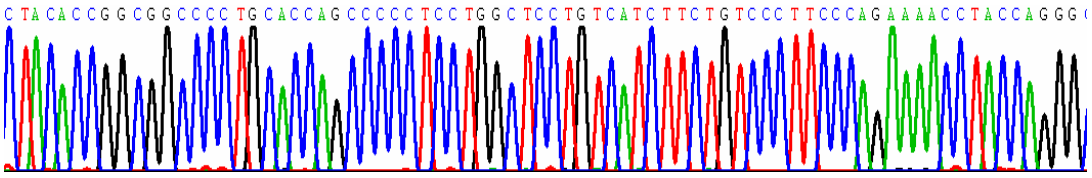

P92L REVERSE SEQUENCE

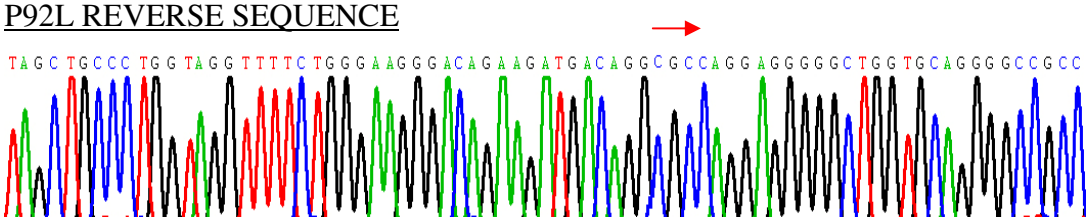

Figure 4.8. The sequence analysis of P92L mutation in the p53 cDNA.

P128S FORWARD SEQUENCE

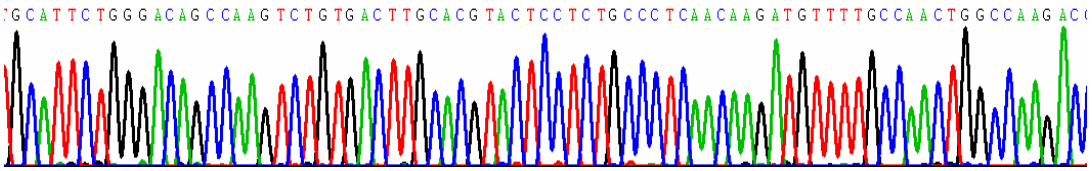

P128S REVERSE SEQUENCE

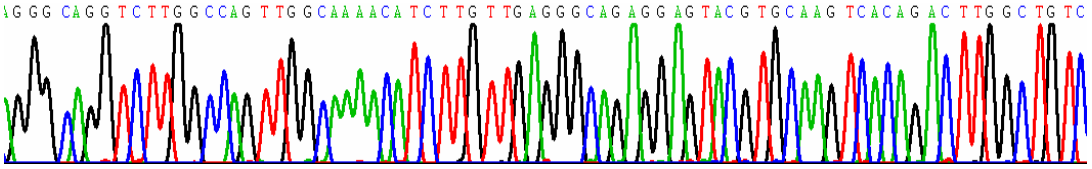

Figure 4.9. The sequence analysis of P128S mutation in the p53 cDNA.

H178Y FORWARD SEQUENCE

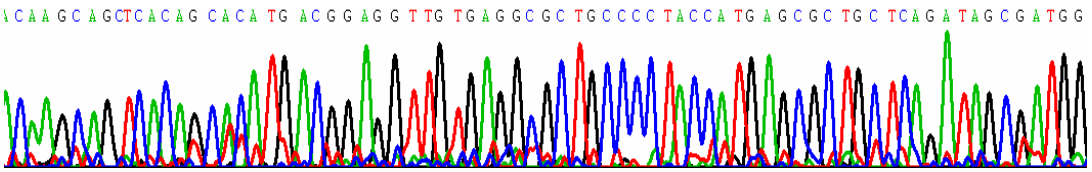

H 178Y REVERSE SEQUENCE

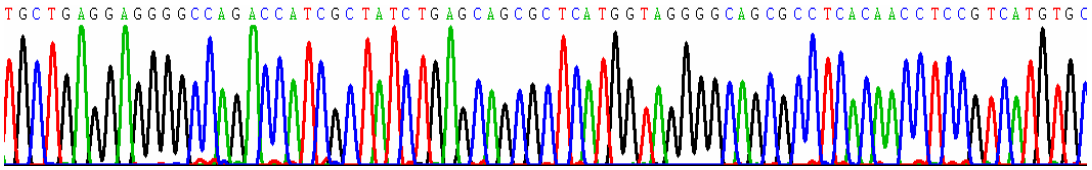

Figure 4.10. The sequence analysis H178Y mutation in the p53 cDNA.

H179Y FORWARD SEQUENCE

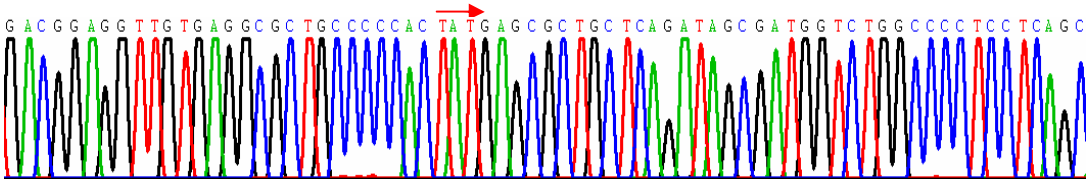

H179Y REVERSE SEQUENCE

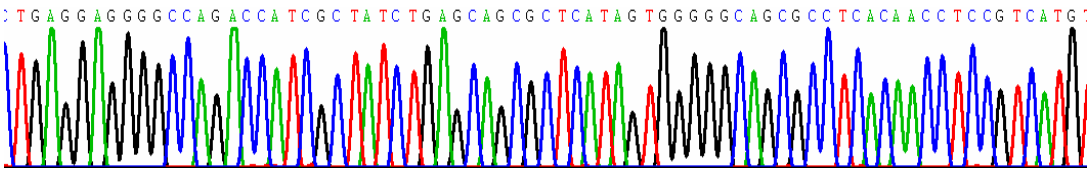

Figure 4.11. The sequence analysis of H179Y mutation in the p53 cDNA.

R201C FORWARD SEQUENCE

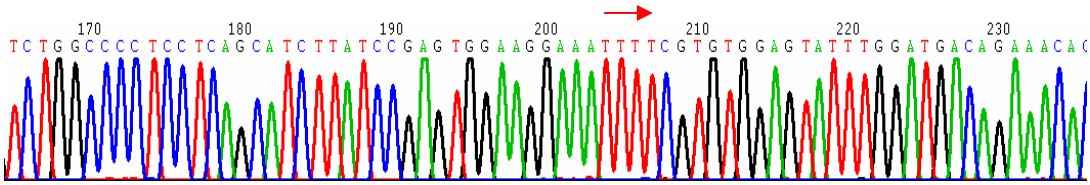

R201C REVERSE SEQUENCE

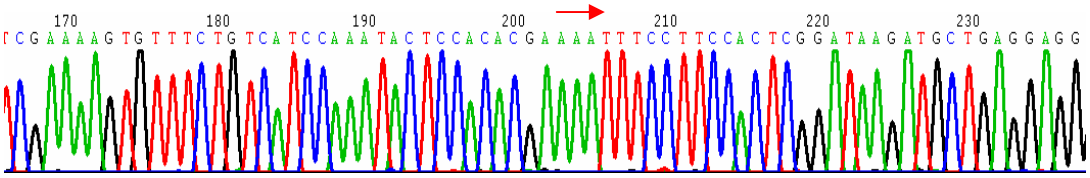

Figure 4.12. The sequence analysis of R201C mutation in the p53 cDNA.

L202F FORWARD SEQUENCE

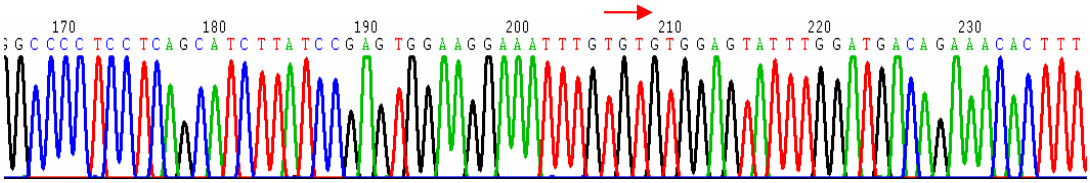

L202F REVERSE SEQUENCE

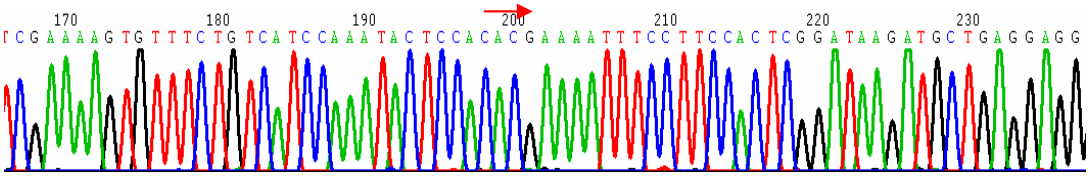

Figure 4.13. The sequence analysis of L202F mutation in the p53 cDNA.

241 FORWARD SEQUENCE

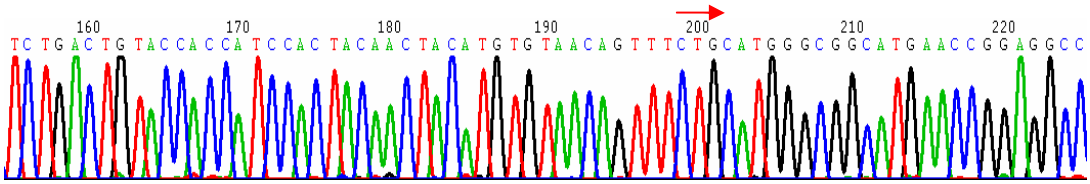

241 REVERSE SEQUENCE

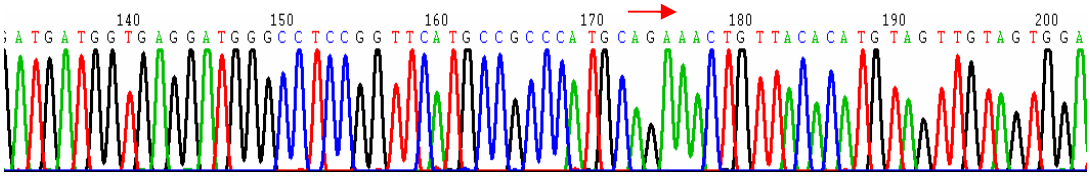

Figure 4.14. The sequence analysis of S241F mutation in the p53 cDNA.

G245S FORWARD SEQUENCE

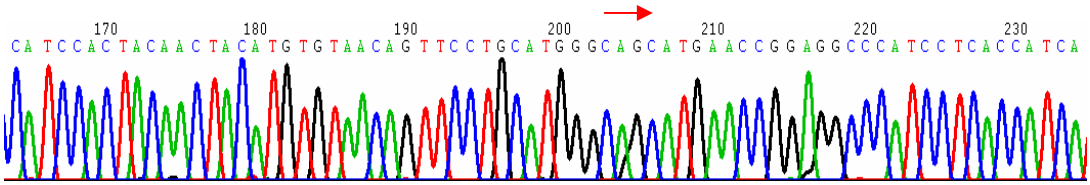

G245S REVERSE SEQUENCE

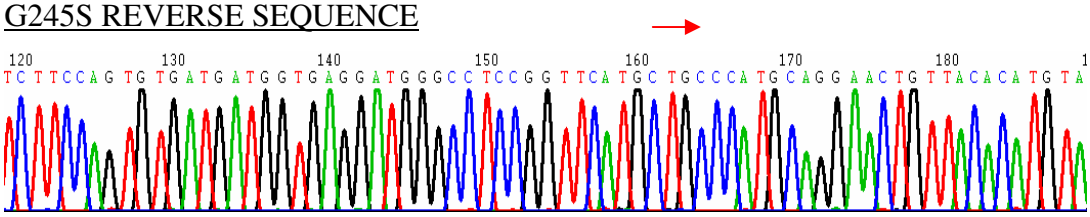

Figure 4.15. The sequence analysis of G245S mutation in the p53 cDNA.

248 FORWARD SEQUENCE

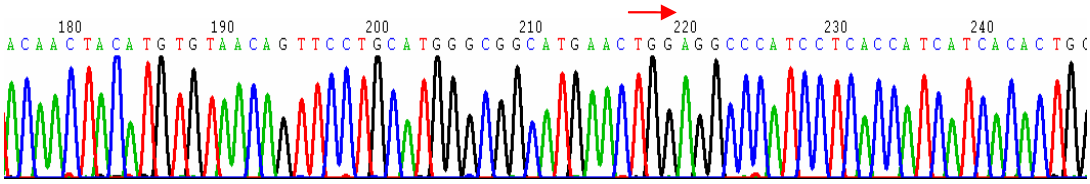

248 REVERSE SEQUENCE

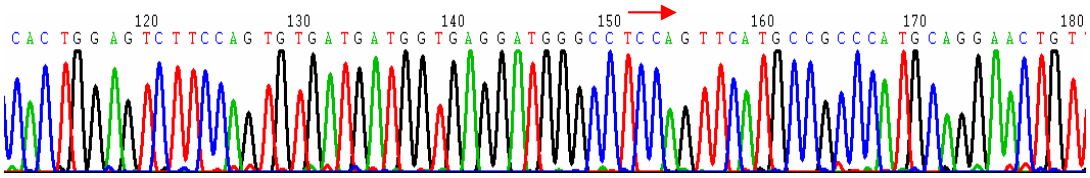

Figure 4.16. The sequence analysis of R248W mutation in the p53 cDNA.

P278L FORWARD SEQUENCE

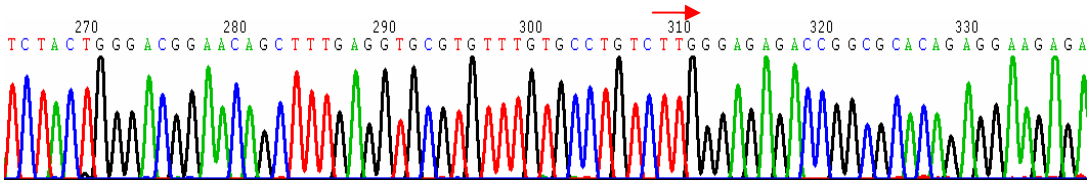

P278L REVERSE SEQUENCE

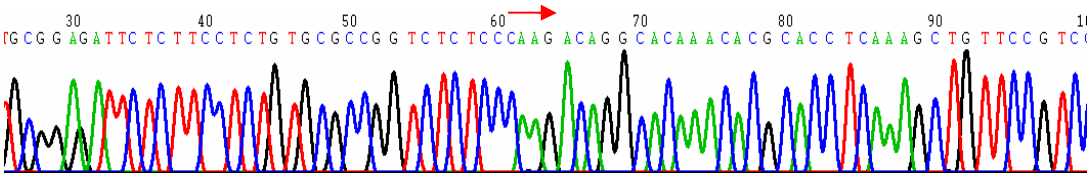

Figure 4.17. The sequence analysis of P278L mutation in the p53 cDNA.

4.6. The confirmation of the Cloning of Mutated pEGFP-p53 Expresion Vector IntoBacterial Cells

After generating the desired mutations and confirming their sequence by using an automated sequence analyzer, the mutated expression vectors were cloned into the XL-1 Blue Supercompetent Cells. The formation of the blue colonies on Kanamycin-containing (30 µg/ml) LB agar plates confirms the presence of cloned cells.

The procedure of this experiment is based on the use of a supercoiled double-stranded DNA (dsDNA) vector with an insert of interest (p53 cDNA) and two synthetic oligonucleotide primers containing the desired point mutation. The primers designed complementary to the opposite strands of the vector are extended with *PfuTurbo* DNA polymerase and they incorporate the point mutation in every cycle. The parental vector containing the non-mutated p53 cDNA is digested during the *Dpn* I treatment. *Dpn* I (target sequence: 5´-Gm6ATC-3´) is specific for methylated and hemimethylated DNA and is used to digest the parental DNA template, and also to select for mutation-containing synthesized DNA. The nicked vector DNA containing the desired mutations is then transformed into XL1-Blue supercompetent cells. One blue colonie was selected and inoculated in 250 ml LB Broth medium and grown overnight at 37 degrees in a shaking incubator. Then Using QIAGEN Maxiprep DNA İsolation Kit, the plasmid DNA was isolated (as explained in detail in section 3.7.2) and used in transfection experiments.

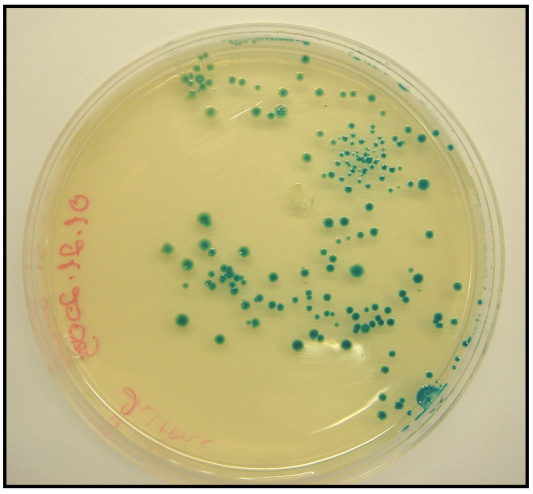

Figure 4.18 Formation of the blue colonies on Kanamycin-agar plates after bacterial transformation.

4.7. Transfection of the Expression Vector into Primary Mouse Fibroblast Cells

After obtaining the mutated plasmids the primary cell culture was done from newborn mice. 16 hours prior to transfection 350000 fibroblast cells were plated in 6 cm petri dishes. 16 hours later the cells were attached to the plates, and reached 60-70 % confluency. The transfection was done using Lipofectamine 2000. To 3 µg DNA, 12 µl Lipofectamine 2000 was added. The vector EGFP-WTp53 was transfected into fibroblast cells to obtain the samples named "Wild Type p53 (WT p53)". The expression vector containing the correspondent mutation was used to test each mutation, and transfected into primary mouse fibroblasts (named "MUT p53). 72 hours post transfection the media of the cells was replaced with 1 X PBS. Half of the the cells were not radiated (named "NO UV WT" and "NO UV MUT") and their media was replaced with fresh DMEM. The remaining cells were subject to UVB radiation and named "UV WT" and "UV MUT" according to the vector they were transfected (Figure **4.19**).

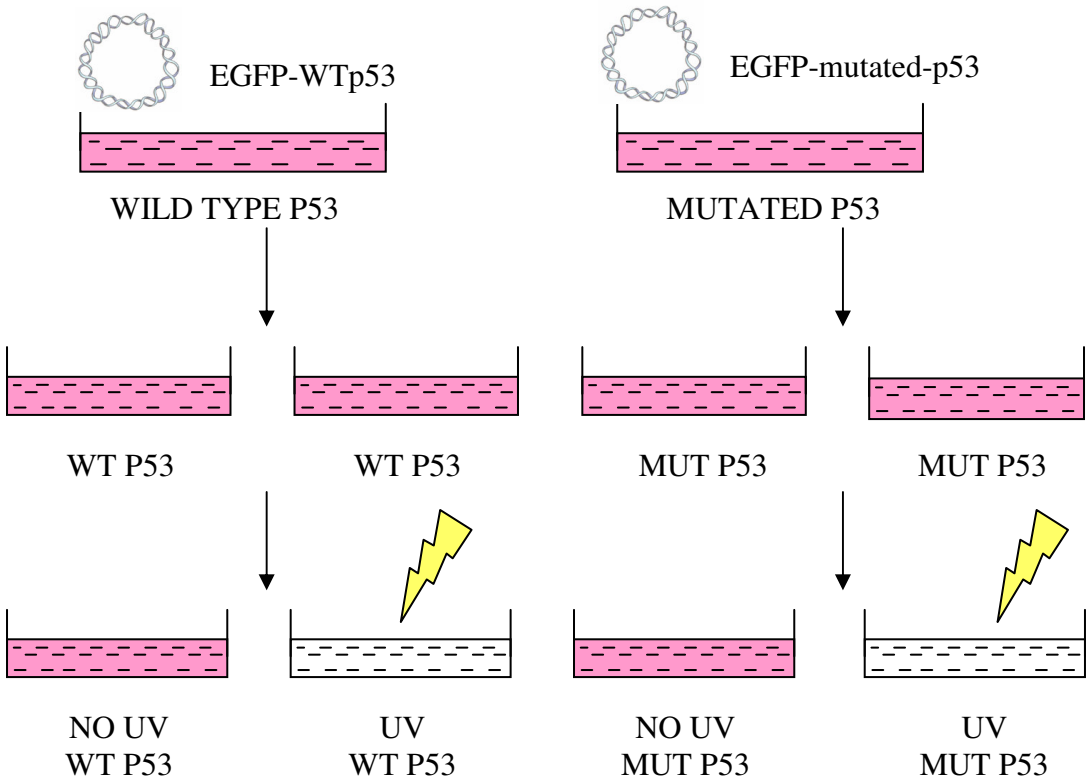

Figure 4.19.The schematic representation of the transfection and UVB radiation experiments in primary mouse fibroblast cells.

4.8. Determination of Apoptosis Using Flow Cytometry

The next day of the UVB radiation the cells were trypsinized and collected separately into 15 ml polypropylene falcon tubes (the media containing the floating cells were also collected). All the samples were incubated with Alexa Fluor 350 and PI. The controls were incubated separately with the proper fluorescent dye as explained in detail in section 3.13. After the completion of annexin assay, the control tubes and the samples were run on the LSR-II Flow Cytometer in order to measure the apoptosis percentage. The figure below shows the reading frames of the flow cytometer for each of the Control Tubes and the blank tube. The histograms of GFP, Alexa Fluor 350 and PI in figure 4.20 show the percentage of the cells in the correspondent control tube that give the fluorescence. For example in the PI Control Tube, 82.59 % of the cells give the PI fluorescence. Again in the GFP Control Tube, 90.20 % of the cells give the GFP fluorescence thus are transfected with the EGFP vector. The fourth reading pane in Figure 4.20 shows the FSC versus SSC chart for the blank tube.

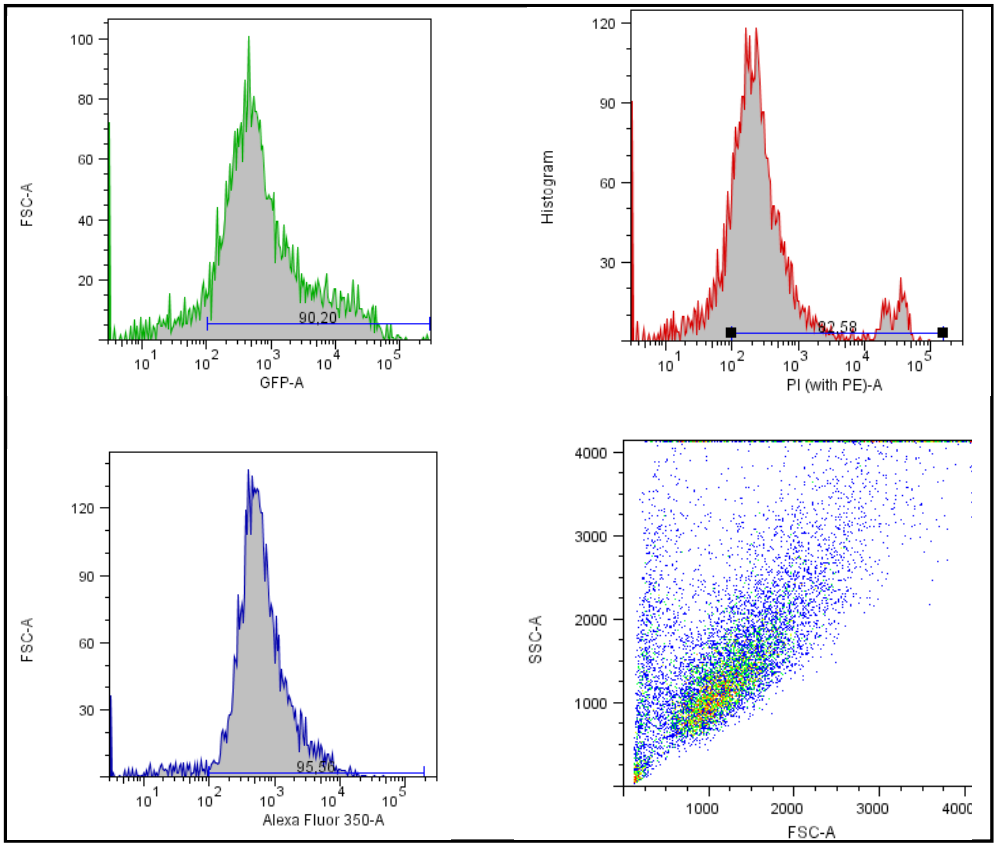

Figure 4.20. The reading frame of LSR-II for the control tubes and the blank tube.

In order to evaluate the results, 10.000 cells containing the GFP signal were selected and the Alexa Fluor 350 versus PI charts were plotted for each of the sample tubes. The figure 4.21 shows the reading frame of LSR-II Flow Cytometer for the Blank Tube (where there are no UV radiation and no transfection). The scale represented in every reading frame is logarithmic. The quadrant separation shown on the image divides the screen into four subpopulations;.

The bottom left quadrant represents the **Live cells** where the cells are Alexa fluor 350 negative and PI negative. According to Figure 4.21, it's 84,02 % of the cells.

The bottom right quadrant represents the **Apoptotic cells** where the population is Alexa positive and PI negative. According to figure 4.21 it's 7,38 **%** of the cells.

The upper right quadrant is the population of **Necrotic cells** in which the cells are Alexa positive and PI positive. According to figure 4.21 it's 4,03 % of the cells.

The upper left quadrant represents the **Debris** where the population is Alexa negative and PI positive and according to figure 4.21 it's 4,57 % of the cells.

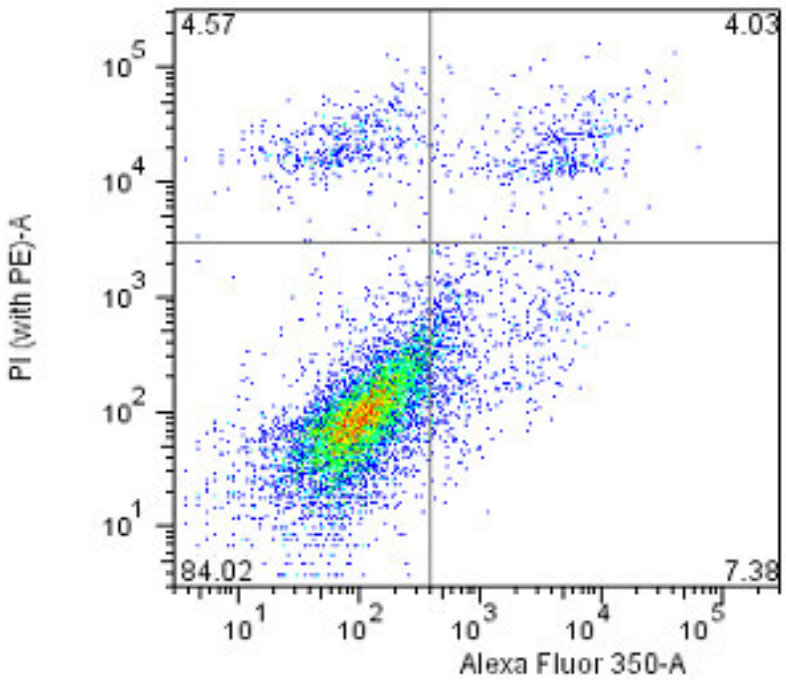

Figure 4.21. The reading frame of LSR-II Flow Cytometer showing the apoptosis percentage of 10000 cells for the Blank tube.

4.9. Evaluation of the Apoptosis Percentage

The output of the LSR-II Flow Cytometer sample tubes were recorded as ".fcs" extension files. The files were read and evaluated in FlowJo (version 5.1) a Java based software. The apoptosis percentage of the sample tubes was recorded and the graphs were drawn using Microsoft Excel.

In order to determine the optimum time after UVB radiation, a time course experiment was carried out. 8 samples of primary mouse fibroblast cells (each containing 350000 cells in 6 cm petri dishes) were plated 16 hours prior to radiation. The day of the experiment the samples were irradiated with 1000 J of UVB. The samples were irradiated and collected 14, 16, 17, 18, 19, 20, 24 and 0 hour post-UVB radiation. The cells were then collected by trypsinization (including the media containing the floating cells) and subjected to Annexin assay. The apoptosis percentage was read using LSR-II flow cytometer and the data was evaluated using FlowJo. The result of the experiment is shown in Figure 4.22. According to the graphic the apoptosis percentage is highest 19 hours after UVB radiation (20.2 %). Thus in every experiment the samples irradiated were harvested 19 hours post-UVB radiation.

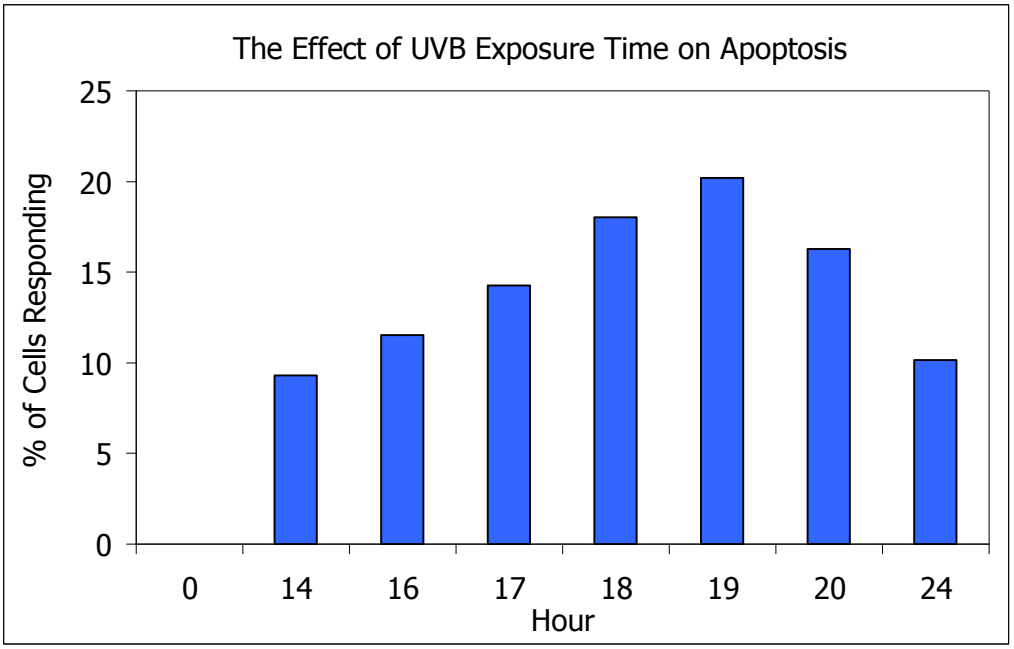

Figure 4.22. The effect of post-UVB exposure time on apoptosis. The cells were harvested in the indicated hours and the apoptosis percentage was plotted.

The effect of the UVB dosage on apoptosis was determined. 5 samples of primary mouse fibroblasts (each containing 350000 cells in 6 cm petri dishes) were plated 16 hours prior to radiation. The day of the experiment 4 of the 5 the samples were irradiated with 250, 500, 750 and 1000 J of UVB and one sample was left non-irradiated. The cells were then collected by trypsinization (including the media containing the floating cells) and subjected to Annexin assay. The apoptosis percentage was read using LSR-II flow cytometer and the data was evaluated using FlowJo. The result of the experiment is shown in Figure 4.23. According to the graphic the apoptosis percentage is highest in 1000 J UVB radiation (15.8 %).

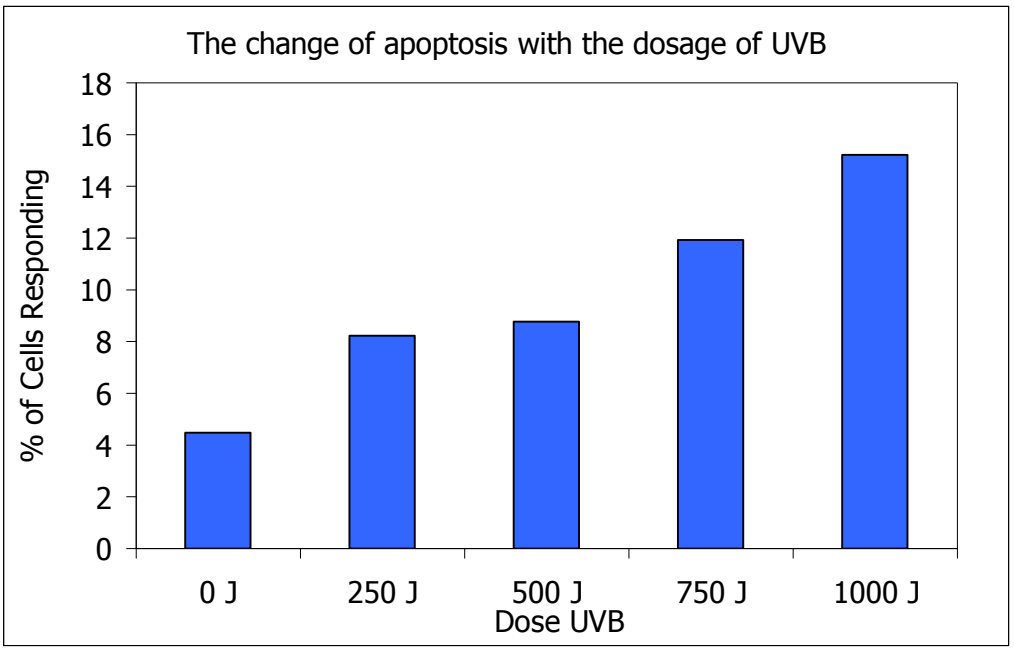

Figure 4.23. The effect of UVB dosage on apoptosis. The cells were irradiated at the indicated dosages and then harvested 19 hours post UVB radiation.

For determining the effect of each mutant on apoptosis, the experiment was designed as explained in detail in section 4.7 and in Figure 4.19. The apoptosis percentage was read using LSR-II flow cytometer and the data was evaluated using FlowJo. The result of the experiments were shown Figure 4.24 to Figure 4.34. The graphics show the average values of 4 experiments for each mutation. The standard deviation values were also indicated.

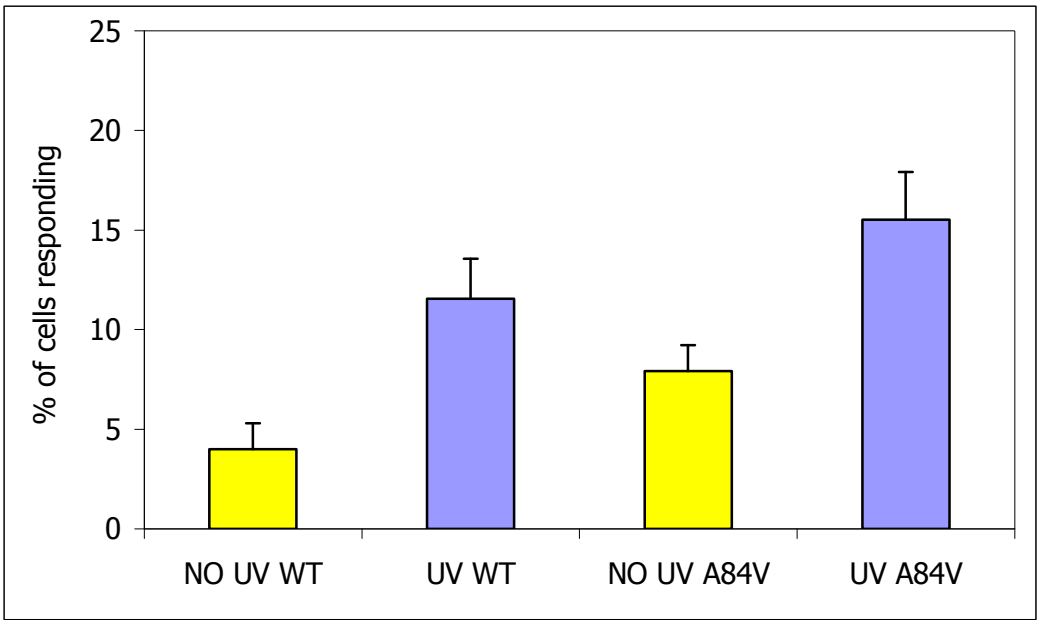

Figure 4.24. The percentage of apoptotic cells in EGFP-WT p53 and EGFP-mut-A84V-p53 transfected fibroblast cells before and after 1000 J UVB radiation.The results were the average of 4 experiments.

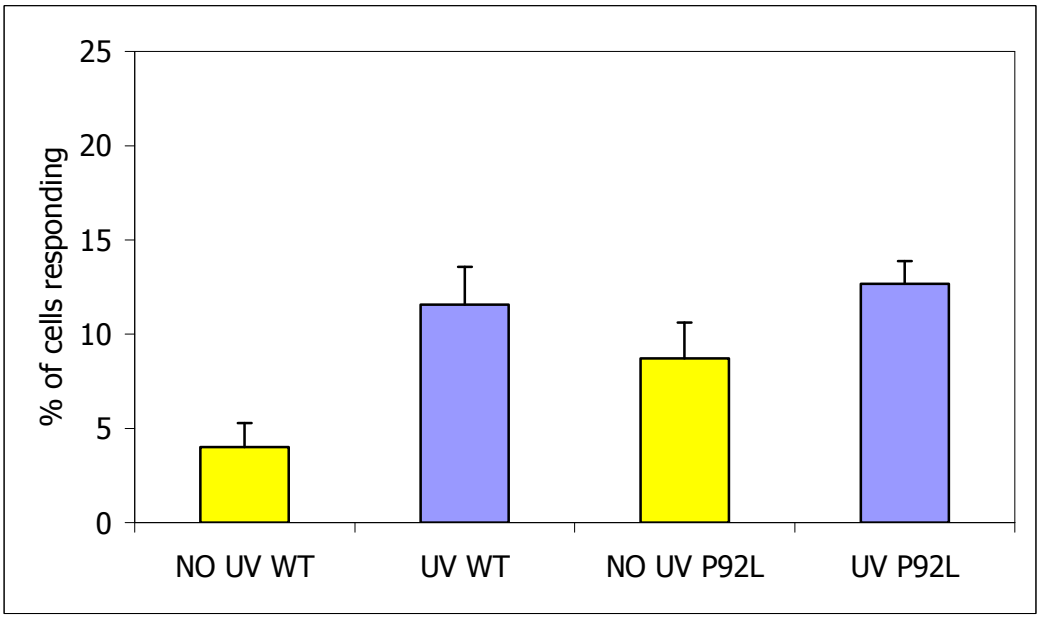

Figure 4.25 The percentage of apoptotic cells in EGFP-WT p53 and EGFP-mut-P92L-p53 transfected fibroblast cells before and after 1000 J UVB radiation. The results were the average of 4 experiments.

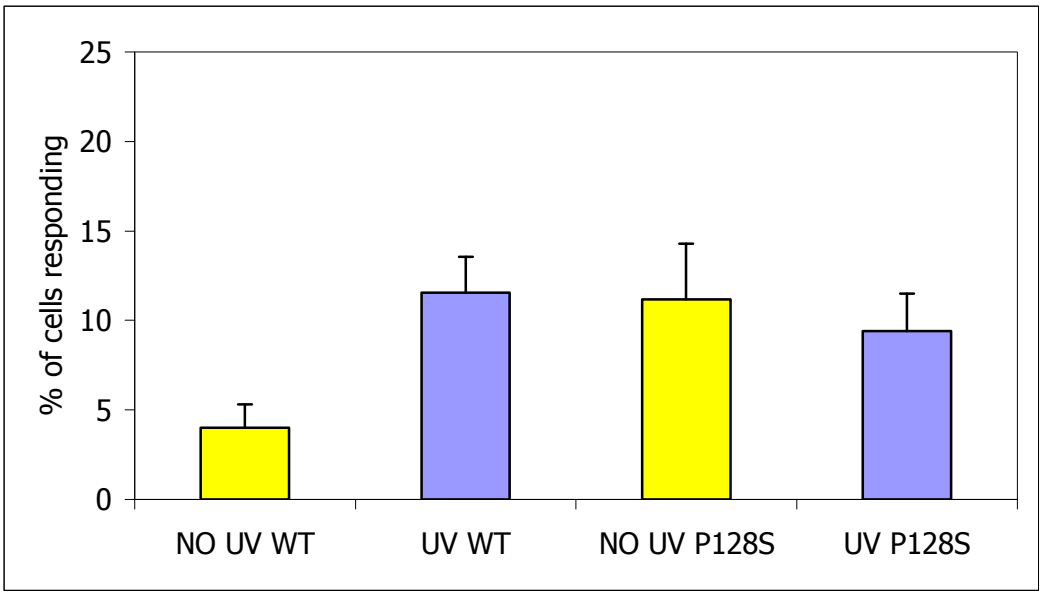

Figure 4.26. The percentage of apoptotic cells in EGFP-WT p53 and EGFP-mut-P128S-p53 transfected fibroblast cells before and after 1000 J UVB radiation. The results were the average of 4 experiments.

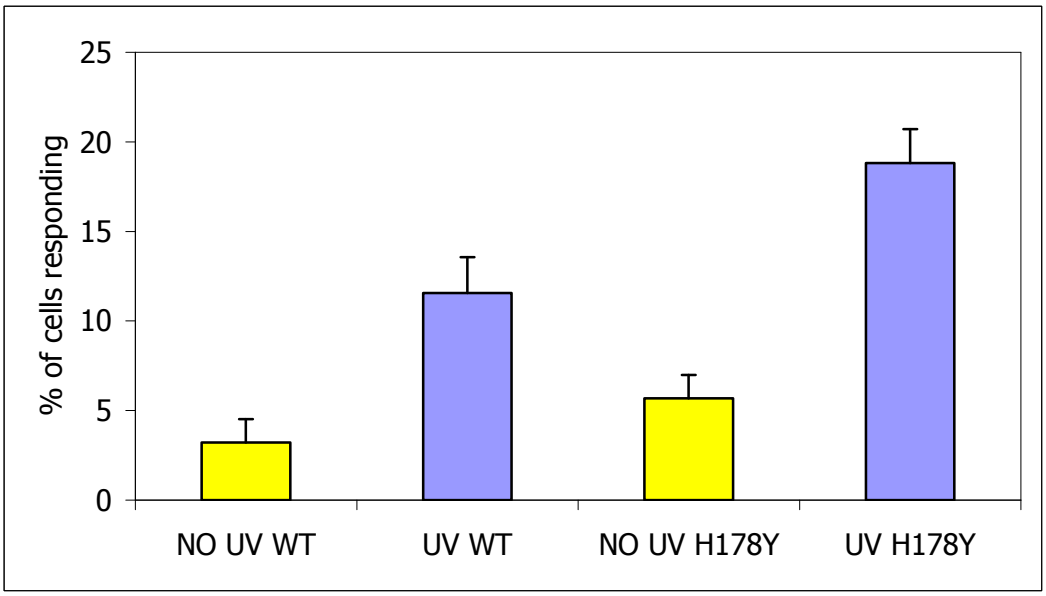

Figure 4.27. The percentage of apoptotic cells in EGFP-WT p53 and EGFP-mut-H178Y-p53 transfected fibroblast cells before and after 1000 J UVB radiation. The results were the average of 4 experiments.

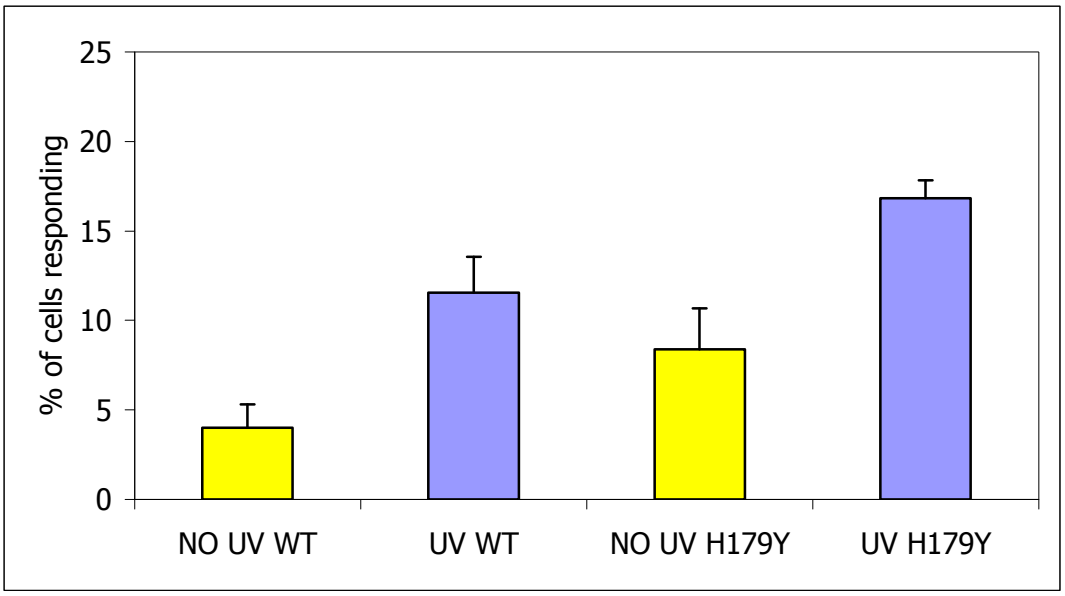

Figure 4.28. The percentage of apoptotic cells in EGFP-WT p53 and EGFP-mut-H179Y-p53 transfected fibroblast cells before and after 1000 J UVB radiation. The results were the average of 4 experiments.

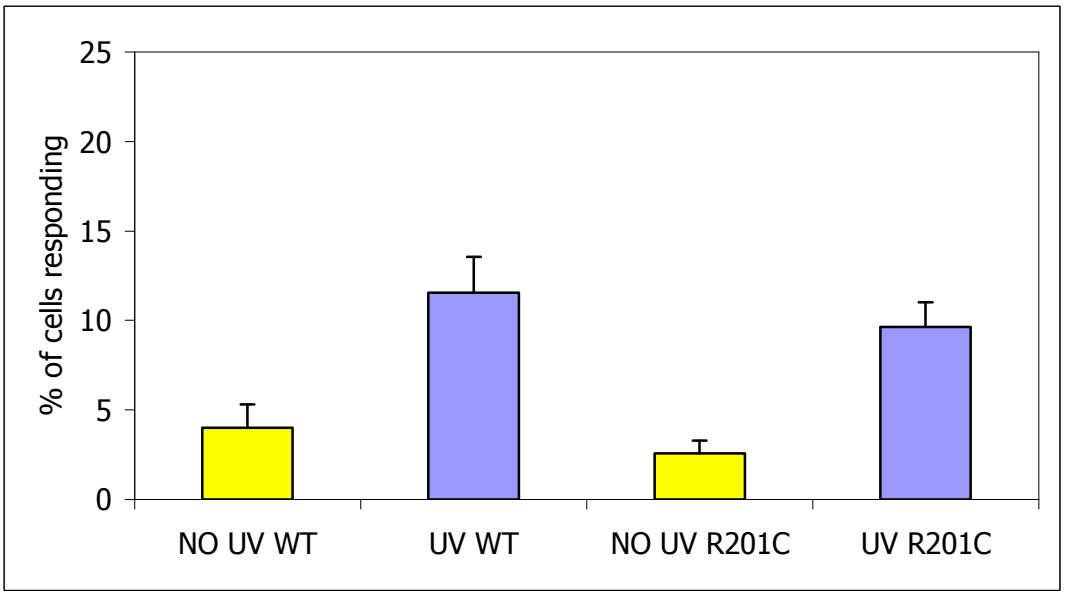

Figure 4.29. The percentage of apoptotic cells in EGFP-WT p53 and EGFP-mut-R201C-p53 transfected fibroblast cells before and after 1000 J UVB radiation. The results were the average of 4 experiments.

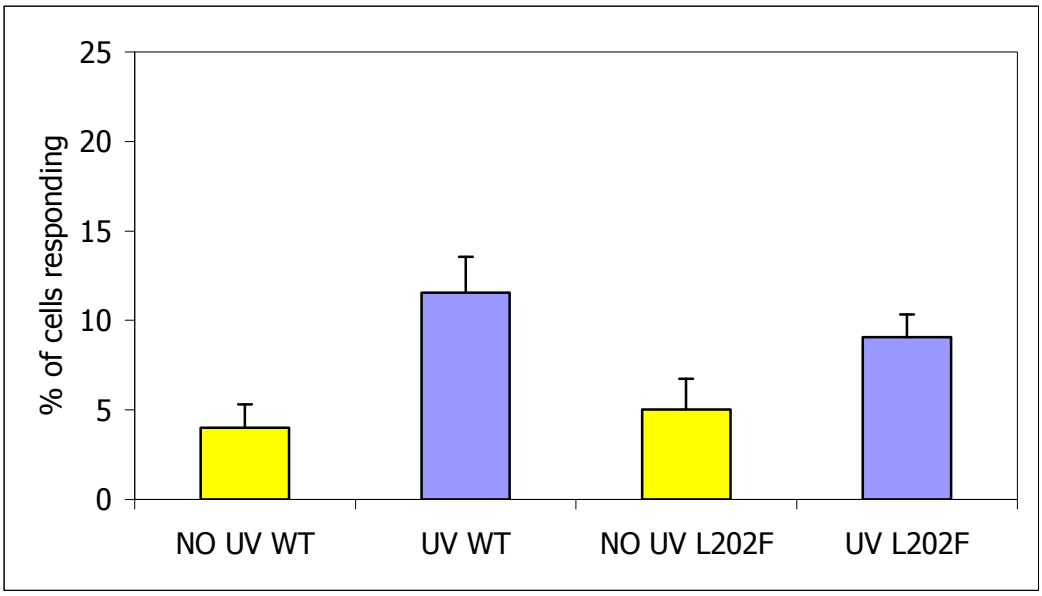

Figure 4.30. The percentage of apoptotic cells in EGFP-WT p53 and EGFP-mut-L202F-p53 transfected fibroblast cells before and after 1000 J UVB radiation. The results were the average of 4 experiments.

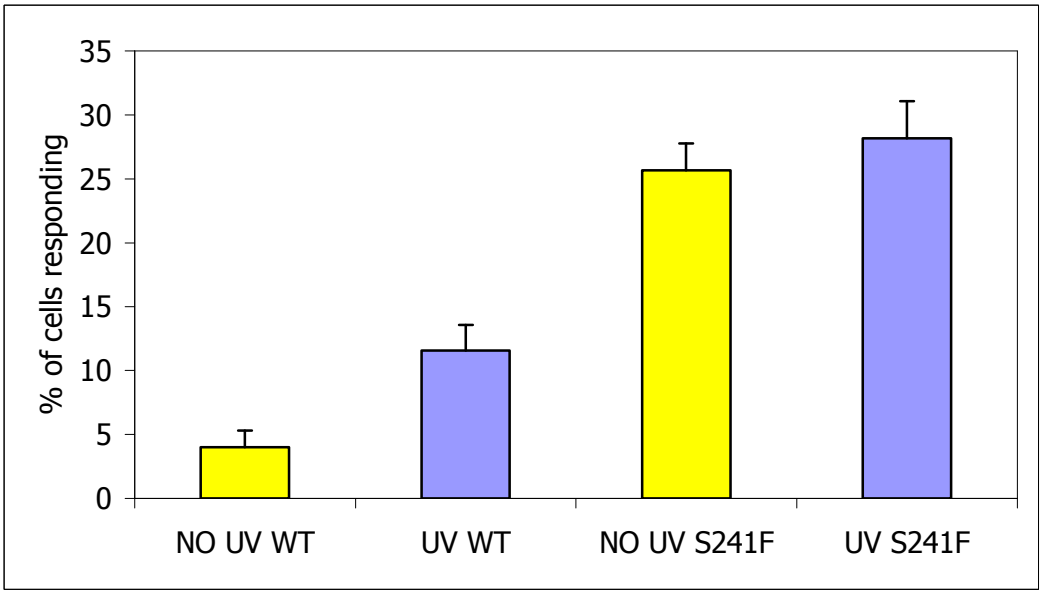

Figure 4.31. The percentage of apoptotic cells in EGFP-WT p53 and EGFP-mut-S241F-p53 transfected fibroblast cells before and after 1000 J UVB radiation. The results were the average of 4 experiments.

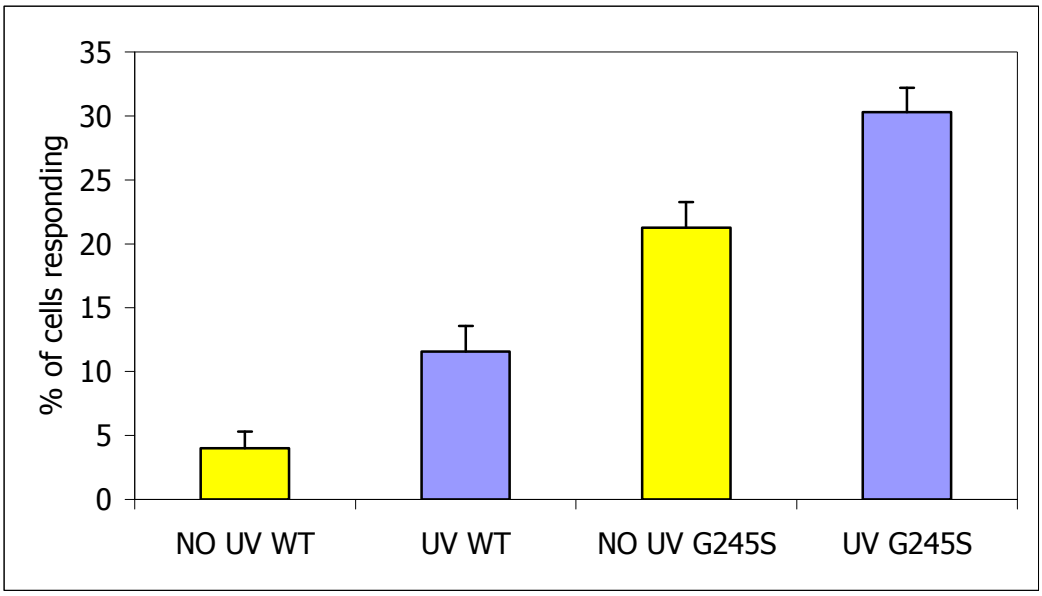

Figure 4.32. The percentage of apoptotic cells in EGFP-WT p53 and EGFP-mut-G245S-p53 transfected fibroblast cells before and after 1000 J UVB radiation. The results were the average of 4 experiments.

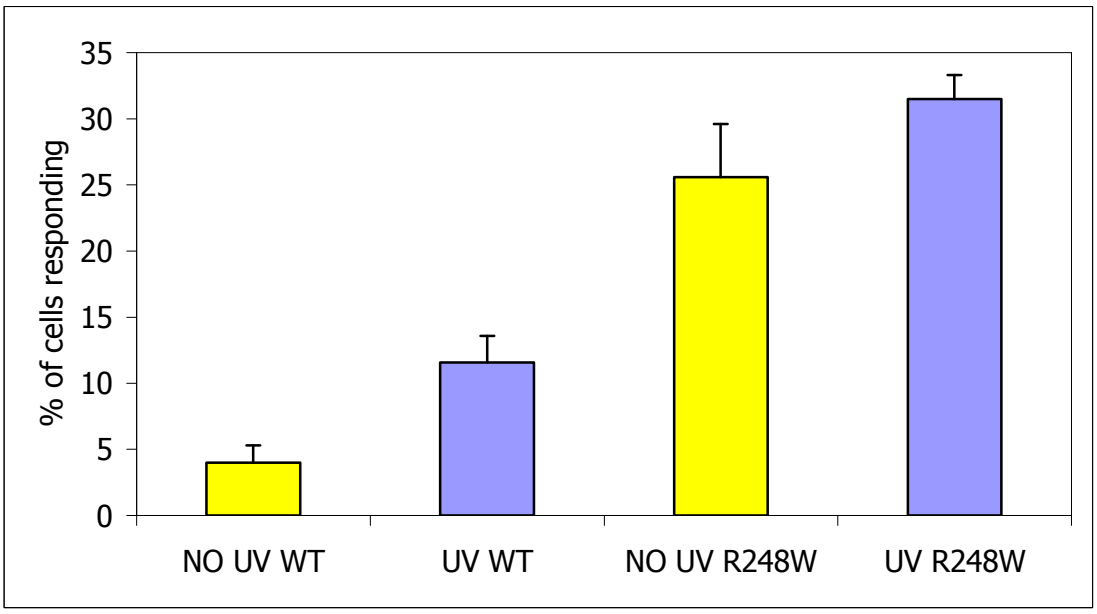

Figure 4.33. The percentage of apoptotic cells in EGFP-WT p53 and EGFP-mut-R248W-p53 transfected fibroblast cells before and after 1000 J UVB radiation. The results were the average of 4 experiments.

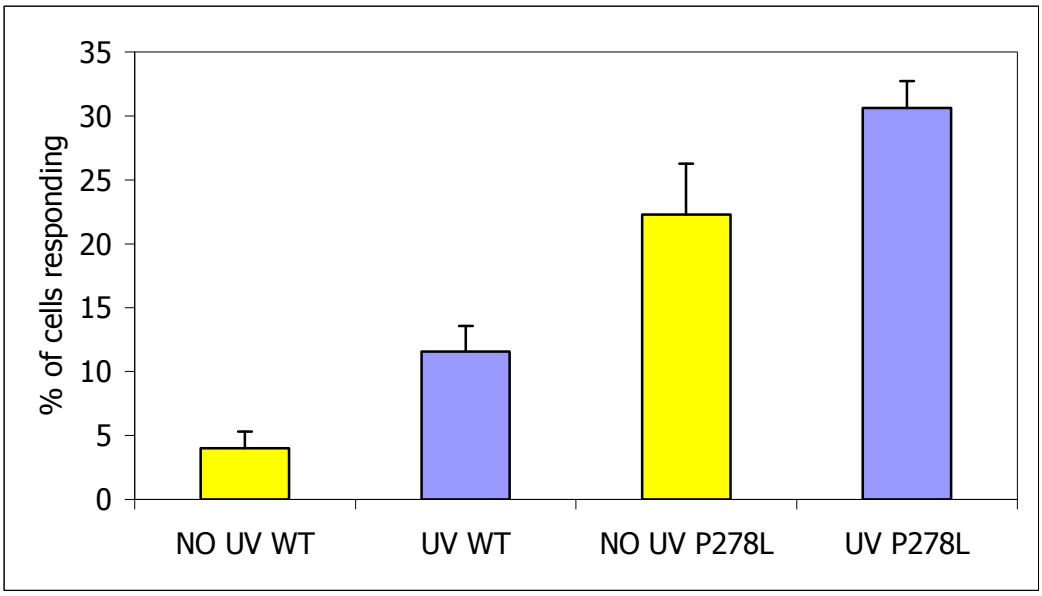

Figure 4.34. The percentage of apoptotic cells in EGFP-WTp53 and EGFP-mut-P278L-p53 transfected fibroblast cells before and after 1000 J UVB radiation. The results were the average of 4 experiments.

The graphic containing all the results together is shown in Figure 4.35. The apoptosis percentage for every sample is listed in Table 4.1. For the mutations A84V and P92L, which take place on the proline-rich domain of P53, there's a slight increase in endogenous apoptosis (7.9 % and 8.7 %, respectively) and a small increase after UVB radiation (15.5 % and 12.7 %, respectively). The endogenous apoptosis increases in P128S (11.2 %) but the response to UVB radiation remains very low (9.4 %) compared to UV WT. For H178Y and H179Y, there's an increase in endogenous apoptosis (5.7 % and 8.4 %, respectively) but the apoptosis percentage in response to UVB is higher (18.8 % and 16.8 %, respectively) compared to UV WT value (which is 11.6 %). For the mutations R201C and L202F, neither the endogenous apoptosis (2.6 % and 5.0 %, respectively) nor the UV-dependent apoptosis percentages (9.6 % and 9.1 %) increase. The endogenous apoptosis percentage was found to be very high in hot spot mutations S241F, G245S, R248W and P278L (25.7 %, 21.3 %, 25.6 % and 22.3 %, respectively). But the response in apoptosis after UVB radiation is very low.

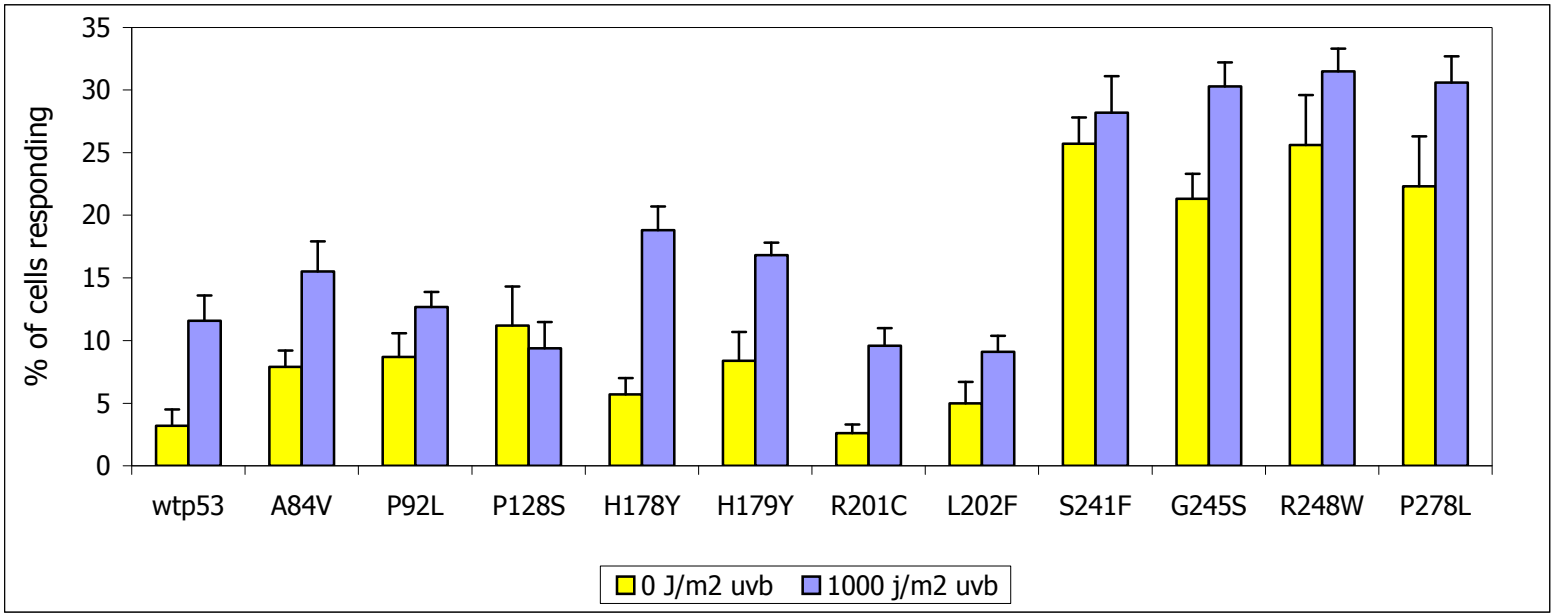

Figure 4.35. The apoptotic percentage of mutated and WT cells before and after UVB radiation

Table 4.1 Apoptosis percentage values and the standard deviations for wild type and mutated cells before and after UVB radiation.

	WT P53	**A84V**	**P92L**	**P128S**	**H178Y**	**H179Y**	**R201C**	**L202F**	**S241F**	**G245S**	**R248W**	**P278L**
0 J/m2 UVB	3.2 ± 1.3	7.9 ±1.3	8.7 ±1.9	11.2±3.1	5.7 ±1.3	8.4 ±2.3	2.6 ±0.7	5.0 ±1.7	25.7±2.1	21.3±2.0	25.6±4.0	22.3±4.1
1000 J/m2 UVB	11.6±2.0	15.5±2.4	12.7±1.2	9.4±2.1	18.8±1.9	16.8±1.0	9.6 ±1.4	9.1 ±1.3	28.2±2.9	30.3±1.9	31.5±1.8	30.6±2.1

4.10. Determining the Protein Expression Levels by Western Blotting

The protein expression analysis was done for the mutations A84V, P92L, P128S and R201C. The protein samples were prepared as explained in detail in section 3.14. The legend for the **Figure 4.36** is as below;

1. NO UV WT
2. UV WT
3. NO UV A84V
4. UV 84V
5. NO UV P92L
6. UV P92L
7. NO UV P 128S
8. UV P128S
9. NO UV R201C
10. UV R201C

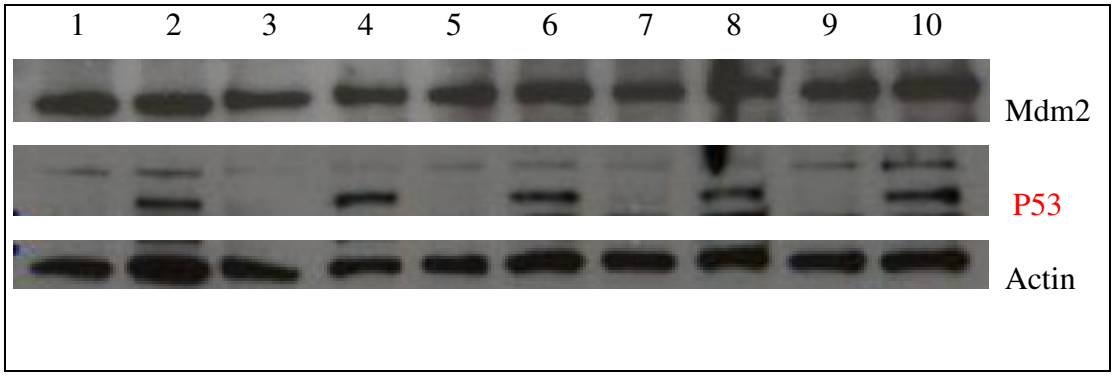

Figure 4.36. The protein expresion levels of the p53, mdm2 and actin proteins by western blotting.

5. DISCUSSION

From it's discovery in 1979, P53 was one of the most intensely studied protein (14). Its role as a tumor suppressor was clarified a 10 years later where its discovery is considered on of the most beneficial serendipity of science (17). Since then the presence of mutated forms of p53 in cancers have been so deeply and widely studied and drove so much interest that in 1993 it was voted as the molecule of the year (68). P53 is mutated in more than 50 % of the cancers (8) and for this reason it has been the focus in cancer research. According to IARC, among the somatic mutations 97 % of them are clustered in the core DNA-binding domain and 73.7 % of them are missense mutations (18).

P53 has distinct functions. Upon the external or internal stimuli it is subjected it activates the transcription of the genes that play roles in cell cycle regulation, apoptosis and DNA repair. It can also repress the activation of some downstream target genes such as Mdm-2 and Bcl-2. Of these proteins Mdm-2 is the negative regulator of p53 and Bcl-2 is an anti-apoptotic protein. P53 activates the transcription of the enzymes involved in various DNA repair mechanisms (such as nucleotide excision repair, as explained in detail in section 2.9 and figure 2.11) (27).

P53 consist of 3 main regions; the N terminal region encodes for the transcriptional activation domain and also has the proline rich domain. The DNA binding domain is the largest domain and takes place in the middle of the protein. The C terminal region encodes for the tetramerization domain and the nuclear localization signal of the protein (15, 17, 19).

Figure 5.1 illustrates the domains of P53, showing the exons, the codons, the evolutionarily conserved regions and the 11 point mutations created in this research. As it can be seen from this figure, 9 of the 11 mutations created in this research are on the DNA binding domain of the protein. The codons 84 and 92 are situated are the proline rich domain. Again except the codons 84, 92, 201 and 202 the mutations were created on evolutionarily conserved regions. 4 of these mutations are hotspot mutations (codons 241, 245, 248 and 278) and 6 of these mutations were not investigated in any publication previously.

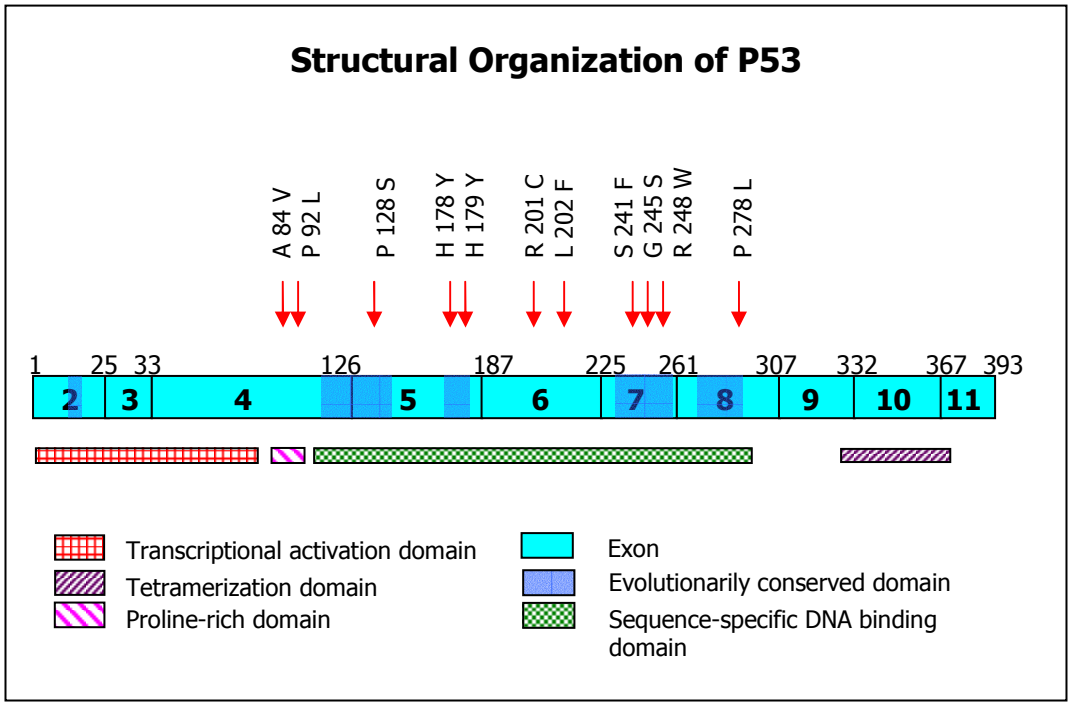

Figure 5.1. Structural Organization of p53. The mutations created were indicated as red arrows.

Before starting the *in vitro* transfection experiments, a series of bioinformatic study was carried out in order to have an insight of what the results may . The design of the study was explained in section 3.2 and the dendrogram obtained was explained in detail in section 4.1 and figure 4.1. The dendrogram only consists of the Non Melanoma Skin Cancer (NMSC) mutations that carry missense point mutations. The frameshift and nonsense mutations were not included in the uploaded data as they will result in the generation of a truncated protein. The proteins that are represented in the 8 columns are as follows; WAF1, MDM2, BAX, 14-3-3-σ, AIP1, GADD 45, NOXA and p53R2 (from left to right, in order of appearance in the dendrogram).

WAF1 is also known as CIP1 or more commonly p21. Its role is to inhibit cyclin-cyclin dependent kinases by binding to cdk's and cyclins, thus inhibiting the cell cycle at G1 to S transition. **MDM2**, as explained in detail in section 2.3 and figure 2.2 is the inactivator of p53-dependent transcription. Mdm2 is the product of an oncogene and forms an autoregulatory loop with p53. **BAX** is a proapoptotic protein, which its transcription is activated by p53 in most of the cells. **14-3-3-σ**, is a new protein,.which sequesters Cyclin B and CDC2 complexes

that initiate mitosis, so they can't enter the nucleus. It serves as adapter, activator, and repressor in response to stress and plays role mainly in cell cycle regulation, and in apoptosis as well. **AIP1** is a potential mediator of p53-dependent apoptosis. When p53 is phosphorylated at the position of Ser-46, AIP1 is upregulated and contributes to the formation of apoptosis. **GADD45** is also induced upon DNA damage. It's directly involved in the NER pathway and it destabilizes the cyclin B-CDC2 complexes like 14-3-3-σ, thus it plays role in inducing the G2/M arrest. **NOXA** is a pro-apoptotic protein that when expressed localizes to the mitochondria, interacts with the anti-apoptotic proteins like Bcl-2 and contributes to the activation of caspase 9. It thus represent a mediator of p53-dependent apoptosis. **P53R2** has an important role in double strand break repair mechanism and its production is induced by radiation. The discovery of p53R2 clarifies a relationship between a ribonucleotide reductase activity involved in repair of damaged DNA and tumor suppression by p53.

These eight protein classified in the dendrogram are all target of p53. Upon activation of p53 these genes are transcriptionally activated, but of course depending on the stimuli p53 is subject to. Mainly WAF1, 14-3-3-σ, GADD45 play role in cell cycle regulation. P53R2 is important in DNA repair. MDM2, BAX, AIP1, NOXA are involved in p53-dependent apoptosis. But they all play role (directly and indirectly) in apoptosis.

According to the dendrogram illustrated in Figure 4.1 we can have a preview of what we can expect at the end of the *in vitro* transfection assays. The logic of the clustering software is to group the data that have similar properties together. Although the colours used in the dendrogram are pseudocolor and cannot be an exact measure of the expression levels, still it can give us a rough idea of the experiment. At a first glance it can be seen that the AK mutations on codons 84, 92, 128, 201 and 202 are groupped together whereas mutations on codons 178, 179, 241, 245, 248 and 278 fall to the same green cluster. Another striking feature is that 7 of the 19 AK mutations (including codons 282 and 222 that are not investigated in this research) are clustered in the same red zone and create a subpopulation of AK's in the dendrogram. On the other hand the remaining 12 AK mutations are spread in the green zone of the dendrogram,

instead of remaining grouped in one area. We can first conclude from the dendrogram that AK mutations unlike BCC and SCC mutations have a wide variety of behavior. On the contrary, if AK mutations were all having the same properties they would be clustered in the same region rather than being spread over the dendrogram. Because of the diversity in their behaviour and knowing that the AK can turn to carcinoma or to the more aggressive SCC (54) in our research we have decided to see the effects of the AK mutations rather than investigationg the effects of the other NMSC. Any new function the mutation will confer to the protein will help us to understand the p53 dependent apoptotic pathway in skin cancers.

If the rows in the dendrogram are examined one by one, it can be concluded that mostly, but with a few exceptions, they are all activated or they all have low expression levels. These few exceptions are, not surprisingly, in the AK mutations. Codons 84, 92, 202, 178 (also investigated in our study) are the ones that have different expression profiles in different promoters. For instance R202C have low expression profile in MDM2, WAF1 and p53R2 but has high expression profile in the remaining promoters. We may expect this mutation to have a decreased response to apoptosis, which in fact is the case (L202F NO UV 5.0 ± 1.7 and L 202F UV 9.1 ± 1.3). This mutation has low percentage of apoptosis after irradiation with UVB. On the other hand GADD45, 14-33-σ levels are high for this mutation. *In vivo* this mutation is defected in p53-dependent apoptosis but probably has gained a new property in the cell cycle regulation. Therefore in the case of damage, this mutation doesn't drive the cell to apoptosis but it halts its pogression in the G2/M phase and leaves a sufficient time for the DNA repair system to eliminate the damage. The similar situation is seen in P128S too. This time the mutation has low expression levels in MDM2 and P52R2 but has high expression levels in the remaining promoters. If we examine Table 4.1 and Figure 4.35 it can be seen again that this mutation has no UV-induced apoptosis (P128S NO UV 11.2 ± 3.1 and P128S UV 9.4 ± 2.1). From these observations we can also make a little remark that P53R2 and MDM2 are essential for the proper functioning of p53-mediated apoptosis. If the MDM2 expression levels are low this means that the mutant P128S and L202F (or the mutant-wt tetramers) will not

be degraded, and the mutations will accumulate and can form mutant clones by clonal epansion.

The remaining mutations are clustered on the same area. According to the dendrogram H178Y, H179Y, S241F, G245S, R248W and P278L have the same expression levels. Comparing with the flow cytometry results and taking a close look at the dendrogram it can be said that H178Y and H179Y fall on the same subpopulation (which is consistent with the apoptosis percentage we have obtained, Table 4.1). The other mutations, which are hotspot mutations, are spread on the green area, and they act in a more similar fashion. Again this finding is consistent with our findings (Figure 4.35 and Table 4.1)

Apoptosis is the programmed cell death and is characterized by various morphological, biochemical and molecular aspects (33). As shown in Figure 2.5 there are two pathways; namely the intrinsic and extrinsic pathways that initiate apoptosis. Unlike necrosis, apoptosis is mitochondria dependent, thus is energy dependent, it doesn't generate an inflammatory response, and its presence is detected by apoptotic bodies and DNA fragmentation (40). As explained in section 3.12 and 3.13 to determine the percentage of the apoptotic cells the annexin assay followed by measurement with flow cytometry was used. The bindin of phosphatidylserine with annexin is the proof of losing the membrane and integrity therefore is the proof to apoptosis. The same condition can be true with late apoptotic cells and necrotic cells too. Because of the membrane disintegration, their PS may bind the Annexin as well. But in that case PI is used to discriminate between apoptotic and necrotic/late apoptotic cells. Since in apoptotic cells the nucleus is condensed in blebbed cells and never exposed to the outside, the cells that bind with PI and Annexin are determined as necrotic/late apoptotic. There are two approaches at this point; determining only the apoptotic cell percentage; or determining the apoptotic cell percentage plus the necrotic/late apoptotic cell percentage and giving the results as the means of "dead cell" and "live cell" percentages. The first approach is more realistic, close to *in vivo* conditions and more accurate. In our research all the results were given in the means of apoptotic cell percentage.

Being on the same protein domain doesn't predict a similar pattern on apoptosis. Being on the same exon also as well doesn't confer the similar behavior to the mutants. For example H178Y and H179Y act different from P128S, although they are all on exon 5. These mutations acquire different properties chemically and physically. In P128S, proline turns to serine; the amino acid becomes linear while normally it's cyclic. Conformationally it's a big change. If the change is examined in the means of charge changes, it can be seen that by turning to serine P128S becomes negatively charged, while normally it's uncharged. In the case of H178Y and H179Y the reverse is true; having the point mutation the amino acid becomes nonpolar (tyrosine) while it was polar previously (histidine). Histidine has an imidazole ring and is basically charged. With this mutation these 2 codons acquire an aromatic ring (tyrosine) and they gain a hydrophobic character.

For P92L and P278L it can be seen that the same amino acid change is occurring; proline turns to leucine. But the effect on apoptosis is totally different P278L has a lot more spontaneous apoptosis but both had only a small increase in UV-induced apoptosis. This is probably because;

a) The hot spot P278L is found on the evolutionary conserved region and creating a mutation here has more drastic effect than creating the same mutation on exon 4 (which is not on an evolutionary conserved region).

b) Exon 8, where P278L is located, is in close contact with the DNA. A mutation occurring here, especially a mutation which causes a change in the shape (circular to linear) occurring here would have a more important effect.

S241F, G245S, R248W and P278L are hot spot mutations and they are all on evolutionary conserved regions. That's a reason why they have such a drastic effect on apoptosis, (with a huge increase in spontaneous apoptosis and a very little apoptosis response after UV). From the information listed in Table 5.1, it can be seen that the chemical property of these mutations changes a lot. S241F and R248W turn to nonpolar while they are normally polar and G245S turns to polar while it's normally nonpolar. Again S241F and R248W turn to aromatic amino acids which is a change that brings a lot of tension on the 3rd dimension of the protein. In the case of R248W, the mutation breaks the main contact with DNA in

the minor groove (59). For P278L the reverse is true, proline turns to leucine. It's important because the side group of proline normally cyclizes onto the backbone and that's how proline creates turning points on the folded protein. With this mutation the cyclized structure is lost, which changes the shape of the active protein a lot.

R201C and L202F are both found on exon 6. They don't take place on one of the evolutionary conserved regions. On the other hand they have important changes both chemically and physically; R201C becomes an aromatic amino acid while normally it's linear. L202F gains a positive charge by turning to Cysteine. Arginine becomes cysteine. The structural change is very dramatic in both of the mutations. But it can be seen that these mutations have no visible effect on apoptosis after UV treatment and they act like WT P53.

The explanations for this situation can be:

a) It's because these mutations are not on an evolutionary conserved region.

b) Exon 6 is not a very functionally important region of the active folded protein. Although the mutations are creating important changes (both chemically and physically) the effect on apoptosis is null. Exon 6 is on the DNA binding region but in the folded active structure it is "hidden" in a hydrophobic region of the protein, or is far away from the DNA, and that's why its effect on apoptosis is not detectable.

c) These two mutations are important, but not for apoptosis. They are important for the cell cycle regulation property of p53 or the DNA repair property, but they have no effect on apoptosis.

d) Or the change is so great that there is total loss of function, a dead protein.

Figure 5.2 was drawn by using the 3D Viewer CHIME, and was an important tool to interpret the conformational change of the amino acids

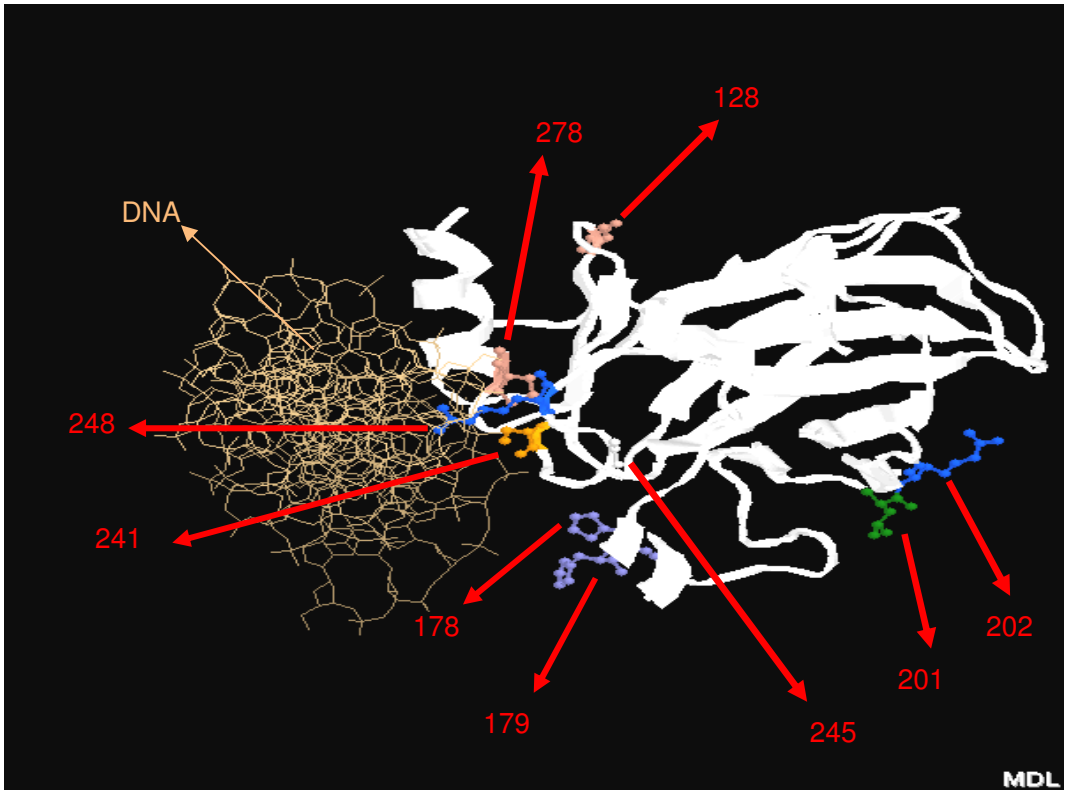

Figure 5.2. The 3D picture of the p53 DNA binding domain and the mutations created on this research drawn with the 3D Viewer CHIME.

In Figure 5.2 the complete sequence of the DNA binding domain of Wild Type p53 and the amino acids mutations created, all indicated with red arrows, can be seen. The codons A84V and P92L are not present in this picture because they are found on the proline-rich domain of p53. This picture only shows the DNA binding domain of p53.

As it can be seen from the picture, R201C and L202F are far away from the "close contact" DNA binding region of the protein. This may be an explanation why changes in these amino acids don't directly affect apoptosis even though they are in the DNA-binding region of amino acids

Also it can be seen that H178Y and H179Y, the only sites in the binding domain that affected spontaneous apoptosis but still allowed UV-induced apoptosis, are also remote from the actual DNA binding surface.

For A84V and P92L the chemical property of the amino acid doesn't change after the mutation is created. In both cases the amino acids are nonpolar. The major change is in P92L, where a cyclic amino acid (proline) turns to a linear

one (leucine). As it's discussed above the "proline to leucine" change in codon P92L doesn't have a huge increase in endogenous apoptosis as it has in codon P278L, but still it has an effect. Mutant vectors 84-128 increase spontaneous apoptosis with little more apoptosis after UV. So, a correlation between the proline rich domain of p53 and apoptosis should be present, or maybe a correlation between exon 4 and apoptosis. In a paper published by Venot *et al*, (20), it's stated that the deletion of the proline rich domain doesn't affect the transactivation of WAF1, MDM2 and BAX, but instead it alters the transcriptional repression, reactive oxygen species production and sequence-specific transactivation of the *PIG3* gene, which are all activities that affect apoptosis. In another work, published by Zhu *et al* (65), different domains of p53 were deleted and the overall effect of all these deletions were investigated. According to this work it was found that the proline-rich region forms an activation domain for pro-apoptotic genes or it inhibits anti-apoptotic genes. As a conclusion of this work they have a schematic representation of the effect of different domains on apoptosis. (PRD is proline rich domain; DBD is DNA binding domain; AD is activation domain; TD is tetramerization domain and NLS is Nuclear localization signal).

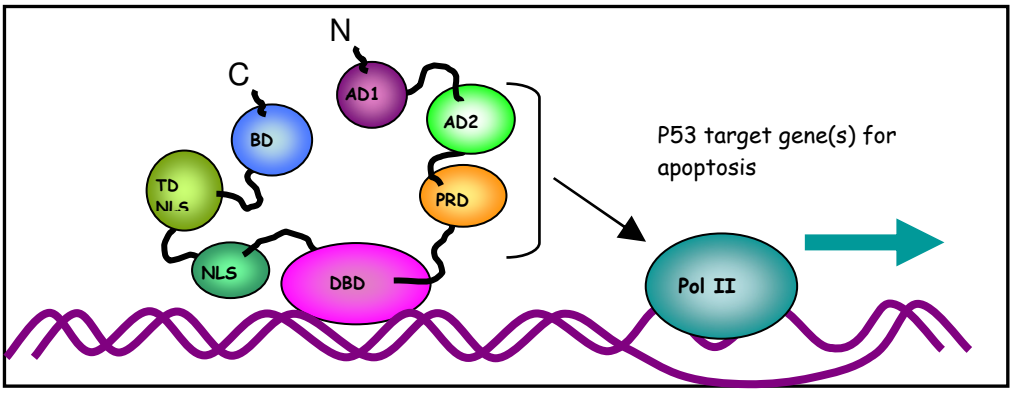

Figure 5.3. Different domains of p53 and apoptosis (65).

According to this model it's suggested that first the binding of DBD to DNA is necessary. Then, AD2 and PRD should together form an active complex that will activate the polymerase and the p53 target genes for apoptosis.

Table 5.1 Properties of the original and mutated codons created in this research.

Name of the Mutant	Original Sequence	Mutated Sequence	Change in amino acid's Chemical Property	Change in amino acid's Physical Property	Exon
A84V	GCC (Ala)	GTC (Val)	Nonpolar → Nonpolar	Aliphatic → Aliphatic	4
P92L	CCC (Pro)	CTC (Leu)	Nonpolar → Nonpolar	Cyclic → Aliphatic	4
P128S	CCT (Pro)	TCT (Ser)	Nonpolar → Polar	Cyclic → non aromatic hydroxil	5
H178Y	CAC (His)	TAC (Tyr)	Polar → Nonpolar	Basic, imidazole → Aromatic	5
H179Y	CAT (His)	TAT (Tyr)	Polar → Nonpolar	Basic, imidazole → Aromatic	5
L201F	TTG (leu)	TTT (Phe)	Nonpolar → Nonpolar	Aliphatic → Aromatic	6
R202C	CGT (Arg)	TGT (Cys)	Uncharged Polar→ (+)'ly charged polar	Basic → Sulfur containing	6
S241F	TCC (Ser)	TTC (Phe)	Polar → Nonpolar	Non aromatic hydroxil → Aromatic	7
G245S	GGC (Gly)	AGC (Ser)	Nonpolar → Polar	Aliphatic → Non aromatic hydroxil	7
R248W	CGG (Arg)	TGG (Trp)	Polar → Nonpolar	Basic → Aromatic	7
P278L	CCT (Pro)	CTT (Leu)	Nonpolar → Nonpolar	Cyclic → Aliphatic	8

6. CONCLUSIONS

In the present study 11 point mutations were created and transiently transfected into P57/BL6 mouse primary fibroblast cells. The wild type and mutated cells were then irradiated with 1000 J/m^2 of UVB and then flow citometry was used to detect the apoptosis percentage before and after UVB radiation. The apoptosis percentage were find as follows;

For cells that are not radiated the percentage is WT p53 3.2 ± 1.3, A84V 7.9 ± 1.3, P92L 8.7 ± 1.9, P128S 11.2 ± 3.1, H178Y 5.7 ± 1.3, H179Y 8.4 ± 2.3, R201C 2.6 ± 0.7, L202F 5.0 ± 1.7, S241F 25.7 ± 2.1, G245S 21.3 ± 2.0, R248W 25.6 ± 4.0 and P278L 22.3 ± 4.0.

After radiation with 1000 J/m^2 of UVB the apoptosis percentage were found as follows: WT 11.6 ± 2.0, A84V 15.5 ± 2.4, P92L 12.7 ± 1.2, P128S 9.4 ± 2.1, H178Y 18.8 ± 1.9, H179Y 16.8 ± 1.0, R201C 9.6 ± 1.4, L202F 9.1 ± 1.3, S241F 28.2 ± 2.9, G245S 30.3± 1.9, R248W 31.5 ± 1.8, P278L 30.6 ± 2.1.

Taking all the results together we can conclude that;

1. The more the amino acid is in close contact with the DNA, the more its effect is visible on apoptosis (like in S241F, G245S, R248W, P278L, H178Y, H179Y).
2. The chemical and physical change of the amino acid is important but not primarily; the physical closeness to the DNA is more important. We can see the evidence of this effect in R201C and L202F.
3. Being on the same exon doesn't predict the same change in apoptosis . For example the codons P128S and H178Y - H179Y are on exon 5. In that case, again the physical closeness to DNA is primarily important, and then the change in the structure plays the role.
4. If we compare P92L and P278L, the two codons that have the same amino acid change but are on different exons (4 and 8, respectively), we can conclude that having the same amino acid change is not enough to see the same effect on apoptosis. Being on an evolutionary conserved region is another important factor. Probably the organism is forcing itself to keep these

regions safe from mutations, but when a mutation occurs its effect becomes more drastic.

In this research 6 of the 11 NMSC mutations were investigated for the first time, thus are not present in any of the p53 mutation databases. Another important aspect of this work is that, the cell type used in transfection experiments was the primary mouse fibroblasts. Generally cell lines like HeLa, Saos-2, HaCat are used to reveal the properties of the p53 mutations. But these cell lines already have defects in their apoptotic or cell cycle pathway. Thus we thought that using primary mouse fibroblasts will reveal more realistic -very close to *in vivo*- results in our experiments.

In the future the mutations created in this project will be tested in p53 KO mouse fibroblasts and see if they repeat the similar behavior or not. By repeting the experiments in p53 deficient cells the p53-dependent apoptotic pathway will be understood a little more. Another project will be to clarify the mitochondrial dependent apoptotic pathways by using the same mutant vectors and siRNA of the pro and anti apoptotic proteins. And finally by using yeast hybrid reporter system, determining the transcriptional activities of these mutations and see if they can transactivate the downstream target genes of the apoptotic machinery.

REFERENCES

1. Lane, D.P., Crawford, L.V. (1979) T antigen is bound to a host protein in SV40-transformed cells. *Nature*. 278 (5701):261-263

2. Reich, N.C., Levine, A.J. (1982) Specific interaction of the SV40 T antigen-cellular p53 protein complex with SV40 DNA. *Virology*. 117(1):286-290

3. Sarnow, P., Hearing, P., Anderson, C.W., Reich, N., Levine, A.J. (1982) Identification and characterization of an immunologically conserved adenovirus early region 11,000 Mr protein and its association with the nuclear matrix. *J Mol Biol*. Dec 15; 162(3):565–583.

4. Szekely, L., Selivanova, G., Magnusson, K.P., Klein, G., Wiman, K.G. (1993) EBNA-5, an Epstein-Barr virus-encoded nuclear antigen, binds to the retinoblastoma and p53 proteins. *Proc Natl Acad Sci U S A*. Jun 15; 90 (12):5455-5459.

5. Wang, X.W., Forrester, K., Yeh, H., Feitelson, M.A., Gu, J.R., Harris, C.C. (1994) Hepatitis B virus X protein inhibits p53 sequence-specific DNA binding, transcriptional activity, and association with transcription factor ERCC3. *Proc Natl Acad Sci U S A*. Mar 15;91(6):2230-2234.

6. May, P., May, E. (1999) Twenty years of p53 research: structural and functional aspects of the p53 protein. *Oncogene*. Dec 13;18(53):7621-7636

7. Oren, M., Reich, N.C., Levine, A.J. (1982) Regulation of the cellular p53 tumor antigen in teratocarcinoma cells and their differentiated progeny. *Mol Cell* Biol. Apr;2(4):443-449.

8. Kress, M., May, E., Cassingena, R., May, P. (1979) Simian virus 40-transformed cells express new species of proteins precipitable by anti-simian virus 40 tumor serum. *J Virol*. Aug; 31(2):472-83.

9. Rotter, V., Prokocimer, M. (1991) p53 and human malignancies. *Adv Cancer Res*. 57257-57272.

10. Crawford, L.V., Pim, D.C., Bulbrook, R.D. (1982) Detection of antibodies against the cellular protein p53 in sera from patients with breast cancer. *Int J Cancer*. Oct 15;30(4):403-408.

11. Angelopoulou, K., Diamandis, E.P., Sutherland, D.J., Kellen, J.A., Bunting, P.S. (1994) Prevalence of serum antibodies against the p53 tumor suppressor gene protein in various cancers. *Int J Cancer*. Aug 15;58(4):480-487.

12. Reich, N.C., Levine, A.J. (1984) Growth regulation of a cellular tumour antigen, p53, in nontransformed cells. *Nature*. Mar 8-14;308(5955):199-201.

13. Milner, J., McCormick, F. (1980) Lymphocyte stimulation: concanavalin A induces the expression of a 53K protein. *Cell Biol Int Rep*. 1980 Jul;4(7):663-667.

14. Calabretta, B., Kaczmarek, L., Selleri, L., Torelli, G., Ming, P.M., Ming, S.C., Mercer, W.E. (1986) Growth-dependent expression of human Mr 53,000 tumor antigen messenger RNA in normal and neoplastic cells. *Cancer Res*. Nov;46(11):5738-5742.

15. Soussi, T., May, P. (1996) Structural aspects of the p53 protein in relation to gene evolution: a second look. *J Biol Mol*, 260, 630-637.

16. Camplejohn, R.S., Rutherford, J. (2001) p53 functional assays: detecting p53 mutations in both the germline and in sporadic tumours. *Cell Prolif.* 34, 1–14.

17. Fisher, D.E., (2001) The p53 Tumor suppressor: Critical regulator of life and death in cancer *Apoptosis,* Vol 6, 7-15.

18. Chao, C., Wu, Z., Mazur, S.J., Borges, H., Rossi, M., Lin, T., Wang, J.Y., Anderson, C.W., Appella, E., Xu, Y. (2006) Acetylation of mouse p53 at lysine 317 negatively regulates p53 apoptotic activities after DNA damage. *Mol Cell Biol*. Sep;26(18):6859-69

19. Walker, K.K., Levine, A.J. (1996) Identification of a novel p53 functional domain that is necessary for efficient growth suppression. *Proc Natl Acad Sci USA*. 93: 15335–15340.

20. Venot, C., Maratrat, M., Dureuil, C., Conseiller, E., Bracco, L., Debussche, L. (1998) The requirement for the p53 proline-rich functional domain for mediation of apoptosis is correlated with specific PIG3 gene transactivation and with transcriptional repression. *Embo J.* 17: 4668–4679.

21. Chen, X., Ko, L.J., Jayaraman, L., Prives, C. (1996) p53 levels, functional domains, and DNA damage determine the extent of the apoptotic response of tumor cells. *Genes Dev*. Oct1;10(19):2438-51.

22. Friedman, P. N., Chen, X., Bargonetti, J., and Prives, C. (1993) The p53 protein is an unusually shaped tetramer that binds directly to DNA. *Proc. Natl. Acad. Sci. USA*, *90:* 3319–3323.

23. Rolley, N., Butcher, S., and Milner, J. (1995) Specific DNA binding by different classes of human p53 mutants. *Oncogene*, *11:* 763–770.

24. Fang, S., Jensen, J.P., Ludwig, R.L., Vousden, K.H., Weissman, A.M. (2000) Mdm2 is a RING finger-dependent ubiquitin protein ligase for itself and p53. *J Biol Chem*. Mar 24;275(12):8945-51.

25. Oren, M. (2003) Decision making by p53: life, death and cancer. *Cell Death and Differentiation*. 10, 431–442

26. Blagosklonny, M.V. (2000) p53 from complexity to simplicity: mutant p53 stabilization, gain-of-function, and dominant-negative effect. *FASEB J*. Oct;14(13):1901-1907.

27. Polyak, K., Waldman, T., He, T-C, Kinzler, K.W., Vogelstein, B. (1996) Genetic determinants of p53-induced apoptosis and growth arrest. Genes Dev. Aug 1;10(15):1945-1952.

28. El-Deiry, W.S., Tokino, T., Velculescu, V.E., Levy, D.B., Parsons, R., Trent, J.M., Lin, D., Mercer, W.E., Kinzler, K.W. and Vogelstein, B. (1993) *WAF1*, a potential mediator of p53 tumor suppression. *Cell* . 75 , 817–825.

29. Deng, C., Zhang, P., Harper, J.W., Elledge, S.J. and Leder, P. (1995) Mice lacking $p21^{CIP1/WAF1}$ undergo normal development, but are defective in G1 checkpoint control. *Cell.* 82, 675–684.

30. Lodish, H., Berk, A., Matsudaira, P., Kaiser, C.A., Krieger, M., Matthew, P.S., Zipursky, S.L., Darnell, J. *Molecular Cell Biology*, 5th Edition, chapter 23, p 889, WH Freeman and Company, New York.

31. Haupt, Y., Oren, M. (1996) p53-mediated apoptosis: mechanisms and regulation *Behring Inst. Mitt.* 97, 32–59.

32. Sionov, V., Hayon, R., Haupt, Y. (2001) The regulation of p53 growth suppression, in Cell Cycle Checkpoints and Cancer. *Landes Bioscience*, 106–125.

33. Save, V., Peter, A., Hall, A., and Coates, P.J. (2004) Apoptotic methods and protocols, methods in molecular biology, *Humana Press*, vol 282, pp 67-86.

34. Adrain, C., Creagh, E. M., Martin, S. J. (2001) Apoptosis-associated release of Smac/DIABLO from mitochondria requires active caspases and is blocked by Bcl-2. *EMBO J*. Dec 3;20(23):6627-36.

35. Hague, A., Paraskeva, C. (2004) Apoptosis and disease: a matter of cell fate. *Nature Cell Death and Differentiation*. 3, 1-7

36. Haupt, S., Berger, M., Goldberg, Z., Haupt, Y. (2003) Apoptosis - the p53 network. *Journal of Cell Science*. 116, 4077-4085.,

37. Csipo, I., Montel, A. H., Hobbs, J. A., Morse, P. A., Brahmi, Z. (1998) Effect of Fas+ and Fas- target cells on the ability of NK cells to repeatedly fragment DNA and trigger lysis via the Fas lytic pathway. *Apoptosis*. 3, 105-114.

38. Johnstone, R. W., Ruefli, A. A., and Lowe, S. W. (2002) Apoptosis: a link between cancer genetics and chemotherapy. *Cell.* 108, 153-164.

39. Zeiss, C. J. (2003) The Apoptosis-Necrosis Continuum: Insights from Genetically Altered Mice. *Vet Pathol.* 40:481-495.

40. Berghe V,. Kalai M., Denecker G., Meeus A., Saelens X., Vandenabeele P. (2006). Necrosis is associated with IL-6 production but apoptosis is not. *Cell Signal*.18(3): p. 328-35.

41. Strano, S., Rossi, M., Fontemaggi, G., Munarriz, E., Soddu, S., Sacchi, A., Blandino, G. (2001) From p63 to p53 across p73. *FEBS Lett*. Feb 16;490(3):163-70.

42. Moll, U.M. (2003) The role of p63 and p73in Tumor Formation and Progression: Coming of Age Toward Clinical Usefulness. *Clinical Cancer Research*. Vol. 9, 5437–5441.

43. Gazziola, C., Megens, E., ,Welboren, W., Denissov, S., Stunnengerg, H., Lohium, M. (2005) Analysis of p53 and p73 binding sites by CHIP-on-chip technology. *FEBS Journal*. 272s1, 355-363.

44. Stone, J.L., Reizner, G., Scotto, J., Elpern, D., Farmer, E.R., Pabo, R. (1986) *Hawaii Med J*. 45, 281-286

45. National Cancer Institute, http://www.nci.com [05/08/2006]

46. Miller, S.J. (1991) Biology of basal cell carcinoma. *J Am Acad Dermatol*. Feb ; 24 (2 Pt 1):161-75.

47. Skin Cancer Foundation http://www.scf.com [05/08/2006]

48. Ziegler, A., Leffell, D.J., Kunala, S., Sharma, H.W., Gailani, M., Simon, J,A,, Halperin, A.J., Baden, H.P., Shapiro, P.E., Bale, A.E., Brash, D.E. (1993) Mutation hotspots due to sunlight in the p53 gene of nonmelanoma skin cancers. *Proc Natl Acad Sci U S A*. May 1;90(9):4216-20.

49. Brash, D.E. (1997) *Trends In Genetics*. 13(10) 410-414.

50. Nelson, D.L., Cox, M.M. Lehninger, 3rd Edition, chapter 10, p 349. Worth Publishing, New York.

51. Goodsell, D.S. (2001) The Molecular Perspective: Ultraviolet Light and Pyrimidine Dimers. *The Oncologist*. 6(3) 298-299.

52. Lodish, H., Berk, A., Matsudaira, P., Kaiser, C.A., Krieger, M., Matthew, P.S., Zipursky, S.L., Darnell, J. Molecular Cell Biology, 5th Edition, chapter 23, pp 966-967, WH Freeman and Company, New York.

53. Sancar, A., Lindsey-Boltz, L.A., Unsal-Kacmaz, K., Linn, S. (2004) Molecular mechanisms of mammalian DNA repair and the DNA damage checkpoints. *Annu. Rev. Biochem*. 73:39-85.

54. Brash, D.E. (1996) Sunlight and Sunburn in Human skin cancer. *J of investigative dermatology symposium proceedings*, 1:136-142. 1996.

55. http://ccr.coriell.org/nigms/pathways/ner.htmll

56. Mullauer, L., Gruber, P., Sebinger, D., Buch, J., Wohlfart, S., Chott, A. (2001) Mutations in apoptosis genes: a pathogenetic factor for human disease. Mutat Res. 488, 211-231

57. Nelson, D.L., Cox, M.M. Lehninger, 3rd Edition, chapter 25, p 949. Worth Publishing, New York.

58. Szymanska, K, Hainaut, P. (2003) TP53 and mutations in human cancer. *Acta Biochim Pol*. 50(1):231-238.

59. The International Agency of Research on Cancer www.iarc.fr/p53/index.html [02/05/2006]

60. Dittmer, D., Pati, S., Zambetti, G., Chu, S., Teresky, A.K., Moore, M., Finlay, C., Levine, A.J. (1993) Gain of function mutations in p53. Nat Genet. 4(1):42-46.

61. Soussi, T., Kato, S., Levy, P.P., Ishioka, C. (2005) Reassessment of the TP53 mutation database in human disease by data mining with a library of TP53 missense mutations. *Hum Mutat*. 25 (1) :6-17.

62. Kato, S., Han, S.Y., Liu, W., Otsuka, K., Shibata, H., Kanamaru, R., Ishioka, C. (2003) Understanding the function-structure and function-mutation relationships of p53 tumor suppressor protein by high-resolution missense mutation analysis. *Proc Natl Acad Sci U S A*. 100(14):8424-8429

63. Olivier, M., Eeles, R., Hollstein, M., Khan, M.A., Haris, C.C., Hainaut, P. (2002) The IARC TP53 Database: new online mutation analysis and recommendations to users. *Hum Mutat*. (6):607-14

64. Noble, J.R., Willetts, K.E., Mercer, W.E., Reddel, R.R. (1992) Effects of exogenous wild-type p53 on a human lung carcinoma cell line with endogenous wild-type p53. *Exp Cell Res*. 203(2):297-304.

65. Zhu, J., Zhang, S., Jiang, J., Chen, X. (2000) Definition of the p53 functional domains necessary for inducing apoptosis. *J. Biol. Chem*. 275, Issue 51, 39927-39934.

66. Ko, L.J., Prives, C (1996) p53: Puzzle and paradigm. *Genes Dev*. 10: 1054–1072

67. Hollstein, M., Sidransky, D., Vogelstein, B., Hariss, C.C. (1991) p53 mutations in human cancers *Science*. 253(5015):49-53.

68. Levine, A.J. (1997) The cellular gatekeeper for growth and division. *Cell*. 88(3):323-31. p53,

69. Andrew, R., Cuddihy1, A., Bristow R.G. (2004) The p53 protein family and radiation sensitivity: Yes or no? *Cancer and Metastasis Reviews* 23: 237–257.

70. Molecular Probes, Vybrant Apoptosis Assay Kit No.6, http://probes.invitrogen.com/media/pis/mp23200.pdf [10/11/2006]

APPENDIX-1 The 3 letter Genetic Code

First Position	Second Position of Codon: T	C	A	G	Third Position
T	TTT Phe [F]	TCT Ser [S]	TAT Tyr [Y]	TGT Cys [C]	T
	TTC Phe [F]	TCC Ser [S]	TAC Tyr [Y]	TGC Cys [C]	C
	TTA Leu [L]	TCA Ser [S]	TAA *Ter* [end]	TGA *Ter* [end]	A
	TTG Leu [L]	TCG Ser [S]	TAG *Ter* [end]	TGG Trp [W]	G
C	CTT Leu [L]	CCT Pro [P]	CAT His [H]	CGT Arg [R]	T
	CTC Leu [L]	CCC Pro [P]	CAC His [H]	CGC Arg [R]	C
	CTA Leu [L]	CCA Pro [P]	CAA Gln [Q]	CGA Arg [R]	A
	CTG Leu [L]	CCG Pro [P]	CAG Gln [Q]	CGG Arg [R]	G
A	ATT Ile [I]	ACT Thr [T]	AAT Asn [N]	AGT Ser [S]	T
	ATC Ile [I]	ACC Thr [T]	AAC Asn [N]	AGC Ser [S]	C
	ATA Ile [I]	ACA Thr [T]	AAA Lys [K]	AGA Arg [R]	A
	ATG Met [M]	ACG Thr [T]	AAG Lys [K]	AGG Arg [R]	G
G	GTT Val [V]	GCT Ala [A]	GAT Asp [D]	GGT Gly [G]	T
	GTC Val [V]	GCC Ala [A]	GAC Asp [D]	GGC Gly [G]	C
	GTA Val [V]	GCA Ala [A]	GAA Glu [E]	GGA Gly [G]	A
	GTG Val [V]	GCG Ala [A]	GAG Glu [E]	GGG Gly [G]	G

APPENDIX 2: The Table of Fluorochromes

Probe	Ex (nm)	Em (nm)	MW	Notes
Reactive and conjugated probes				
R-Phycoerythrin (PE)	480;565	578	240 k	
PE-Cy5 conjugates	480;565;650	670		*aka* Cychrome, R670, Tri-Color,
PE-Cy7 conjugates	480;565;743	767		
Fluorescein	495	519	389	FITC; pH sensitive
TRITC	547	572	444	TRITC
PerCP	490	675		Peridinin chlorphyll protein
Texas Red	589	615	625	Sulfonyl chloride
Alexa Fluor dyes				
Alexa Fluor 350	346	445	410	
Alexa Fluor 430	430	545	701	
Alexa Fluor 488	494	517	643	
Alexa Fluor 532	530	555	724	
Alexa Fluor 546	556	573	1079	
Alexa Fluor 555	556	573	1250	
Alexa Fluor 568	578	603	792	
Alexa Fluor 594	590	617	820	
Alexa Fluor 633	621	639	1200	
Alexa Fluor 647	650	668	1250	
Alexa Fluor 680	679	702	1150	
Alexa Fluor 700	696	719		
Nucleic acid probes				
Hoechst 33258	345	478	624	AT-selective
SYTOX Blue	431	480	~400	DNA
SYTOX Orange	547	570	~500	DNA
Ethidium Bromide	493	620	394	
7-AAD	546	647		7-aminoactinomycin D
Acridine Orange	503	530/640		DNA/RNA
Propidium Iodide (PI)	536	617	668.4	
Fluorescent Proteins				
GFP uv	385	508		
EGFP	489	508	26k	Quantum yield ~0.60
DsRed	558	583	~110k	Quantum yield 0.79.